I. THE CRYSTAL STRUCTURES OF CERTAIN INTERMETALLIC COMPOUNDS

(a) The Nature of the Bonds in the Iron Silicide FeSi and Related Crystals

(b) A Study of the Structures of the Intermetallic Compounds Mg_2Tl, Mg_2In, and Mg_2Ga

II. METALLIC VALENCE AND X-RAY EMISSION FINE STRUCTURE: A DISCUSSION

III. CRYSTAL STRUCTURES OF CERTAIN INORGANIC COMPOUNDS

(a) Crystal Structure of Sodium Borohydride

(b) A Redetermination of the Structural Parameters in the Cubic Modification of Arsenious Oxide

Thesis by

Albert Mills Soldate

In Partial Fulfillment of the Requirements

For the Degree of

Doctor of Philosophy

California Institute of Technology

Pasadena, California

1950

Acknowledgments

The investigations of this thesis resulted from suggestions by Professor Linus Pauling to whom I am further indebted for advice and encouragement in the course of completing them.

I wish to express my gratitude to Professor J. H. Sturdivant for his generous expenditure of time and effort in offering much helpful advice and constructive criticism to me during my graduate studies at the Institute.

Abstracts

Abstract of Part I.

Section (a)*

The structure of the iron silicide FeSi was determined by means of X-ray single-crystal photography. The previously reported structure was verified. The structure is based upon the space group $T^4 - P2_13$ with $a_o = 4.489 \pm 0.005$ Å. Four iron and four silicon atoms are in the positions (xxx; $x+\frac{1}{2}, \frac{1}{2} - x, \bar{x}; \nu$) with $x_{Fe} = 0.1370 \pm 0.0020$ and $x_{Si} = 0.842 \pm 0.004$.

A detailed discussion of the structure was given in terms of the resonating-valence-bond theory developed by Professor Pauling.

---

* The work of this section was done in collaboration with Professor Linus Pauling.

Abstract of Part I.

Section (b)

An investigation of the structures of the intermetallic compounds Mg_2Tl, Mg_2In, and Mg_2Ga was made. The methods of X-ray single-crystal and powder photography were employed. The structures of Mg_2Tl and Mg_2In are based upon the space group D_{3h}^3 - $C\bar{6}2m$ with three molecules in a unit cell of dimensions $a_o = 8.068 \pm 0.005$ Å, $c_o = 3.457 \pm 0.0007$ Å; $a_o = 8.324 \pm 0.005$ Å, $c_o = 3.457 \pm 0.0007$ Å, respectively. The three thallium or indium atoms are in the positions

1: (a) 000,

2: (c) $\frac{1}{3}\ \frac{2}{3}\ \frac{1}{2}$; $\frac{2}{3}\ \frac{1}{3}\ \frac{1}{2}$.

The six magnesium atoms are in the positions

3: (f) $x_1 00$; $0 x_1 0$; $\bar{x}_1 \bar{x}_1 0$

3: (g) $x_2 0 \frac{1}{2}$; $0 x_2 \frac{1}{2}$; $\bar{x}_2 \bar{x}_2 \frac{1}{2}$.

In the case of Mg_2Tl $x_1 = 0.3746 \pm 0.0028$ and $\bar{x}_2 = 0.2866 \pm 0.0038$. It was not possible to fix the parameters x_1 and x_2 accurately in the instance of Mg_2In, but it is highly probable that they do not differ greatly from the corresponding values of Mg_2Tl.

A discussion of the structure of Mg_2Tl in terms of the resonating-valence-bond theory [1), (2)] was given and it was found that the valences of the thallium atoms are larger than that exhibited in the elementary substance.

The structure of Mg_2Ga is apparently similar to that of Mg_2Tl and Mg_2In. The positions of the atoms, however, necessitate a doubling of the unit cell dimension along the c axis. It was not possible to determine the exact position of the atoms.

Abstract of Part II.

A discussion is given of the relationship between metallic valence and the fine structure of the X-ray emission bands of metals, alloys, and intermetallic compounds. The study of fine structure seems to offer a chance to gain valuable information concerning metallic valences; there is, however, a great need for more experimental information.

Abstract of Part III.

Section (a)

The structure of sodium borohydride was investigated by means of X-ray powder photography and found to be based on a face-centered cubic lattice. The unit cell of dimensions $a_o = 6.151 \pm 0.009$ kX contains four sodium and four boron atoms arranged in the following manner:

4 Na at ooo, $o\frac{1}{2}\frac{1}{2}$, $\frac{1}{2}o\frac{1}{2}$, $\frac{1}{2}\frac{1}{2}o$

4 B at $\frac{1}{2}\frac{1}{2}\frac{1}{2}$, $\frac{1}{2}oo$, $o\frac{1}{2}o$, $oo\frac{1}{2}$

It is probable that the structure consists of tetrahedral BH_4^- ions and Na^+ ions. The dimensions of the ions would permit oscillation or rotation of the BH_4^- tetrahedra.

Abstract of Part III.

Section (b)

The structural parameters of the cubic modification of arsenious oxide have been redetermined by means of X-ray powder and single crystal photography and found to agree closely with those reported by Almin and Westgren[5].

The structure is based upon the packing of As_4O_6 molecules which have the same dimensions as those found for the molecules of the gas[2], [12].

Table of Contents

I. THE CRYSTAL STRUCTURES OF CERTAIN INTERMETALLIC COMPOUNDS

(a) The Nature of the Bonds in the Iron Silicide FeSi and Related Crystals

Reprinted from *Acta Crystallographica*, VOL. 1, PART 4, September 1948

PRINTED IN GREAT BRITAIN

Acta Cryst. (1948). **1**, 212

The Nature of the Bonds in the Iron Silicide FeSi and Related Crystals*

BY L. PAULING AND A. M. SOLDATE

Gates and Crellin Laboratories of Chemistry, California Institute of Technology, Pasadena, Cal., U.S.A.

(*Received* 7 *June* 1948)

The iron silicide FeSi has been reinvestigated by X-ray photography of single crystals, and the reported structure for the substance has been verified. The space group is T^4–$P2_13$, with

$$a_0 = 4{\cdot}489 \pm 0{\cdot}005 \text{ A.}$$

Four iron atoms and four silicon atoms are in positions $(x, x, x;\ x+\frac{1}{2}, \frac{1}{2}-x, \bar{x};\ \swarrow)$, with

$$x_{Fe} = 0{\cdot}1370 \pm 0{\cdot}0020 \quad \text{and} \quad x_{Si} = 0{\cdot}842 \pm 0{\cdot}004.$$

A detailed discussion of the structure and the values of the interatomic distances has been given, by application of the resonating-valence-bond theory, and it has been shown that the interatomic distances are compatible with those found for elementary iron and elementary silicon.

Introduction

The structure of the iron silicide FeSi was first investigated by Phragmén (1923), who found it to be based upon the space group T^4–$P2_13$, with a unit cell containing four iron atoms in the positions $(x, x, x;\ x+\frac{1}{2}, \frac{1}{2}-x, \bar{x};\ \swarrow)$ and four silicon atoms in a similar set. The edge of the cubic unit cell (a_0) was given as 4·48 A., and it is evident from Phragmén's drawing of the structure that x_{Fe} and x_{Si} were taken as approximately $\frac{1}{6}$ and $\frac{5}{6}$. Wever & Moeller (1930) later studied this structure by use of powder photography and reported the values $x_{Fe} = 0{\cdot}1340 \pm 0{\cdot}0020$, $x_{Si} = 0{\cdot}8445 \pm 0{\cdot}0020$, and $a_0 = 4{\cdot}467$ A. (It is mentioned in the *Strukturbericht*, **2**, p. 241, however, that the authors have stated in a personal communication that an error was made in their determination of the parameters.) Another powder photographic study of this substance was made by Borén (1933), who reported $x_{Fe} = 0{\cdot}139 \pm 0{\cdot}001$, $x_{Si} = 0{\cdot}845 \pm 0{\cdot}001$, and $a_0 = 4{\cdot}478$ A.

The structure found for FeSi and other silicides (CrSi, MnSi, CoSi, NiSi) (Borén, 1933) is interesting as an example of co-ordination number 7. Each iron atom is surrounded by seven silicon atoms, and each silicon atom by seven iron atoms, at the distances 2·28 A. (one ligand), 2·35 A. (3), and 2·50 A. (3) (calculated with the parameter values of Borén; those of Wever & Moeller lead to values agreeing with these to within 0·03 A.). Each iron atom also has six iron neighbors at 2·75 A. We became interested in the structure in connection with our efforts to develop a rational theory of metals and intermetallic compounds (Pauling, 1938, 1947), and attempted to find an explanation of the choice by these substances of this unusual structure, in preference to the sodium chloride, nickel arsenide, or cesium chloride structure, and also an explanation of the

* Contribution no. 1172 from the Gates and Crellin Laboratories.

unusually small interatomic distances shown by the crystal. These small distances make themselves evident when an effort is made to calculate the valences of the iron and silicon atoms from the bond distances, with use of the recently proposed relation between bond distance and valence (Pauling, 1947):

$$R_n = R_1 - 0{\cdot}300 \log n. \qquad (1)$$

The bond numbers obtained from the reported interatomic distances lead, when summed, to the valences 6·98 for iron and 6·93 for silicon, in obvious disagreement with those usually accepted, 5·78 and 4·00, respectively.

The seriousness of the apparent anomaly in valence and the incompleteness of the published details of the only single-crystal investigation of the structure that has been reported (Phragmén, 1923) caused us to consider the possibility of an error in the structure determination, and led us to verify the structure and to redetermine the parameters by single-crystal X-ray methods.

Experimental methods and results

A preparation which consisted of silicide crystals embedded in a silicon-rich α-iron matrix was made by slowly cooling a mixture of reagent-grade iron and silicon containing 25 (wt.) % of silicon from the molten state, under 40 mm. of hydrogen. A residue of silicide crystal fragments and silica was obtained by the decomposition of the sample with hot aqua regia. A single-crystal fragment with longest dimension less than 0·1 mm. was selected, and its individuality as a single crystal was demonstrated by the preparation of heavily exposed symmetrical Laue photographs. The Laue point group was found to be T_h–$2/m\bar{3}$. The value of a_0 was found to be $4{\cdot}489 \pm 0{\cdot}005$ A. from equatorial measurements of 15° oscillation photographs; no re-

flections requiring a larger cell were observed on the Laue or oscillation photographs.* The lattice is primitive, restricting the space group to

$$T^1\text{–}P23, \quad T^4\text{–}P2_13, \quad T_h^1\text{–}Pm3, \quad T_h^2\text{–}Pn3,$$

or T_h^6–$Pa3$ (*Internationale Tabellen...*).

T_h^2–$Pn3$ is eliminated by the observation of reflections $(0kl)$ with $k+l$ odd, and T_h^6–$Pa3$ by $(0kl)$ with k odd.

The density 5·95 g.cm.$^{-3}$ reported for a specimen containing 33·0 (wt.) % of silicon (Landolt-Börnstein, 1931, p. 330) leads to $3{\cdot}86 \sim 4$ atoms of iron and $3{\cdot}86 \sim 4$ atoms of silicon in the unit cell. It is assumed that the iron and silicon atoms are distributed in a definite, non-statistical fashion. The final correspondence between calculated and observed structure factors constitutes the ultimate justification of this assumption. (Furthermore, there seems to be no reasonable statistical distribution involving four iron and four silicon atoms for any one of the three possible space groups.)

It is impossible to place four iron and four silicon atoms in sets of equivalent positions of the space groups T^1–$P23$ and T_h^1–$Pm3$ which are not also equivalent positions of the space group T_d^1–$P\bar{4}3m$ (which has the Laue symmetry O_h–$4/m\bar{3}2/m$). The structure must therefore be based on the space group T^4–$P2_13$. The observed absence of reflections of the type $(h00)$ with h odd is consistent with the choice of this space group. Four iron and four silicon atoms may be placed in sets of equivalent positions in only one manner, namely, in two sets of equivalent positions of the type $(x, x, x;\ x+\frac{1}{2}, \frac{1}{2}-x, \bar{x};$ etc.$)$.

A set of 15° oscillation photographs about a twofold axis was prepared in a cylindrical camera with a radius of 5 cm. by use of Mo $K\alpha_1$, α_2 radiation filtered by zirconium foil. Three films interleaved with 0·001 in. copper foil were used for each exposure (Hughes, 1941). Intensities of reflections observed in the photographs were estimated visually. Absorption corrections, omitted here, were estimated to be small. The atomic scattering factors for iron were taken as averages between those of Pauling & Sherman (1932) and of Thomas & Fermi (*Internationale Tabellen...*), and the atomic scattering factors for silicon as averages between those of Pauling & Sherman and of James & Brindley (*Internationale Tabellen...*). A temperature factor

---

* The Mo $K\alpha_1$ components of well-resolved doublets were used for these measurements; the value 0·70926 A. was assumed for λ. It is probable that earlier measurements of a_0 are reported in kX. units. If this is the case, the measurement of the present investigation is in good agreement with the measurements of Phragmén (1923) and Borén (1933).

† Owing to the experimental arrangement the $K\alpha_2$ component of the reflection (10.0.0) was coincident with the $K\alpha_1$ components of the reflections (10.1.0) and (10.$\bar{1}$.0) on one exposure and the $K\alpha_1$ components of the reflections (1.10.0) and ($\bar{1}$.10.0) on another exposure. The well-known intensity ratio of the $K\alpha_1$ to the $K\alpha_2$ line, 2 : 1, was used to make the intensity comparisons involving these coincidences shown in Fig. 1.

exp $[0{\cdot}5\{(\sin\theta)/\lambda\}^2]$ was applied to calculated structure-factor values.

Table 1. *Intensities of X-ray reflections on oscillation photographs of* FeSi

(*hkl*)	Obs.	Calc.	(*hkl*)	Obs.	Calc.	(*hkl*)	Obs.	Calc.
110	11	9·5	710	<3·0	3·1	490	3·1	2·5
020	8·8	11	550	4·5	4·6	940	Abs.	1·6
120	13	12	460	7·0	6·6	770	<3·0	2·4
210	26	33	640	6·8	6·6	680	<3·0	1·8
220	2·5	2·7	270	Abs.	0·2	860	<3·0	1·8
130	5·6	4·7	720	5·6	5·9	0.10.0	6·8	5·6
310	5·9	6·9	370	3·3	4·1	1.10.0	3·7	3·1
230	14	13	730	4·2	4·4	10.1.0	3·0	2·2
320	8·4	7·0	560	9·1	9·0	2.10.0	Abs.	1·2
040	25	25	650			10.2.0	Abs.	1·2
140	Abs.	0·6	080	7·2	6·4	590	<3·0	2·0
410	8·5	10	180	Abs.	1·2	3.10.0	4·1	4·0
330	7·4	6·3	810	6·3	6·4	10.3.0	Abs.	1·8
240	4·6	5·1	470	Abs.	0·9	780	Abs.	1·2
420	4·8	5·1	740	Abs.	0·6	870	Abs.	0·4
340	<1·9	2·3	280	Abs.	0·8	4.10.0	4·9	4·3
430	3·8	3·4	820	Abs.	0·8	10.4.0	4·5	4·3
150	5·9	6·2	660	4·4	4·2	690	6·1	4·5
510	3·9	4·3	380	Abs.	0·7	960	Abs.	1·0
250	18	19	830	<3·0	2·7	1.11.0	3·5	3·4
520	6·5	7·2	570	4·5	4·4	11.1.0	Abs.	0·7
440	16	15	750	Abs.	0·3	2.11.0	Abs.	1·6
350	2·7	3·0	480	5·9	5·2	11.2.0	6·0	4·3
530	3·3	3·2	840	5·7	5·2	5.10.0	Abs.	1·1
060	11	11	190	<3·0	2·4	10.5.0	2·8	2·3
160	5·6	5·8	910	3·1	3·7	880	4·0	2·9
610	8·9	9·9	670	Abs.	1·1	790	Abs.	0·6
260	2·4	2·9	760	6·2	5·2	970	4·5	3·6
620	2·6	2·9	290	8·2	7·7	3.11.0	2·3	2·3
450	7·5	6·9	920	<3·0	2·7	11.3.0	Abs.	1·3
540	<3·0	2·3	580	<3·0	2·0	6.10.0	2·8	2·3
360	5·8	6·3	850	5·8	5·5	4.11.0	Abs.	1·1
630	4·9	5·3	390	Abs.	0·7	11.4.0	Abs.	1·1
170	4·4	4·2	930	4·4	4·2			

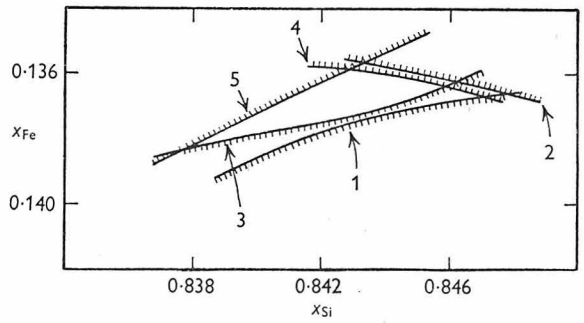

Fig. 1. Determination of parameters.

Curve	Comparison
1	$2F^2_{10,0,0} < 4F^2_{1,10,0} + F^2_{10,0,0}$
2	$2F^2_{10,0,0} > 4F^2_{10,1,0} + F^2_{10,0,0}$
3	$\|F\|_{920} > \|F\|_{830}$
4	$\|F\|_{850} > \|F\|_{840}$
5	$\|F\|_{4,10,0} > \|F\|_{3,10,0}$

Structure factors calculated with $x_{Fe}=0{\cdot}1370$ and $x_{Si}=0{\cdot}8420$ show good agreement with those calculated from the observed intensities (Table 1). Intensity comparisons between reflections having nearly identical angle-dependent factors and observed on the same side of a given film were used to establish the limits of error shown graphically in Fig. 1.† Presumably reliable

values of x_{Fe} and x_{Si} are $0{\cdot}1370 \pm 0{\cdot}0020$ and $0{\cdot}842 \pm 0{\cdot}004$, respectively. These are in essential agreement with those of Wever & Moeller (1930) and of Borén (1933).

Discussion of the structure

The interatomic distances

The ligands of each iron atom in FeSi are seven silicon atoms at distances 2·29 A. (1), 2·34 A. (3) and 2·52 A. (3), and six iron atoms at 2·75 A., these distances being reliable to about 0·01 A. The corresponding bond numbers, calculated with the assumption of the normal single-bond radii 1·165 A. for iron and 1·173 A. for silicon (Pauling, 1947), are 1·21, 1·00, 0·50 and 0·20, respectively; the sum of these values for the bonds formed by an iron atom is 6·91, which differs significantly from the expected value 5·78. Each silicon atom is surrounded by seven iron atoms at 2·29 A. (1), 2·34 A. (3) and 2·52 A. (3), and six silicon atoms at 2·78 A., the corresponding bond numbers being 1·21, 1·00, 0·50 and 0·19, and the calculated valence of silicon 6·85, which is very much greater than the normal value 4.

Let us now consider the electronic structure that would be expected for the iron silicide crystal according to the resonating-valence-bond theory of metals (Pauling, 1948). According to this theory, silicon, with only four stable orbitals in its outer shell, could not form more than four electron-pair bonds, which might, however, resonate among more than four positions. In order for metallic resonance of the valence bonds to occur, some of the atoms must possess an extra orbital, the metallic orbital; it is not necessary, however, that the silicon atom itself possess a metallic orbital, inasmuch as its four bonds might undergo pivoting resonance about it, if the surrounding atoms possess the metallic orbital. Moreover, it is to be expected that the resonance of the four bonds of the silicon atom would be of such a nature as to lead to the assignment to the interatomic positions of bond numbers equal to simple fractions, such as $\frac{1}{2}$, $\frac{1}{3}$, $\frac{2}{3}$, ... We note that the observed interatomic distances 2·34 A. (for three bonds) and 2·52 A. (for three) differ by just 0·18 A., which corresponds to a factor $\frac{1}{2}$ in bond number, and that the remaining bond distance, 2·29 A., is slightly smaller (0·05 A.) than the smaller of the other two, suggesting that its bond number is slightly greater. These distances hence suggest that the corresponding bond numbers are 1, $\frac{2}{3}$, and $\frac{1}{3}$, their sum thus being equal to the normal valence 4 for silicon. We assume, as has been found necessary for other crystals also, that the valence of the silicon atom is concentrated entirely into the bonds with its nearest neighbors, and that the six silicon neighbors at 2·78 A. are not bonded by the silicon atoms, the bond number 0·19 given by equation (1) being illusory.

The silicon atom is thus to be described as using one

of its four tetrahedral sp^3 bond orbitals in forming an essentially non-resonating single bond with one iron atom, at 2·29 A.; the other three orbitals resonate between the three iron atoms at 2·34 A., and the three at 2·52 A., the latter set being the less favored, by the factor $\frac{1}{2}$, presumably because of their less satisfactory relation to the tetrahedral directions (the angle with the non-resonating bond being 40° less than the tetrahedral angle, as compared with 26° more for the former set).

When the two longer distances are corrected by 0·11 and 0·29 A. for bond numbers $\frac{2}{3}$ and $\frac{1}{3}$, respectively, and the single-bond radius of silicon is also subtracted, there are obtained the values 1·12, 1·06 and 1·06 A., respectively, for the single-bond radius of iron. Moreover, we expect that the iron atom has the valence 6 (rather than the valence 5·78 found in elementary iron), for reasons described below; of this valence four units are used in bonds with silicon, leaving two valences to be divided among the six iron–iron bonds. The iron–iron distance 2·75 A., when corrected by the amount 0·29 A. corresponding to bond number $\frac{1}{3}$, leads to 1·23 A. for the single-bond radius of iron. These four values show striking deviation from the single-bond radius 1·165 A. found for elementary iron (Pauling, 1947).

However, it is known (Pauling, 1948) that elementary iron represents a resonance average between two valence forms of iron. In one of these, Fe_A, two of the eight outer electrons of the atom are atomic electrons, contributing to the ferromagnetic moment, and the other six are valence electrons. Of the nine stable outer orbitals of the iron atom, two are used for the atomic orbitals, and the remaining seven, d^3sp^3, are for the six valence bonds and the metallic orbital. The metallic orbital accordingly has $\frac{3}{7}$ or 42·9 % d character, on the assumption that the hybrid character of the metallic orbital is the same as that of the bonding orbital. The other kind of iron atoms, Fe_B, contains three atomic electrons in three of the d orbitals, the other six orbitals (d^2sp^3) constituting five bonding orbitals and the metallic orbital. These six orbitals have 33·3 % d character. The ferromagnetic saturation moment, 2·22 magnetons, shows that the structures A and B contribute 78 and 22 %, respectively, to elementary iron, the average amount of d character thus being 39·7 %. The corresponding single-bond radius is 1·165 A. The single-bond radius for sp^3 bonds, with no d character, is found by linear extrapolation (Pauling, 1947) to be 1·481 A. On the assumption (Pauling, 1947, 1948) that there is a linear relation between the single-bond radius formed by a hybrid orbital and the amount of d character, there can be derived the equation

$$R_1(\mathrm{Fe}) = 1{\cdot}481 - 0{\cdot}797\,\delta, \qquad (2)$$

where the symbol δ means the fractional amount of d character in the bond orbital. This leads, for example, to the value 1·138 A. for the single-bond radius of the d^3sp^3 bonds formed by Fe_A, which is sexivalent.

We may now use equation (2) in interpreting the

values 1·12, 1·06, 1·06, and 1·23 A. found for the single-bond radius of iron for the different kinds of bonds formed in the FeSi crystal. Application of equation (2) leads to the values 45, 53, and 31 % d character, respectively, for these bonds. Since there are altogether three d orbitals available for use in the six bond orbitals and the metallic orbital, the difference between 3 and the summed amount of d character for the bond orbitals is the d character of the metallic orbital. This difference is found to be 34 %, an entirely reasonable value.

The state of the iron atom in FeSi may thus be described in the following way. The iron atom is sexivalent iron, Fe_4. It uses four of its orbitals in forming bonds with the seven surrounding silicon atoms—one single bond, three $\frac{2}{3}$ bonds, and three $\frac{1}{3}$ bonds—and two of the remaining orbitals, and the corresponding valence electrons, in forming six $\frac{1}{3}$ bonds with six neighboring iron atoms. The orbitals involved in the bonds with silicon are different in hybrid character from those involved in the bonds with iron; they have between 45 and 53 % of d character, whereas the bonds with iron have only 31 % d character. The metallic orbital has essentially the same hybrid character, 34 % d, as the bond orbital with the smallest d character.

It is interesting to note that the four iron–silicon bond orbitals make use of just two of the three available d orbitals, the third being used by the two bond orbitals involved in iron–iron bonds and the metallic orbitals. Moreover, the distribution of the d orbitals among the orbitals of each class is essentially uniform; the four orbitals involved in bonds with silicon have approximately one-half d character, and the two orbitals involved in iron–iron bonds and the metallic orbital have approximately one-third d character. If it is assumed that the amounts of d character for these classes of orbitals are precisely $\frac{1}{2}$ and $\frac{1}{3}$, respectively, the bond numbers calculated for the four kinds of bonds become 0·85, 0·70, 0·35 and 0·33, respectively, adding up to the valence 6. It is not clear whether the treatment of the distances in which the bond numbers are supposed to be simple (1, $\frac{2}{3}$, $\frac{1}{3}$) or the slightly different treatment in which the amounts of d character are supposed to be simple ($\frac{1}{2}$, $\frac{1}{3}$) is to be preferred.

It has hence been found that the interatomic distances in FeSi are compatible with those in metallic iron and elementary silicon, with the principal difference that the iron atom in FeSi is sexivalent iron, rather than iron with the average valence 5·78, and the effective radius of iron for the different non-equivalent bonds that have formed in FeSi is different because of a difference in the amount of d character. These values of the iron radius are, however, related to that shown in elementary iron, and may be derived from it.

The compounds CrSi, MnSi, CoSi and NiSi were found by Borén (1933) to have the same structure as FeSi, and he reported values for a_0 and for the two atomic parameters differing very little from those for FeSi. The corresponding bond distances are given in

Table 2, together with the single-bond radii of the metallic atoms calculated from them with the same assumption about bond numbers as made above for FeSi. The values for the amount of d character (δ) are also given, as calculated by the following equation (Pauling, 1948):

$$R_1(\delta, z) = 1{\cdot}825 - 0{\cdot}043\,z - (1{\cdot}600 - 0{\cdot}100\,z)\,\delta. \quad (3)$$

Here z is the atomic number minus 18. It is seen that the amounts of d character lie in the neighborhood of 50 % for the bonds between the metal atom and silicon, and of 30 % for the metal–metal bonds. The values found for the d character of the metallic orbital show rather wide fluctuations, which presumably have little significance. (The magnetic data reported for MnSi, FeSi, and CoSi (Foëx, 1938) are difficult to interpret because of lack of correspondence with the Weiss-Curie equation, and hence are not useful in this case as a criterion of electronic structure.)

Table 2. *Bond distances and bond character in* FeSi *and related crystals*

(All distances in A.)

	M–Si			*M*–*M*	
	1 bond $n=1$	3 bonds $n=\frac{2}{3}$	3 bonds $n=\frac{1}{3}$	6 bonds $n=\frac{1}{3}$	Metallic orbital
			CrSi ($a_0=4{\cdot}620$)		
Bond distance	2·32	2·43	2·58	2·83	
$R(1)$	1·15	1·15	1·12	1·27	
% d character	42	42	45	30	69
			MnSi ($a_0=4{\cdot}548$)		
Bond distance	2·30	2·39	2·55	2·79	
$R(1)$	1·13	1·11	1·09	1·25	
% d character	43	46	48	30	57
			FeSi ($a_0=4{\cdot}489$)		
Bond distance	2·29	2·34	2·52	2·75	
$R(1)$	1·12	1·06	1·06	1·23	
% d character	45	53	53	31	34
			CoSi ($a_0=4{\cdot}438$)		
Bond distance	2·28	2·33	2·47	2·73	
$R(1)$	1·11	1·05	1·01	1·22	
% d character	47	56	61	31	18
			NiSi ($a_0=4{\cdot}437$)		
Bond distance	2·28	2·33	2·47	2·73	
$R(1)$	1·11	1·05	1·01	1·22	
% d character	47	57	64	29	17

The choice of the FeSi *structure*

Some general considerations about the selection of the FeSi structure by iron silicide and related substances may now be formulated. It is clear that the sodium chloride structure would not be a satisfactory one—in this structure an atom has as its neighbors only six atoms of the other kind, all more distant neighbors being so far removed as not to permit the formation of a significant bond with them; the effective valences of the two kinds of atoms are hence the same, and the structure is accordingly an unsuitable one for two elements with such different valences as 4 and 6. On the other hand, the nickel arsenide structure, with

small axial ratio, such as shown by AuSn (Pauling, 1947), might be assumed by FeSi. The axial ratio could adjust itself in such a way that the silicon atom would use its valence of 4 in forming four bonds with the surrounding six iron atoms, and the iron atom would use its extra valence 2 in forming two iron–iron single bonds, one with each of the iron atoms above and below it along the *c* axis. Similarly, the cesium chloride structure might be assumed by FeSi, each silicon atom then forming eight half-bonds with the iron atoms surrounding it in a cubic arrangement, and each iron atom forming eight half-bonds with silicon atoms, and six one-third bonds with the six adjacent iron atoms. It seems not unlikely that co-ordination number 6 (bond number $\frac{2}{3}$) is more suitable for silicon in an intermetallic compound than co-ordination number 8* (bond number $\frac{1}{2}$), and that, moreover, resonating iron–iron bonds, with bond number $\frac{1}{3}$, are more stable than non-resonating bonds, with bond number 1. The actual FeSi structure would thus be preferred to the cesium chloride structure for the first reason, and to the nickel arsenide structure for the second reason.

* A substance in which the four bonds of the silicon atom show pivoting resonance among eight positions is Mg_2Si, with the fluorite structure (Pauling, 1948).

We are grateful to Prof. J. H. Sturdivant for assistance with the experimental part of this investigation. The work reported in this paper is part of a series of studies of metals and alloys being carried on with the aid of a grant from the Carbide and Carbon Chemicals Corporation.

References

BORÉN, B. (1933). *Ark. Kemi Min. Geol.* **11** A, 1.
FOËX, G. (1938). *J. Phys. Radium*, **9**, 37.
HUGHES, E. W. (1941). *J. Amer. Chem. Soc.* **63**, 1737.
Internationale Tabellen zur Bestimmung von Kristallstrukturen (1935). Berlin: Borntraeger.
LANDOLT, H. & BÖRNSTEIN, R. (1931). *Physikalisch-chemische Tabellen*. Berlin: Springer.
PAULING, L. (1938). *Phys. Rev.* **54**, 899.
PAULING, L. (1947). *J. Amer. Chem. Soc.* **69**, 542.
PAULING, L. (1948). *Nature, Lond.*, **161**, 1019.
PAULING, L. & SHERMAN, J. (1932). *Z. Krystallogr.* **81**, 1.
PHRAGMÉN, G. (1923). *Jernkontor. Ann.* **107**, 121.
WEVER, F. & MOELLER, H. (1930). *Z. Krystallogr.* **75**, 362.

I. THE CRYSTAL STRUCTURES OF CERTAIN INTERMETALLIC COMPOUNDS

(b) A Study of the Structures of the Intermetallic Compounds Mg_2Tl, Mg_2In, and Mg_2Ga

A Study of the Structures of the Intermetallic Compounds Mg_2Tl, Mg_2In, and Mg_2Ga.

Introduction

The metallic elements gallium, indium, and thallium are members of the ascending branches of the first, second, and third long periods of the periodic table in the sense first discussed by Pauling[1]. Elements of the ascending branches typically show a variety of valences in the formation of intermetallic compounds and it has been shown theoretically that the three elements of Group III B can exhibit valences ranging from five downwards, although the elementary valences for gallium, indium, and thallium are $3\frac{1}{2}$, $2\frac{1}{2}$, and 2 respectively[1], [2]. Intermetallic structures involving valences differing from the elementary values are generally of interest, and the present investigation was undertaken with the expectation that the phases Mg_2Tl, Mg_2In, and Mg_2Ga[3] would have structures in which such differences in valence are exhibited. This expectation is made reasonable by the existence of a number of intermetallic compounds of different stoichiometric proportions in each of the binary systems of magnesium with thallium, indium, or gallium. In the magnesium-thallium system the phases Mg_5Tl_2, Mg_2Tl, and MgTl have been reported, all with narrow regions of homogeneity[4]; in the magnesium-indium system phases of composition Mg_5In_2, Mg_2In, MgIn, and $MgIn_2$ were found in X-ray studies, although the explicit details of the phase diagrams have not been worked out; and

in the magnesium-gallium system the phase diagram indicates the existence of the intermetallic compounds Mg_5Ga_2, Mg_2Ga, MgGa, and $MgGa_2$[5], in agreement with an X-ray investigation of the system[6]. The structures of MgTl, $MgIn_2$, and MgIn are known[3],[7]; no structural determinations have been made for the other compounds.

It has been reported that the structures of Mg_5Ga_2, Mg_5In_2, and Mg_5Tl_2 are similar and are based on an orthorhombic unit cell containing 28 atoms (Z = 4)[3]. In addition a common structure based on a hexagonal unit cell with 18 atoms (Z = 6) was implied for the compounds Mg_2Ga, Mg_2In, and Mg_2Tl. The hexagonal structure seemed the simpler of the two, a priori, and thus a structural study of the three intermetallic compounds Mg_2Ga, Mg_2In, and Mg_2Tl was undertaken.

General Experimental Details

(a) Preparation of Compounds

Use of the following method was found to effect easy and rather accurate syntheses from the elementary substances. A molten mixture of KCl and LiCl (11:9 by weight) was added to an alundum extraction thimble and then heated to incipient red heat, about 450° C. A calculated amount of heavy metal was then added and the molten mass was again brought to about 450° C. Next, the specimen of magnesium was added to the melt, and the mixture was stirred vigorously for ten minutes with a clay rod and allowed to cool to room temperature. Heating was accomplished with an oxygen-gas flame from a hand torch clamped into position under the alundum

thimble. Changes in composition due to heating losses during the course of the X-ray powder photography were estimated to be small. In view of previous reports concerning the existence of the compounds and the verification found here for the essential results of the X-ray studies of them[3], [7], no attempt was made to check the composition by means of chemical analyses.

(b) Preparation of Specimens and Powder Photography

The intermetallic compounds prepared, especially Mg_2Tl, were found to corrode when left unprotected from the atmosphere. The preparation of specimens suitable for X-ray powder photography was therefore carried out in a dry box under a carbon dioxide or argon atmosphere. Filings from clean surfaces of the melts were sieved with a 200 mesh screen and the resulting powder was loaded into thin-walled pyrex capillaries. The open end of each capillary was then capped with vaseline in order to secure temporary protection from the atmosphere upon removal from the dry box. After removal each capillary was quickly sealed off with an oxygen-gas flame. The breadth of the high angle lines in X-ray photographs of specimens prepared in this manner revealed the presence of lattice distortions; annealing of the specimens for short periods at low temperatures effected a satisfactory sharpening of the high-angle reflections. In the cases of Mg_2Tl and Mg_2In an annealing period of one hour at 100° C was found sufficient. A somewhat higher temperature was apparently necessary for the Mg_2Ga specimens, one hour at 200° C being

effective. The annealed specimens always appeared clean and free of oxides upon microscopic examination, and no X-ray evidence was found for impurities other than those resulting from the presence of other intermetallic compounds in the system concerned, such as MgTl, MgIn, etc.

Powder photographs were prepared with copper radiation filtered through nickel. The cylindrical camera generally used had a radius of 5 cm., and a system of 0.6 mm. slits was used to define the incident beam. After the present investigation was well under way, the laboratory acquired a 57 mm. camera employing the Straumanis mounting. Several powder photographs were taken with the use of this equipment.

The Structural Determination of Mg_2Tl

The reflections which appeared on powder photographs of the compound Mg_2Tl and which were not due to the presence of small amounts of MgTl or Mg_5Tl_2 were successfully indexed on the basis of a hexagonal unit cell of approximate dimensions $a_o = 8.04$ Å, $c_o = 3.64$ Å*. This cell is half as large as

---

*The powder photographs of annealed specimens prepared from a melt of calculated composition Mg_2Tl contained a few reflections of low intensity which could be indexed on the basis of the cubic unit cell of MgTl. With the addition of a small amount of magnesium to the melt and subsequent powder photography, these lines disappeared, and a small number of faint reflections in other positions appeared which presumably due to the presence of a small amount of Mg_5Tl_2. In this way the lines which were those of Mg_2Tl could be identified with certainty.

that proposed by Haucke[3], the value for c_o being approximately one-half his reported value for Mg_2Ga. The smaller cell was accepted on a tentative basis and was confirmed in subsequent experiments. A density determination with the use of the displacement technique gave the value 2.75~3 for the number of molecules of Mg_2Tl in the unit cell*.

It was noticed at once that reflections of the type hk·2n were faint or absent when $h-k \neq 3m$, but were generally strong when $h - k = 3m$. This suggested the approximate positions 000, 1/3 2/3 1/2, 2/3 1/3 1/2 for the three thallium atoms, from the following argument. In a hexagonal lattice it is always possible to use a triply primitive hexagonal cell with a volume three times that of the smallest

---

*The low value for this number is reasonable in view of the extreme reactivity of the substance and the resulting tendency to measure a displacement volume which is too high. Thiophene-free benzene of high purity was used as the liquid and was dried by refluxing over P_2O_5 for several hours with a subsequent distillation. Even after this precaution was taken to ensure an inert liquid, bubbles of gas were slowly evolved upon contact with the specimen. It was, of course, considered futile to attempt the removal of occluded gases by boiling.

During the determination the specimen was never directly in contact with the atmosphere, but was in contact with CO_2 when not immersed in the purified benzene. All necessary transferences were made in a dry box under CO_2. The surface of the specimen used was scraped free of oxide initially.

hexagonal cell. The $\underline{A}$ axes of the large cell are inclined at 30° to corresponding $\underline{a}$ axes of the smallest hexagonal cell and lattice translations of $n \cdot \frac{\underset{\sim}{A}_1 - \underset{\sim}{A}_2}{3}$, n = 0, 1, 2,... exist which lead to the extinction of reflections of the type H - K ≠ 3m. Since Mg_2Tl reflections of the type hk·0, h - k ≠ 3m are weak or absent and reflections of the type hk·0, h - k = 3m are strong, the projections of the thallium atoms on the base of a suitably chosen primitive hexagonal cell are indicated to be at the positions 00, 1/3 2/3, 2/3 1/3 (the vectors from the origin to the positions are 0, 1, $2 \cdot \frac{\underset{\sim}{a}_1 - \underset{\sim}{a}_2}{3}$, respectively). The absence or weakness of reflections of the type hk·2n, h - k ≠ 3m indicates that one or two of the atoms lie approximately on the horizontal plane halfway along the vertical cell edge ($z = \frac{1}{2}$). The choice of one or two of the atoms in any combination to be placed in this plane is arbitrary; there is only one resulting vector diagram. One convenient choice has been indicated, with the three thallium atoms at 000; 1/3 2/3 1/2; 2/3 1/3 1/2; another convenient choice is 0 0 1/2; 1/3 2/3 0; 2/3 1/3 0.

The general intensity relationships among the remaining reflections observed for which ℓ is odd were satisfied by the proposed arrangement for the thallium atoms. It was considered probable that the proposed positions were exactly correct, and the chance of determining the magnesium positions was considered promising. A diagram of the spatial arrangement of the thallium atoms with the use of the radius observed in

the elementary substance indicated that the large vacancies in the structure were centered about the positions $x_1\ 0\ 0$, $0\ x_1 0$, $\bar{x}_1\bar{x}_1 0$; $\bar{x}_2 0\ \frac{1}{2}$, $0\ \bar{x}_2\frac{1}{2}$, $x_2 x_2\frac{1}{2}$ where $x_1, x_2 > 0$. From considerations of symmetry it seemed reasonable that these are the true positions of the magnesium atoms; if the radius of elementary magnesium is used, there are no steric hindrances for suitable values of x_1 and x_2. The completed arrangement is based upon the space group D_{3h}^3 - $C\bar{6}2m$. Preliminary calculations were made to see if the values of x_1 and x_2 could be determined from the powder photographic data, but it was immediately apparent that it is impossible to do so. Reflections of the type for which the scattering contributions of the thallium atoms cancel according to the proposed arrangement were observed in one instance only, and the thallium contributions were so large in the remaining cases that the scattering contributions of the magnesium atoms could be changed appreciably without determinable changes in intensities. It became apparent that, if the structure of Mg_2Tl were to be determined in the present investigation, it would be necessary to obtain additional information from single-crystal X-ray photography.

It was obvious that certain rather formidable difficulties would have to be overcome in the preparation of suitable single crystals of the substance. The substance was very reactive and would have to be protected from the atmosphere at all times. The substance was soft and it would not be possible to pulverize a melt to small particles which were

single crystals. Since the adjoining phases Mg_5Tl_2 and MgTl were so close in composition to that of Mg_2Tl, a successful chemical separation of single crystals grown from a two-phase melt was considered unlikely. Accordingly, the following technique was first tried. A melt of calculated composition Mg_2Tl was prepared in the usual way with a KCl - LiCl flux in an alundum crucible. While the mass was molten, at a temperature of about 450° C, a clay tube with a 0.5 mm. bore was lowered into the crucible and a cylindrical casting was formed by sucking up Mg_2Tl in the liquid state with a vacuum pump which was attached to the upper end of the clay tube. Cooling took place immediately and the tube was quickly and carefully demolished under a binocular microscope with a razor blade and ordinary dissecting instruments. The casting thus obtained was immersed in a protective layer of vaseline-ligroin solution--- initially some gas evolution was noted which soon ceased without visible corrosion of the specimen. In this manner specimens were prepared which consisted of clumps of acicular crystals; the long axes of the needles were misaligned by a few degress in each clump. The problem of isolating a single individual from such an aggregate seemed difficult, and an attempt was made to grow crystals by a slower cooling process. Crystals were grown in a two-phase melt by slow cooling in a Swedish iron crucible under a protective atmosphere of argon. Upon cooling the crystals were again clumped together and grew

on the surface of the molten mixture. One promising specimen was removed from the solid mass by a systematic procedure of excavation in which selected regions of the surrounding matrix were exposed to moisture and the resulting products of the reaction were removed with a dissecting needle. At the conclusion of the procedure the specimen removed was found to consist of the usual clump of aciculae; it was therefore decided to attempt the isolation of one individual from such a clump without further expenditure of time and effort in trying to grow individuals. A specimen was selected which was indicated by means of Laue photography to be nearly a single individual on one side and over a reasonable length. The specimen, always under a coating of vaseline-ligroin solution, was fastened to a thin Pyrex fiber by dried shellac using the hot-wire technique. One side of the specimen was systematically dissolved with 20% nitric acid, and the course of the isolation was followed and directed with Laue photography. The apparatus used in the controlled dissolution was designed to accomplish the grinding of small crystals to cylindrical form; it was modified here by replacing the abrasive surface of the grinding wheel with hardened filter paper which served as a very gentle rubbing surface which could bring the surface of the metal into contact with absorbed acid solution.

At the conclusion of the procedure the original specimen was shaped at one end to a cylinder 0.1 mm. in diameter and 0.5 mm. long. The cylinder was almost a single individual with its long axis nearly parallel to the c axis of the

crystal. The specimen was then washed repeatedly with vaseline-ligroin solution and, after a day, a coating of material formed from the reaction of the remaining acid was removed by gentle abrasion with a dry surface. The specimen was then removed from the Pyrex rod and sealed in a thin-walled Pyrex capillary. It was held rigidly in position by a small shellac joining between the inner surface of the capillary and the untreated end of the specimen. All photographs of the crystal were taken with the c axis vertical. Orientation of the crystal was accomplished with Laue photography. During photography the specimen was always in such a position that the incident beam of radiation did not pass through the untreated part of the specimen.

In Figure 1_a and 1_b prints are shown of two Laue photographs taken for two symmetrical settings of the crystal. The c axis is vertical in both cases; in Figure 1_a the incident beam is parallel to one of the a axes and in Figure 1_b the specimen has been rotated 30° about the c axis from this position. Although considerable differences in the spot shapes are caused by absorption effects and the presence of other individuals on one side of the specimen, it can be seen in both figures that the local intensity relationships around each spot indicate two perpendicular mirror planes, one vertical, the other horizontal. This indicates that the Laue point group of the crystal is $D_{6h} - \frac{6}{m}mm$. As a check to this conclusion, symmetrical Laue photographs were prepared with a specimen which consisted of a clumped aggregate with a very

Figure 1_a

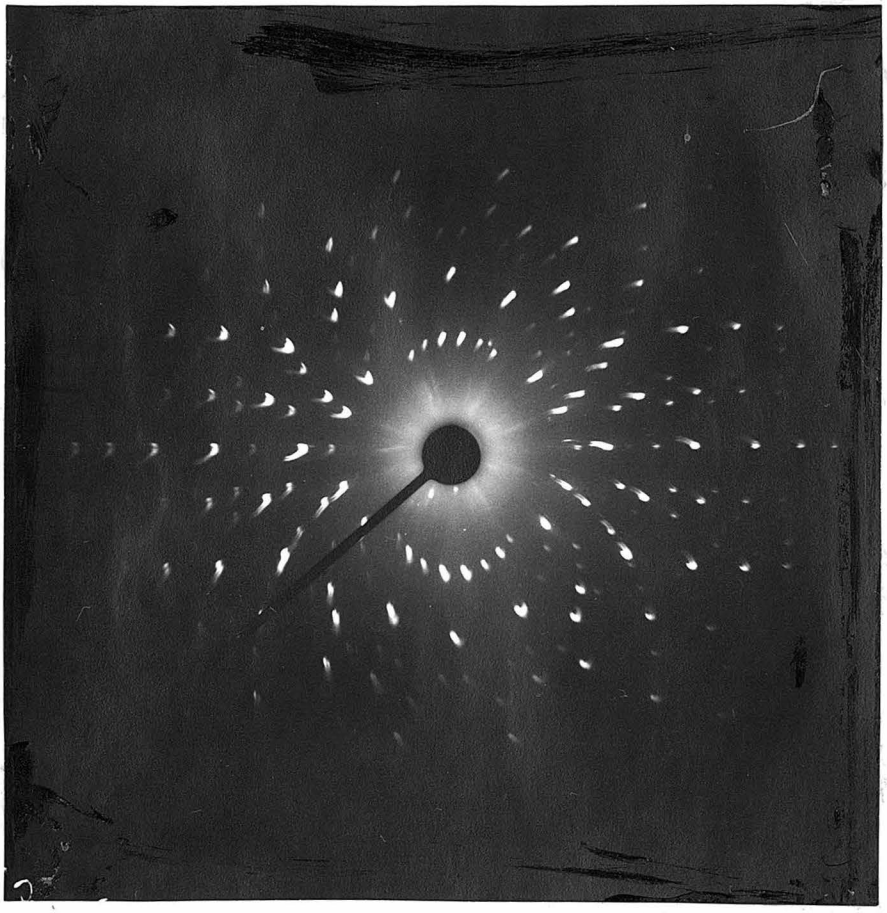

$\underset{\sim}{c}$ vertical

$\underset{\sim}{s}_o \parallel \underset{\sim}{a}$

Figure 1_b

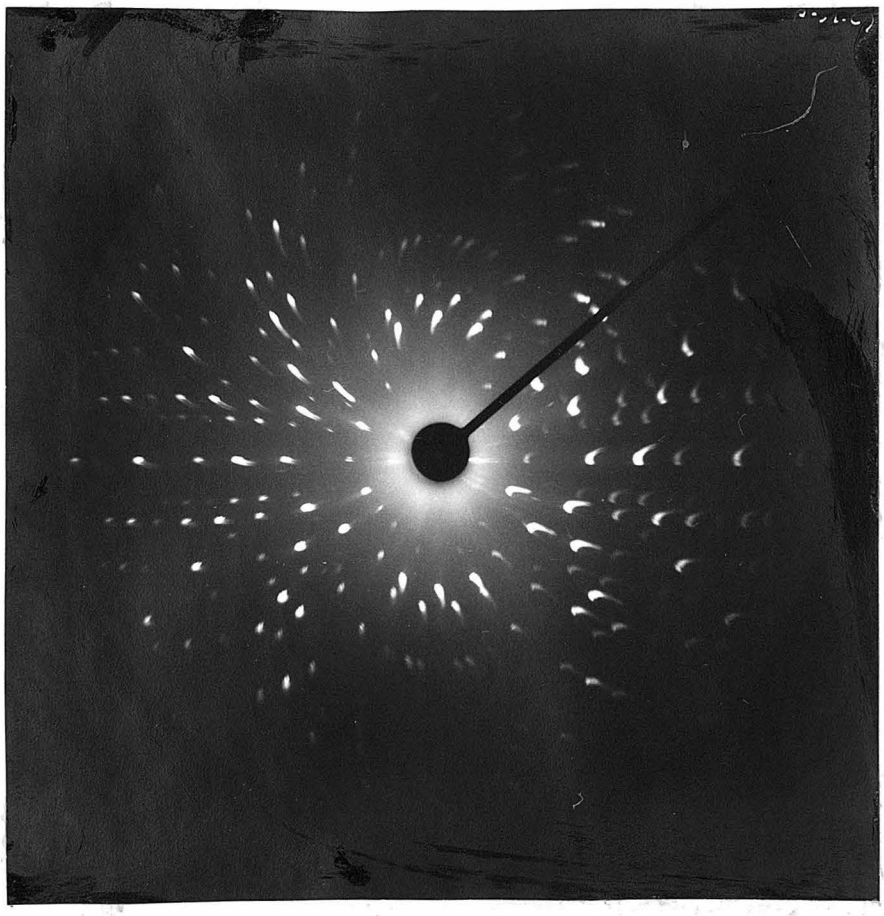

$\underset{\sim}{c}$ vertical

$\angle (\underset{\sim}{s}_o, \underset{\sim}{a}) = 30^\circ$

small single crystal tip. The incident beam touched only the tip and extremely long exposures were necessary. The photographs are reproduced in Figures 2_a and 2_b. The settings correspond to those of Figures 1_a and 1_b. Although the background is high and reproduction of the photographs difficult, it is evident that the symmetry found in the preceding photographs is confirmed.

Additional Laue photographs of the cylindrical specimen were prepared with the incident beam inclined at small angles to $\underset{\sim}{a}$. The positions of the reflections of only one side of the photographs could be accurately determined in gnomonic projections; the sides projected correspond to the left side of the reproductions of Figure 1. No reflections were found which required the assumption of a unit cell larger than the one proposed from the powder photographic data. The first order reflections observed in the symmetrical photographs are listed in Tables 1 and 2.

In the application of the Laue photographic data to the determination of structure, it is safe to assume first that the unit cell and Laue point group found holds at least for the positions of the thallium atoms; it is conceivable that the positions of the magnesium atoms permit neither the unit cell nor the Laue symmetry found, but that the contributions to scattering from these atoms are negligible with respect to the contributions from the thallium atoms. The correctness of the positions proposed for the thallium atoms are tested by an examination of the ways in which three atoms, either crystallographically equivalent or not, in any combination, could be

Figure 2_a

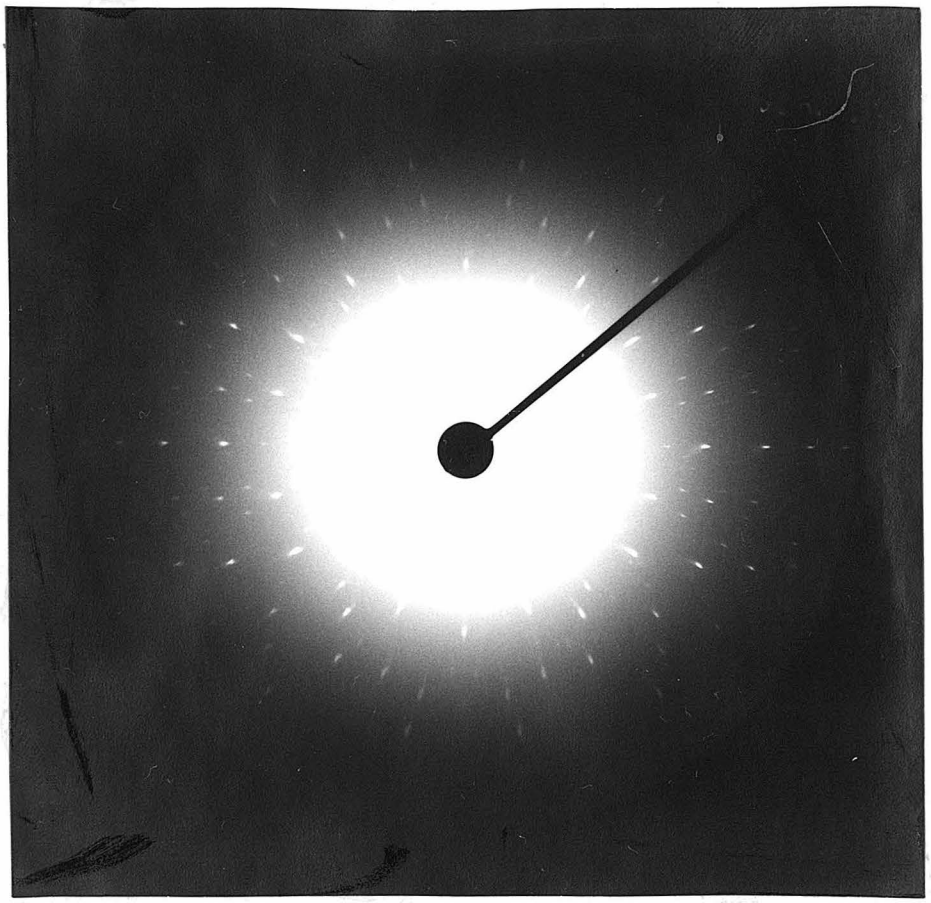

$\underset{\sim}{c}$ vertical

$\underset{\sim}{s}_o \parallel a$

Figure 2_b

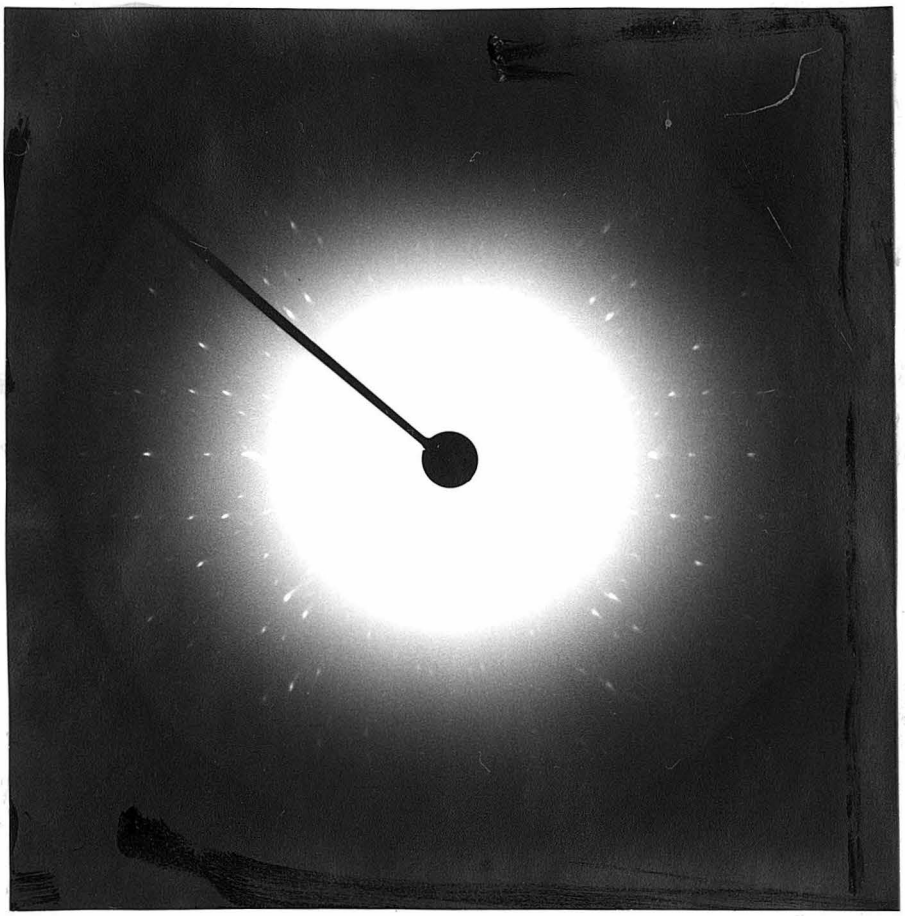

$\underset{\sim}{c}$ vertical

$\angle\ (\underset{\sim}{s}_o, \underset{\sim}{a}) = 30^\circ$

placed in a unit cell based upon a space group of the Laue point group D_{6h}. Thus all space groups were examined belonging to the point groups $D_{6h} - \frac{6}{m}mm$, $D_6 - 62$, $C_{6v} - 6mm$, and $D_{3h} - \bar{6}2m$. The only possible arrangement which does not lead to gross disagreement with the intensities of the reflections observed in the powder photographs is the one previously proposed, thallium atoms at 0 0 0; $\frac{1}{3}\ \frac{2}{3}$ z; $\frac{2}{3}\ \frac{1}{3}$ z with the value of z close to $\frac{1}{2}$. The intensity relationships between the reflections of the Laue photographs show that it is very unlikely that z differs from $\frac{1}{2}$ by as much as 0.05. This statement is derived from the following argument. If z is $\frac{1}{2}$, the geometrical structure factor formulae for the thallium positions are

$\ell = 2n$, $n = 0, 1, 2, \ldots$

$S = 3$, $h - k = 3m$, $m = 0, 1, 2, \ldots$

$S = 0$, $h - k \neq 3m$

$\ell = 2n + 1$

$S = -1$, $h - k = 3m$

$S = 2$, $h - k \neq 3m$

On the other hand, if z differs from $\frac{1}{2}$ by 0.05 and

$\ell = 5$

$S = \pm 2i$, $h - k = 3m$

$S = 1 \pm i$, $h - k \neq 3m$.

In a few instances the intensity of a reflection of the type hk·5, h - k = 3n could be compared to that of a reflection

of the type hk·5, h - k ≠ 3n. In every case the observed intensity of the reflection of the first type is much smaller than that of the reflection of the second type. This would be expected if z is precisely $\frac{1}{2}$; on the other hand if z differs from $\frac{1}{2}$ by as much as 0.05, it would be predicted that the reverse of the observed relationship should hold. Furthermore, only four very faint reflections of the type hk·5, h - k = 3n were observed to twenty-one of the type hk·5, h - k ≠ 3n, which were generally of moderate intensity. There are approximately one-half as many reflections of the first type as of the second type (in a given sphere of reflection) and the much greater preponderance of reflections of the second type would be unexpected, if the thallium contributions to reflections of the first type were greater than those to reflections of the second type to the extent indicated for z = $\frac{1}{2}$ ±0.05.

The positions of the thallium atoms having been fixed with some degree of accuracy, it is now profitable to discuss the possibility that the size of the unit cell found is not correct with respect to the positions of the magnesium atoms. It can be noted from Tables 1 and 2 that a few reflections of the type hk·0, h - k ≠ 3n are observed. There is no doubt that the contributions made to the intensities of these reflections by the scattering of the thallium atoms exactly cancel one another, and that the intensities of the reflections are due only to scattering by magnesium atoms. Since it is possible to observe reflections which depend on magnesium scattering alone, it is reasonable to expect that,

if the true unit cell were larger than the one proposed, some evidence should be found to this effect from the Laue photographs. It was, therefore, considered safe to proceed with the assumption that the unit cell found is correct.

With the thallium parameter z fixed in the range $\frac{1}{2} \pm 0.05$, the scattering contributions of the magnesium atoms should have an appreciable effect upon the intensities of many of the reflections observed in the Laue photographs. For instance if $z = \frac{1}{2} \pm 0.05$ and $l = 1$,

$$S_{rl} = -0.902 - 0.618i, \quad h - k = 3n$$

$$S_{rl} = 1.902 + 0.309i, \quad h - k \neq 3n.$$

Thus, even if z were to differ from $\frac{1}{2}$ by as much as 0.05, still only one thallium atom out of three would contribute to the intensity of the first type of reflection and two out of three to the second type. The maximum magnesium contribution in any case would be that for which six magnesium atoms would scatter in phase. A reasonable average value for the values of $\sin \frac{\theta}{\lambda}$ observed in Tables 1 and 2 is 0.30/0.37 = 0.81. At this value of $\sin \frac{\theta}{\lambda}$ the ratio of the atomic scattering factor of magnesium to that of thallium is about 0.075. The maximum contribution of magnesium would therefore be 6 x 0.075 = 0.45 compared to approximately 1 for the thallium contribution in the case $h - k = 3m$, $l = 1$. It is improbable, of course, that the maximum magnesium contribution would be realized; it is, however, reasonable to expect that the contributions would be large enough to be able to lead to

contradictions of the observed Laue symmetry for reflections of the type h - k = 3m, ℓ = 1, at least. No contradictions to the general symmetry relationships were observed and the Laue point group D_{6h} can be assigned to the structure without reasonable doubts.

It is now possible to derive the space group of the structure from the following considerations. If all the space groups of the Laue point group D_{6h} are considered in which it is possible to place three thallium atoms in the positions 0 0 0, $\frac{1}{3}\ \frac{2}{3}$ z, $\frac{2}{3}\ \frac{1}{3}$ z or an equivalent set, it is found that the only positions for six magnesium atoms which are not immediately eliminated by gross steric hindrances are

(1) x 0 0; 0 x 0; $\bar{x}\ \bar{x}$ 0; $\bar{x}$ 0 0; 0 $\bar{x}$ 0; x x 0

(2) x 0 $\frac{1}{2}$; 0 x $\frac{1}{2}$; $\bar{x}\ \bar{x}\ \frac{1}{2}$; $\bar{x}$ 0 $\frac{1}{2}$; 0 $\bar{x}\ \frac{1}{2}$; x x $\frac{1}{2}$

(3) x 0 z; 0 x z; $\bar{x}\ \bar{x}$ z; $\bar{x}$ 0 z; 0 $\bar{x}$ z; x x z

(4) x, 2x, 0; $\overline{2x}$, $\bar{x}$, 0; x $\bar{x}$ 0; $\bar{x}$, $\overline{2x}$, 0; 2x, x, 0; $\bar{x}$ x 0

(5) x, 2x, $\frac{1}{2}$; $\overline{2x}$, $\bar{x}$, $\frac{1}{2}$; x $\bar{x}\ \frac{1}{2}$; $\bar{x}$, $\overline{2x}$, $\frac{1}{2}$; 2x, x, $\frac{1}{2}$; $\bar{x}$ x $\frac{1}{2}$

(6) x, 2x, z; $\overline{2x}$, $\bar{x}$; z; x $\bar{x}$ z; $\bar{x}$, $\overline{2x}$, z; 2x, x, z; $\bar{x}$ x z

(7) x y 0; $\bar{y}$, x - y, 0; y - x, $\bar{x}$, 0; y x 0; $\bar{x}$, y - x, 0; x - y, $\bar{y}$, 0

(8) x y $\frac{1}{2}$; $\bar{y}$, x - y, $\frac{1}{2}$; y - x, $\bar{x}$, $\frac{1}{2}$; y x $\frac{1}{2}$, $\bar{x}$, y-x, $\frac{1}{2}$; x-y, $\bar{y}$, $\frac{1}{2}$

(9) x y 0; $\bar{y}$, x-y, 0; y-x, $\bar{x}$, 0; $\bar{y}$ $\bar{x}$ 0; x, x-y, 0; y-x, y, 0

(10) x y $\frac{1}{2}$; $\bar{y}$, x-y, $\frac{1}{2}$; y-x, $\bar{x}$, $\frac{1}{2}$; $\bar{y}$ $\bar{x}$ $\frac{1}{2}$; x, x-y, $\frac{1}{2}$; y-x, y, $\frac{1}{2}$

(11) x $\bar{x}$ 0; x, 2x, 0; $\overline{2x}$, $\bar{x}$, 0 (two sets)

(12) x $\bar{x}$ $\frac{1}{2}$; x, 2x, $\frac{1}{2}$; $\overline{2x}$, $\bar{x}$, $\frac{1}{2}$ (two sets)

(13) three atoms in (11) and three atoms in (12)

(14) x 0 0, 0 x 0, $\bar{x}$ $\bar{x}$ 0 (two sets)

(15) x 0 $\frac{1}{2}$, 0 x $\frac{1}{2}$, $\bar{x}$ $\bar{x}$ $\frac{1}{2}$ (two sets)

(16) three atoms in (14) and three atoms in (15).

In the discussion of the various arrangements listed above, the positions 0 0 0, $\frac{1}{3}$ $\frac{2}{3}$ z, $\frac{2}{3}$ $\frac{1}{3}$ z will be assigned the three thallium atoms with z in the range $\frac{1}{2} \pm 0.05$. The generality of the discussion is not affected by this choice.

It will be noted that the majority of the permissible arrangements (1) to (16) are planar. These arrangements might be eliminated at once by a consideration of the 00: 2n - 1 intensities. Unfortunately there were no reflections of this type which were observed unambiguously in the powder photographs, and it was not considered feasible to attempt single crystal photography of the specimen prepared in such a way as to observe them. If intensities of the type hk·0 are considered, arrangements (1), (2), (3), (9), (10), (14), (15), and (16) differ only in that one or two magnesium parameters x are possible. The various structure factor

expressions can be made formally identical to that of arrangement (14) with two parameters x_1 and x_2 by letting $x_1 = \pm x_2$ in certain cases. A discussion of these arrangements will be deferred until later.

It is necessary now to have some idea of the sizes of the various atoms without making assumptions which would vitiate the eliminations of the remaining space groups. A lower limit of 2.50 Å for both the thallium-magnesium and magnesium-magnesium distances seems safe. A minimum bond number of 2.6 was calculated for a thallium-magnesium distance of 2.50 Å with the assumption of the normal single bond radius of magnesium and the single bond radius of quinquevalent thallium, 1.387 Å[1],[2]. The bond number 2.4 was calculated for a magnesium-magnesium distance of 2.50 Å. Bond numbers significantly greater than one are rarely, if ever, observed in intermetallic compounds.

By graphical means it was seen that arrangement (5) is not permissible if the lower limits to both magnesium-thallium and magnesium-magnesium distances are to be maintained. In this arrangement the value of the parameter x must be between 0.84 and 0.88 if the magnesium atom at $x\ \bar{x}\ \frac{1}{2}$ is to be fitted between the thallium atoms at 0 0 0 and $\frac{2}{3}\ \frac{1}{3}\ \frac{1}{2}$. As a result pairs of magnesium atoms, such as those at 2x, x, $\frac{1}{2}$ and x, 2x, $\frac{1}{2}$ are at a distance between 1.8 and 2.3 Å apart. A similar argument can be used to eliminate arrangements (8) and (12). Arrangements (9) and (10) are permissible for values of x between 0.31 and 0.35 and of y between 0.03 and

-0.03. Because of the small allowable value of y these arrangements can be considered as nearly equivalent to those of arrangements (14) and (15) with $x_1 \approx \bar{x}_2$. Further discussion of arrangements (9) and (10) will therefore be postponed. Arrangements (4) and (11) are permitted only for values of x between 0.78 and 0.83. If x or x_1 and $\bar{x}_2$ are taken as 0.80 it is easy to show that the gross intensity relationships between the small angle powder reflections are not satisfied. For example, the reflection for the planes {30.0} was observed to be about twice as strong as the adjacent reflection for the planes {22.0} . Since the thallium contributions and the frequency factors for the two reflections are the same, the magnesium contribution in the case of {30.0} must reinforce that of thallium much more strongly than it does in the case of {22.0} . On the other hand, the geometrical structure factor for arrangements (4) and (11) with x = 0.80 is -1.73 for {30.0} and -1.97 for {22.0} , the geometrical structure factor for thallium being 3.0 in each case. Arrangements (4) and (11) are thus eliminated. In arrangement (7) steric considerations show that x must again be close to 0.80 and the value of $\bar{y}$ must not differ from that of x by more than about 0.05. Arrangement (7) may therefore be eliminated by the argument used to eliminate arrangements (4) and (11).

In the case of arrangement (6) it is easy to show that x must be between 0.78 and 0.88. At x = 0.78 the previous calculations indicate that the calculated intensities of

{30.0} and {22.0} fail completely to satisfy the observed relationship. At x = 0.88 the geometrical structure factors for arrangement (6) are -1.60 and -1.91 for {30.0} and {22.0} respectively; again the observed intensity relationship is not satisfied. Arrangement (6) is accordingly eliminated. Arrangement (13) may be split into two divisions. In the first, the two values of x lead to an arrangement which, when projected on the base of the unit cell, is nearly identical to arrangement (5); the observed intensity relationship between {30.0} and {22.0} may be used to eliminate this possibility. In the second, one value of x lies between 0.84 and 0.88; the other value lies in the neighborhood of $\frac{1}{2}$ within rather wide limits. The latter arrangement leads to a very unfavorable type of coordination, one of the thallium atoms having nine nearest magnesium neighbors and the other two having only three nearest neighbors. For this reason the arrangement was eliminated from further consideration.

All possible arrangements have now been eliminated except those which are formally equivalent to the arrangement

(17) $x_1\ 0\ z_1$; $0\ x_1\ z_1$; $\bar{x}_1\bar{x}_1 z_1$; $x_2\ 0\ z_2$; $0\ x_2\ z_2$; $\bar{x}_2\ \bar{x}_2\ z_2$.

All the arrangements of this type with the exception of arrangement (16) require that all the magnesium atoms be in one plane. Such a degree of planarity was felt to be unlikely, and it was considered that hk·0 data from single crystal photographs together with the powder photographic data would be sufficient to complete the determination of

structure.

In order to determine the positions of the magnesium atoms it is necessary, as discussed previously, to observe as many hk·0 reflections of the type h - k $\neq$ 3n as possible. The Laue data of Tables 1 and 2 was found to be useless for this purpose; only a small number of such reflections were observed, and the possibility of intercomparison of intensities, which is necessary for a parameter determination, is denied by the fact that the reflections are observed at greatly different values of $n\lambda$ and $\sin\theta$. It was deemed impractical to attempt a systematic program of Laue photography with successive orientations of the crystal in such a manner as to observe selected pairs of the reflections at identical wave lengths. Instead a program of monochromatic photography was undertaken in order to complete the determination of structure.

A series of oscillation photographs with the c axis vertical were prepared with the use of Cu K radiation filtered through nickel. In this manner all the hk·0, h - k $\neq$ 3n reflections were obtained which it was possible to observe under the experimental conditions. The choice of copper Kα radiation instead of molybdenum Kα radiation, the only other feasible choice, was made for the following reasons. It was realized that heavy exposures would be required in order that the reflections of the type desired could be observed with sufficient intensity to afford

reliable intercomparisons. Previous experience with the apparatus available at the time coupled with the fact that the mass absorption coefficients for both copper Kα and molybdenum Kα radiation are high, 231 and 136 respectively, led to the conclusion that heavy exposures could not be obtained in a reasonable length of time with molybdenum radiation. Furthermore, filtered radiation of the highest possible spectral purity was desired; filtered copper K radiation is much cleaner than is filtered molybdenum K radiation. Finally, the existence of a high temperature factor was indicated by both the powder and Laue photographic data, and it is doubtful whether the larger sphere of reflection gained with molybdenum Kα radiation could be used to good advantage even under favorable experimental conditions.

The exposures necessary for the preparation of suitable 30° oscillation photographs were of the order of 15 x 168 = 2520 milliampere hours. The successive oscillation ranges overlapped 5° and the total oscillation range was over 60°. Three films were used for each exposure in accordance with the multiple film technique[8] and the intensities were estimated visually. No reflections were observed on any of the films which necessitated an enlargement of the unit cell chosen.

In Figure 3 the most heavily exposed film of one set of three is reproduced. It shows the same general asymmetry as that shown in the Laue photographs, one side of the specimen apparently consisting of several large individuals inclined

at small angles to one another. The equatorial reflections on one side of the film, however, are reasonably well formed and permit fairly reliable intensity estimations. The powder lines of the intermetallic compound MgTl are also observed in the photograph indicating its presence as an impurity; little difficulty was occasioned by this complication.

The cylindrical absorption factors of Claassen[9] were applied to the observed intensities together with the frequency factor and the usual angle-dependent factors. The corrected intensities so obtained are listed in Table 3.

If arrangement (16) is chosen for the magnesium atoms, the space group is D_{3h}^{3} - $C\bar{6}2m$ and the z parameter of the thallium atoms must be exactly $\frac{1}{2}$. The lower limit of 2.50 Å for the magnesium-thallium and magnesium-magnesium distances requires that $0.312 \leq x_1 \leq 0.492$ and $0.212 \leq \overline{x}_2 \leq 0.372$. This parameter region includes any of the parameter regions sterically permissible for the remaining possible arrangements. Complete generality with regard to the choice of any one of the arrangements formally equivalent to arrangement (17) is therefore preserved.

The observed relationships between the intensities of the reflections 21·0, 31·0, 32·0, and 50·0 are approximately satisfied only in the sub region $0.402 \leq x_1 \leq 0.352$, $0.252 \leq x_2 \leq 0.302$. In this region curves were calculated for each ratio between the corrected observed intensities of adjacent reflections. From the points of intersection of

Figure 3

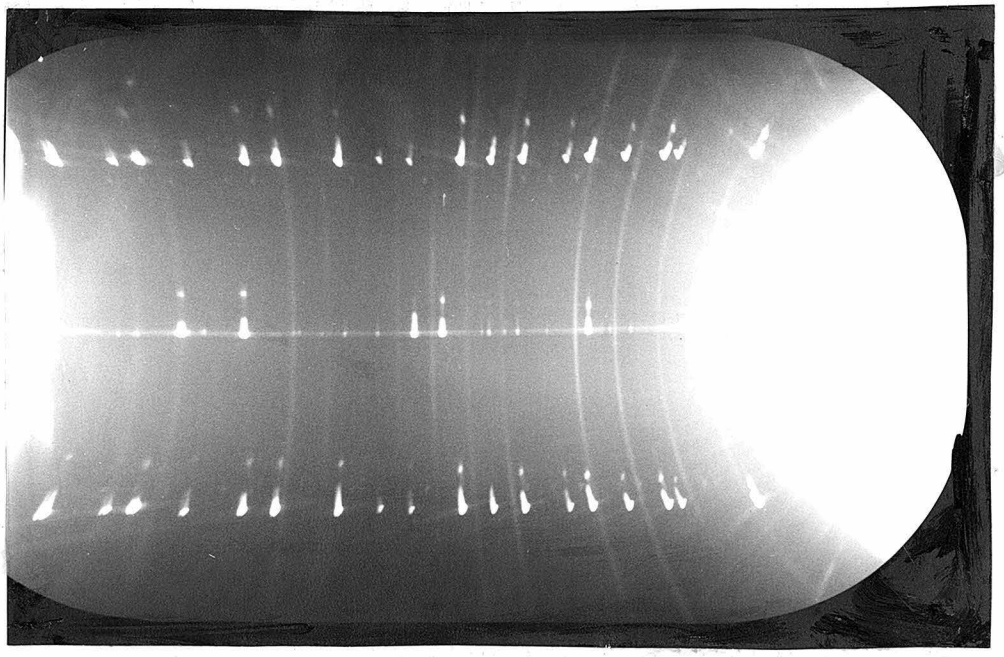

Left side of specimen, 30° oscillation

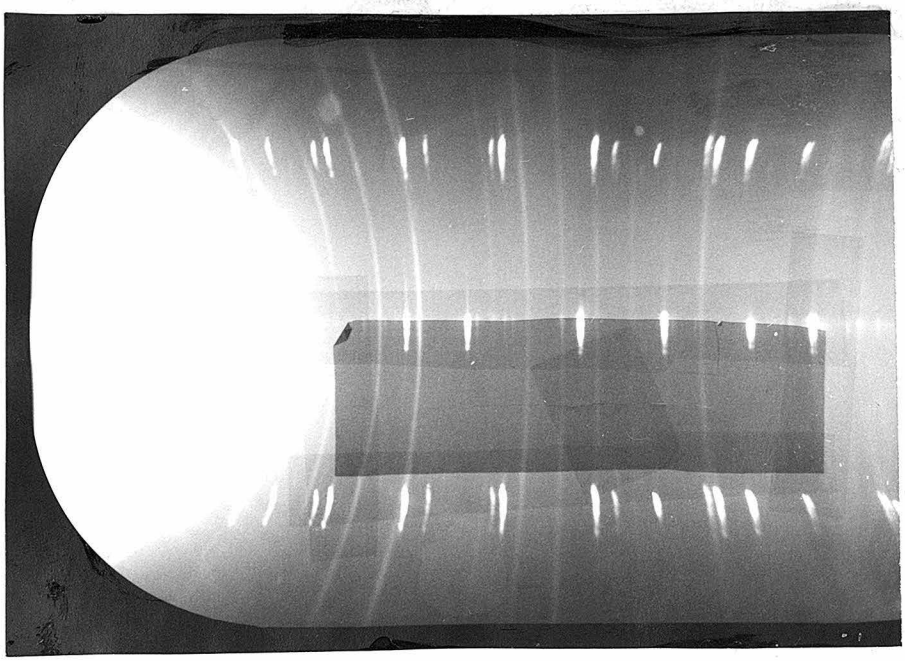

Right side of specimen, 30° oscillation

these curves the approximate parameters $\frac{x_1}{2} = 0.187$, $\frac{x_2}{2} = 0.142$ were obtained. With the use of these parameters the temperature factor B in the expression $I_{calc.} \propto |F|^2 \exp\left\{-2B\frac{\sin^2\theta}{\lambda^2}\right\}$ was found to be approximately 1.65. This temperature factor was used to correct the intensities listed in Table 3 and the final values of the parameters were determined by the points of intersection of the corrected curves, calculated as before.

In the final parameter determination the coordinates of the various points of intersection were given the weights 0, 1, or 2 by the use of the following scheme. If the point of intersection does not lie within the region $0.402 \leq x_1 \leq 0.332$, $0.252 \leq x_2 \leq .302$, the weight is zero*. If the angle of intersection is close to 90°, both coordinates should be weighted heavily, subject to the remaining considerations of the scheme. On the other hand, if the angle of intersection is very small, but both curves are nearly perpendicular to one axis (x_1 or x_2 axis), the coordinate along this axis should be determinable with some certainty. Finally the magnitude of the slope of a given ratio along a given axis at the point of intersection should be large if the corresponding coordinate is to receive a maximum weight.

---

*Only two curves were completely removed from this region, those involving the observed intensity of the reflection 43·0. During the estimation of intensities it was noticed that this spot was ill-formed, apparently because of absorption effects, and some doubt was felt at the time as to whether or not an attempt should be made to estimate its intensity.

A number of curves lying well within the region were parallel to the extent that no included points of intersection existed.

The values of $\frac{x}{2}_1$ and $\frac{\bar{x}}{2}_2$ derived from each point of intersection, together with the assigned weights, are given in Table 4. The final values of the parameters and the corresponding probable errors determined by the weighted averaging of the data of Table 6 are $\frac{x}{2}_1 = 0.1873 \pm 0.0014$, $\frac{\bar{x}}{2}_2 = 0.1433 \pm 0.0019$. The calculated values of the hk·0, h - k $\neq$ 3n intensities, corrected for thermal motion, are given in Table 3 and generally are in satisfactory agreement with the observed intensities, although the discrepancies are appreciably greater than those observed in the usual structure determinations made under more favorable experimental conditions. It is felt, however, that the final parameter values are reliable to the extent indicated. Because the values of x_1 and x_2 differ greatly, it is possible to eliminate arrangements (1), (2), (3), (9), and (10) for the magnesium atoms. The only possible arrangements are (14), (15), and (16), all of which lead to the space group D^3_{3h} - C$\bar{6}$2m and the exact value $\frac{1}{2}$ for the thallium parameter.

In order to verify the conclusion made previously that arrangement (16) represents the actual configuration of the magnesium atoms, a set of multiple film powder photographs were prepared and the intensities of the observed reflections were estimated visually. The use of arrangement (16) leads to satisfactory agreement between calculated and observed intensities; on the other hand it is easy to show that gross disagreements would exist if either arrangement (14) or (15) were used. For example, the reflection for the planes {00.2}

is observed to be about $2\frac{1}{2}$ times as intense as that for the planes $\{30.1\}$. With arrangement (14) the calculated ratio $I_{\{00.2\}} / I_{\{30.1\}}$ becomes about 19; with arrangement (15) the ratio becomes 0.85. The corresponding ratio calculated for arrangement (16) is approximately 2.4. Arrangement (16) was therefore chosen.

In order to obtain the best possible agreement between calculated and observed intensities the expression

$$I_{calc} \propto p|F|^2_{calc} \exp\left\{-2B\left(\frac{\sin^2\theta}{\lambda^2} + \frac{b\,l^2}{4c_o^2}\right)\right\}$$

was used. This expression contains the general form of the temperature factor for a biaxial crystal derived with the assumption of central linear restoring forces. The value of the parameter B was found to be 1.80 from a consideration of the $\{hk\cdot 0\}$ powder reflections, necessarily those for which $h - k = 3n$. This value is in good agreement with the value 1.65 which was found for B from the intensities of Table 3. The parameter b was given the value 1.26 because of the close equality of the intensities of the reflections $\{33.0\}$ and $\{22.2\}$; its magnitude is not of such an order as to affect the argument used in the elimination of arrangements (14) and (15). Observed intensities, corrected with Lorentz, polarization, and absorption factors[9] are listed in Table 5, as are the corresponding calculated intensities.

The structural investigation was completed with a precise determination of the dimensions of the unit cell. The best value for a_o was found to be 8.086 Å from the $\{hk\cdot 0\}$ powder spacings with the use of the extrapolation

method of Nelson and Riley[10]. In this procedure values of a_o calculated from each $\{hk \cdot 0\}$ spacing were plotted against corresponding values of the function $\frac{1}{2}\left(\frac{\cos^2\theta}{\sin\theta} + \frac{\cos^2\theta}{\theta}\right)$. The plot so obtained was approximately linear with a slope which is a measure of the magnitude of the absorption error in the values of the observed spacings.

At the position $\theta = 90^o$ the absorption effect vanishes and the intercept of a straight line drawn through the points of the plot with the a_o axis represents the correct value of a_o, if shrinkage and eccentricity errors are negligible. Three plots of the type described were made from three different powder photographs. Two of the photographs were of the usual type with both ends of the film in the back reflection region; the third photograph was prepared with the mounting first used by Straumanis[11]. In each case shrinkage corrections were made and eccentricity errors were assumed to be negligible. The three values of a_o found from the plots were 8.087 Å, 8.086 Å, and 8.085 Å. A reasonable limit of error was estimated to be 0.005 Å from a consideration of the changes in the value of a_o on drawing other reasonably well-fitting straight lines through the points of each plot. The values of λ for the $K\alpha_1$, and $K\alpha_2$ components of the copper $K\alpha$ line were taken as 1.5405 Å and 1.5443 Å, respectively. One of the plots is reproduced in Figure 4.

The extrapolation procedure of Nelson and Riley could not be used directly in the determination of c_o because no

more than four reflections of the type $\{00.l\}$ lie within the range in which the lines of the powder photograph could be indexed with certainty, and of these only $\{00.2\}$ could be observed free from the interference of other reflections. Thus it was necessary to determine c_o from general $\{hk \cdot l\}$ data. Again three determinations were made with the use of the three photographs mentioned previously. In each determination the value of a_o was taken from the $\{hk \cdot 0\}$ data in the manner first described. The spacings of as many of the $\{hk \cdot 2\}$ reflections as could be measured accurately were corrected for absorption shifts by the use of the a_o plots in the following way. According to Nelson and Riley[10] and Taylor and Sinclair[12], under certain experimental conditions which are commonly satisfied,

$$(a) \quad -\frac{dD}{D} \propto \frac{1}{2}\left(\frac{\cos^2\theta}{\sin\theta} + \frac{\cos^2\theta}{\theta}\right)$$

where D is the true spacing and $D_{obs} = D + dD$. In the instance of hk·0 reflections $\frac{dD}{D} = \frac{da_o}{a_o}$ and we find that

$$(b) \quad -\left(a_o^{obs} - a_o\right) \propto \frac{a_o}{2}\left(\frac{\cos^2\theta}{\sin\theta} + \frac{\cos^2\theta}{\theta}\right),$$

the proportionality constants of Equations (a) and (b) being equal. The proportionality constant is determined from the plot of the type shown in Figure 4 concerned, more accurately from the slope of the straight line drawn through the points of the plot, and is then used to find the correction dD to be applied to the observed spacings of the $\{hk \cdot 2\}$ reflections. The value of a_o derived from the $\{hk \cdot 0\}$ spacings of the photo-

Figure 4

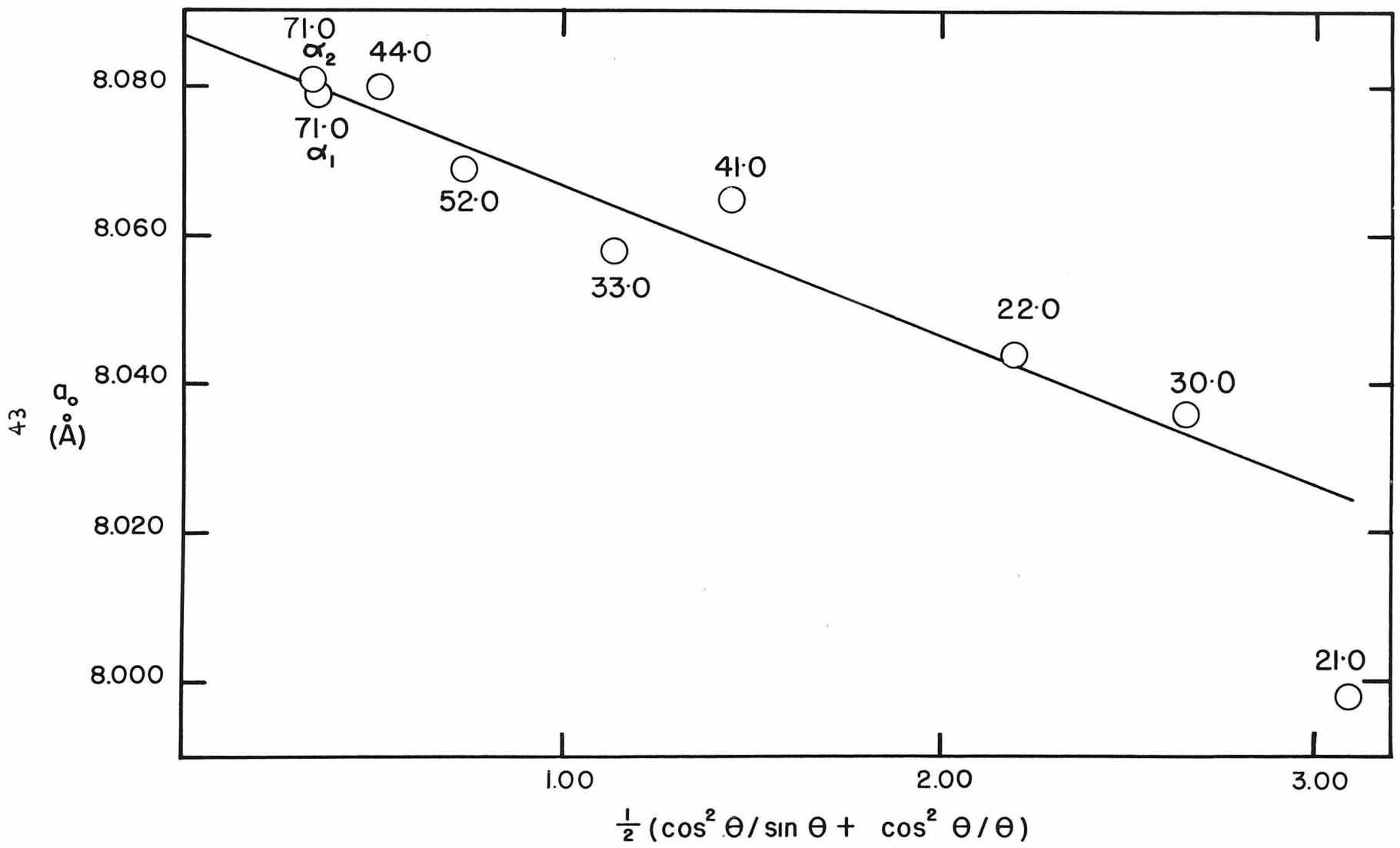
71·0
α2
44·0
71·0
α1
52·0
41·0
33·0
22·0
30·0
21·0
8.080
8.060
8.040
8.020
8.000
a₀
(Å)
1.00
2.00
3.00
½ (cos² θ/sin θ + cos² θ/θ)

graph in question, together with the values of the corrected $\{hk\cdot 2\}$ spacings were then used to calculate corresponding values of c_o. These values were then averaged to obtain the best value of c_o for each photograph. The probable error in each case was estimated from the internal consistency of the set. The three values of c_o and the corresponding probable errors are 3.674 ± 0.003 Å, 3.670 ± 0.005 Å, and 3.672 ± 0.005 Å. The final value of c_o was taken as 3.672 ± 0.007 Å.*

Structural Summary

The structure of the intermetallic compound Mg_2Tl is based upon the space group D^3_{3h} - $C\bar{6}2m$ with a unit cell of dimensions $a_o = 8.086 \pm 0.005$ Å, $c_o = 3.672 \pm 0.007$ Å. Three thallium atoms and six magnesium atoms are contained in the unit cell. The thallium atoms are in the positions

1: (a) 000

2: (c) $\frac{1}{3}\ \frac{2}{3}\ \frac{1}{2}$; $\frac{2}{3}\ \frac{1}{3}\ \frac{1}{2}$

---

*The increased value of the error assigned to the final value of c_o represents the sum of the average probable error from the three determinations and one-half the error assigned to value of a_o. The determination of c_o is partially dependent upon the determination of a_o. A rather qualitative argument was formulated to show that this partial dependence of c_o upon a_o could be expressed reasonably by the calculation of the error for c_o in the manner described.

The magnesium atoms are in the positions

$$3: \ (f) \ x_1 0 \ 0; \ \ 0 \ x_1 \ 0; \ \ \bar{x}_1 \ \bar{x}_1 \ 0$$
$$3: \ (g) \ x_2 \ 0 \ \tfrac{1}{2}; \ \ 0 \ x_2 \ \tfrac{1}{2}; \ \ \bar{x}_2 \ \bar{x}_2 \ \tfrac{1}{2}.$$

The values 0.3746 ± 0.0028 and 0.2866 ± 0.0038 were found for x_1 and $\bar{x}_2$, respectively.

Structural discussion

The positions found for the magnesium and thallium atoms in the structure Mg_2Tl lead to the following details of coordination. The thallium atom at 000, hereafter to be denated Tl I, is surrounded by six magnesium atoms at 2.96 Å which lie on the corners of a trigonal prism, and by three magnesium atoms at 3.03 Å which are situated on lines perpendicular to the rectangular faces of the prism and passing through the point 000. A closest thallium atom is at 001, 3.67 Å distant; this distance is not considered to be a bonded distance. Each thallium atom of the positions 2: (c), hereafter Tl II, is surrounded by six magnesium atoms at a distance of 3.14 Å and three magnesium atoms at a distance of 2.90 Å. The coordination polyhedron is very similar to that of Tl I; the six magnesium atoms at 3.14 Å form a trigonal prism, and the three magnesium atoms at 2.90Å are again situated on lines which are perpendicular to the rectangular faces of the prism and which pass through its center. Each magnesium atom of the set 3:(f), hereafter Mg I, is surrounded by four thallium atoms at the distance 3.14 Å and one thallium atom 3.03 Å away. The polyhedron

is a rectangular pyramid with the magnesium atom close to the base on the line drawn through the apex and perpendicular to the base. Each magnesium atom of positions 3:(g) is surrounded by two thallium atoms at a distance of 2.96 Å and two thallium atoms at a distance of 2.90 Å. The coordination polyhedron in this case is an approximately regular tetrahedron.

In addition there exist magnesium - magnesium distances of about 3.30 Å which are perhaps non-bonded distances; the decision as to the nature of these distances will be attempted subsequently. Each atom Mg I is surrounded by six Mg II atoms, four at a distance of 3.30 Å and two at a distance of 3.31 Å. Six Mg I atoms surround each Mg II atom, four at 3.30 Å and two at 3.31 Å. The coordination polyhedron in both cases is very nearly a trigonal prism.

The nearest or very near neighbor distances found in the structure can be used to derive the valences exhibited by the various types of atoms with the application of the rules proposed by Pauling[1], [2]. The procedure is based upon the relationship

(c) $R_n = R_1 - 0.300 \log n$

which is now too well known to require further explanation. The principal difficulty in the application of this relation between distance and bond number is the uncertainty as to the correct value of the single bond radius R_1. As a start in the discussion of valence we shall assume that the value of R_1 for both types of magnesium atoms is normal, 1.364 Å[2].

We shall now seek a self-consistent solution of the thallium valences, defining a self-consistent solution as one in which the use of single bond radii derived from assumed valences in a manner to be described leads to valences equal to those assumed. As an example, let us assume that the valence of Tl I is 4.00. If we assume that the d character of all bonding and metallic orbitals is the same, we find that the use of the relationship

(d) $R_1(\delta, z) = 1.850 - 0.030\ z - (1.276 - 0.070\ z)\delta$

leads to the value 1.419 Å for $R_1^{(2)}$. The use of Equation (c) now leads to the valence 4.20 for Tl I. Thus 4.00 is a nearly self-consistent solution for the valence of Tl I. The exact self-consistent valences of Tl I and Tl II were found to be 4.14 and 3.63 with the respective single bond radii 1.414 Å and 1.433 Å. We can now calculate the valences of the magnesium atoms by the use of the self-consistent single bond radii of the thallium atoms. If the short magnesium distances are non-bonded, the calculated valences of MgI and MgII are 1.45 and 2.35. If the magnesium- magnesium distances are bonded, the corresponding valences are 2.10 and 3.00. The magnesium valences in either case seem improbable, and thus the validity of the self-consistent solutions for the thallium valences is to be questioned.

It is worthwhile at this point to consider the effect of small variations in the distances upon the results of the

preceding calculations. The Tl I - Mg I distance of 3.03 Å is very sensitive to the value of the parameter x_1 and is independent of x_2. A reasonable minimum value of x_1 is $0.3746 - 3 \cdot 0.0028 = 0.3662$. The Tl I - Mg I distance is now decreased to 2.96 Å; the Tl II - Mg I distance, previously taken as 3.14 Å, is not decreased appreciably. The self-consistent valence of Tl I is now 4.36, the self-consistent valence of Tl II being about 3.63. Corresponding valences of Mg I and Mg II are 1.56 and 2.32 with the assumption that magnesium-magnesium distances are non-bonded. Although the maximum allowable decrease in the value of x_1 brings the magnesium valences closer to the expected value 2.00, the shift is not nearly great enough. An increase in the value of x_1 would obviously make matters worse.

If the value of x_1 found experimentally is retained, and variations in the value of x_2 are considered, we have the following situation. If the value of $\bar{x}_2$ is increased to $0.2866 + 3 \cdot 0.0038 = 0.2980$, the Tl II - Mg II distance is decreased to 2.85 Å and the Tl I - Mg II distance is increased to 3.04 Å. The self-consistent valences of Tl I and Tl II are now 3.60 and 3.90 with the single bond radii 1.434 Å and 1.423 Å, respectively. Corresponding magnesium valences are 1.45 (I) and 2.37 (II) if short magnesium- magnesium distances are assumed to be non-bonded. Although the thallium valences are changed appreciably by an increase in the value of $\bar{x}_2$, the magnesium valences are essentially unchanged.

If the value of $\overline{x}_2$ is decreased to 0.2866 - 3·0.0038 = 0.2752, the Tl II - Mg II distance is 2.96 Å and the Tl I - Mg II distance is 2.89 Å. The self-consistent valences of Tl I and Tl II are 4.71 and 3.35 with single bond radii of 1.396 Å and 1.445 Å. The valence of Mg I is 1.48; that of Mg II is 2.34. It is assumed again that no magnesium-magnesium bonds exist.

It is evident therefore that with the largest reasonable variations of x_1 and x_2 from the most probable values, the magnesium valences calculated in the manner previously indicated are essentially unchanged. It is improbable that the magnesium valences are correctly indicated in the preceding calculations, either with or without the assumption that the magnesium - magnesium distances are non-bonded. One immediate objection to the method employed in the calculations is that the assumption of the equality of the percentages of d character of all the bonding and metallic orbitals for a given thallium atom may well be incorrect. In order to avoid this assumption it is necessary to attack the problem in an entirely different way. We first assume the principle, first enunciated by Pauling[1], that bond numbers should always be equal to ratios of small integers $\frac{2}{3}$, $\frac{1}{2}$, $\frac{1}{4}$, $\frac{1}{3}$, etc. The occurence of numbers greater than about 5 in the ratios seems to be unlikely; this enables us to make a decision as to the nature of the short magnesium- magnesium distances. The bond number of a magnesium - magnesium distance of 3.31 A

is 0.107 $\sim \frac{1}{10}$ with the use of the single bond radius 1.364 Å. It seems likely, in view of the principle just cited, that the bond number $\frac{1}{10}$ has no physical significance and that the magnesium - magnesium distances are non-bonded.

It is hard to see why the valences of the magnesium atoms should differ from two. Electron transferences appear improbable because of the small differences between the electronegativities of magnesium and thallium, and the resulting difficulty in satisfying the principle of electroneutrality[13] if significant formal charges exist. Thus it seems wholly reasonable that the valences of both types of magnesium atoms are 2.00. In accordance with this valence requirement we now select bond numbers for the various distances which seem satisfactory. From the bond numbers and the single bond radius of magnesium, 1.364 Å, the corresponding single bond radii of the thallium atoms is calculated with the use of Equation (c). The number of d orbitals employed in bond formation is then calculated from the application of Equation (d). The valence of a given thallium atom is determined initially from the bond numbers assumed, and must be compatible with the number of d orbitals employed in bond formation, as calculated in the manner just described. If valences are incompatible with amounts of d character employed in bond formation, the initial choice of bond numbers is incorrect. A new choice of bond numbers must be made then and the procedure repeated. When valences are found to be compatible with the number of d orbitals employed, a decision is reached

concerning the valences of the thallium atoms, the bond numbers of the various distances, and the numbers of d orbitals employed in bonding.

Application of the method described above, with the use of the most probable values of x_1 and x_2 led to the conclusion that the valence of Tl I is 4.40 and the valence of Tl II is 3.80. Each atom Mg I forms one bond with Tl I of order $\frac{2}{3}$ and four bonds with Tl II of order $\frac{1}{3}$. Each atom Mg II forms two bonds of order $\frac{2}{5}$ with Tl I and two bonds of order $\frac{3}{5}$ with Tl II. Every thallium atom I forms six $\frac{2}{5}$ bonds with the use of 0.67 d orbitals and three $\frac{2}{3}$ bonds without the use of d orbitals; 0.30 metallic orbitals are employed which have 10% d character. Thallium II forms three $\frac{3}{5}$ bonds with the use of 0.29 d orbitals, and six $\frac{1}{3}$ bonds without the use of d orbitals. Thallium II has 0.60 metallic orbitals which have 19% d character. This description of valences and distances in the structure of Mg_2Tl seems the most reasonable.

The Structural Determination of Mg_2In

Preliminary powder photography indicated that the structure of Mg_2In was isomorphous to that of Mg_2Tl. Experience gained in the determination of the structure of Mg_2Tl led to the conclusion that, if the structural parameters of Mg_2In were to be determined accurately, it would be necessary to obtain single-crystal data. Accordingly, a number of attempts to prepare single crystals were made along the lines described

in the preceding section. These experiments were unsuccessful. Additional experiments were made to prepare slowly cooled cylindrical castings of the compound with the use of the small bore clay tubing described previously. Several single crystals were prepared by this method, but all of them were found to have the Laue symmetry O_h. Since the only known phase in the magnesium-indium system with the Laue symmetry O_h is that of $MgIn_2$[3], it was assumed that large decreases in the magnesium content of the melt occurred whenever the molten material was in prolonged contact with the clay tubing.

Although the procedure followed in the preparation of slowly cooled castings was unsuccessful in the present investigation, it will be described in detail with the hope that some future use can be made of it in the preparation of single crystals in systems of less reactive metals. A tubular furnace was prepared by winding a double helix of resistance wire around a piece of clay tubing in such a way that both leads were situated at one end of the tube. The inside diameter of the tube was of such a size as to permit an easy, but snug fit with the small bore tubing in which the casting was to be prepared. A sheath of large-bore clay tubing surrounded the winding and was attached to each end of it with sodium silicate. The end of the intermediate tube at which the leads of the winding emerged, and which projected beyond the sheath tube, was then sealed with silver chloride

to the small-bore tubing on the inside, and to a piece of Pyrex tubing on the outside. These seals were made vacuum tight. The Pyrex tube was connected to a two-way stopcock and pump. The innermost, small bore tube projected into the Pyrex tube at one end and through the ends of the sheath and intermediate tube at the other; thus forming a passageway from the pump to the atmosphere. The spacing of the furnace winding was increased from one end to the other so that a large difference between the steady-state temperatures at either end of the furnace could be obtained. In this way a sudden decrease in the power input produced a cooling front which traveled along the length of the furnace. It was hoped that cooling in this manner would encourage the formation of fewer, and larger single crystals. When a casting was to be prepared, the furnace was brought to a steady state temperature with the lower end of the furnace somewhat above the estimated melting point of the alloy and the upper end about 100° C cooler. The pump was turned on, but was isolated from the innermost tube by means of the two- way stopcock. The casting assemblage was lowered into the crucible until the tip of the small-bore tube touched the bottom; the rest of the furnace was well above the surface of the molten compound. The pump was then connected to the system by a quick turn of the stopcock and the molten material was sucked into the small-bore tube. In most cases solidification occurred toward the top of the furnace before metal was sucked

into the Pyrex tube. The assemblage was withdrawn from the crucible and the power input to the tubular furnace was discontinued. After a few minutes of cooling the casting was removed by careful demolition of the entire furnace assemblage and quickly placed under a protective coating of vaseline-ligroin solution. Very rarely did the casting consist of a continuous rod. Usually sections of alloy were interspersed by regions of solidified flux. The crystallinity of the various particles obtained was tested by means of Laue photography. As was stated previously, several single crystals of identical structures with the Laue symmetry O_h were obtained; no single crystals of hexagonal symmetry were found.

Because of the failure to prepare single crystals, it was necessary to rely on powder photographic data for the determination of structure. Two sets of multiple-film photographs were prepared in the usual way, one of which was an extremely heavy exposure. Intensities were estimated visually; the data is given in Table 6. A few lines of very low intensity which were identified as belonging to MgIn and Mg_5In_2 were observed in the photographs. The presence of both the phases was attributed to the fact that Mg_2In probably melts incongruently. It is well known that, in the case of incongruent melting, it is often possible to obtain three solid phases from the cooling of a liquid phase[14].

In order to verify the identification of the Mg_5In_2 lines, a melt of calculated composition Mg_5In_2 was prepared

and photographed. During the course of the attempts to prepare single crystals, some alloys were prepared which had large percentages of the phase MgIn, and no difficulty was found in the identification of these lines in the final Mg_2In powder photographs.

The powder reflections which were those of Mg_2In were indexed with a unit cell of dimensions $a_o = 8.324 \pm 0.005$ Å, $c_o = 3.457 \pm 0.007$ Å. The determination of precise unit cell dimensions was carried out by the use of the extrapolation procedure of Nelson and Riley[10] in the manner previously described.

The observed intensities of Table 6 show the same general relationships found in the powder pattern of Mg_2Tl, and it is evident that the structures of Mg_2In and Mg_2Tl are isomorphous. It was not possible to fix the magnesium parameters x_1 and x_2 with precision, because only a small number of reflections of the form hk·2n, h-k≠3m were observed. The intensity relationships between the reflections $\{22\cdot1\}$ and $\{30\cdot1\}$, $\{31\cdot3\}$ and $\{32\cdot3\}$, $\{21\cdot3\}$ and $\{61\cdot1\}$, $\{72\cdot1\}$ and $\{81\cdot1\}$ limit the parameters to the region $0.170 \leq \frac{x_1}{2} \leq 0.200$, $0.130 \leq \frac{x_2}{2} \leq 0.170$. In the derivation of this region a lower limit of 2.50 A was assumed for magnesium-magnesium and magnesium - indium distances.

Intensities calculated with the parameter values $\frac{x_1}{2} = 0.187$, $\frac{x_2}{2} = 0.143$ are in satisfactory agreement with observed intensities, as is shown in Table 6. The temperature factor $\exp\left\{-4.00\left(\frac{\sin^2\theta}{\lambda^2} + \frac{0.59\,l^2}{4c_o^2}\right)\right\}$ was applied to the calculated

intensities.

The structural details of Mg_2In are, therefore, very similar to those of Mg_2Tl and the two structures are apparently isomorphous. It is not considered safe to state more than this without additional diffraction data.

The Structural Determination of Mg_2Ga

At the outset of this investigation it was decided to attempt the complete determination of structure with powder photographic data. The previous difficulty found in growing single crystals and the pressure to complete the work in a reasonable length of time led to this decision.

A melt of calculated composition Mg_2Ga and several specimens suitable for powder photography were prepared in the usual way. A heavy multiple-film exposure was made and the intensities of the observed reflections were estimated visually. The reflections of the photograph were indexed successfully with the assumption of a unit cell of dimensions $a_o = 7.807$ Å, $c_o = 6.900$ Å*.

The dimensions of the unit cell found here are in essential agreement with those found by Haucke[3], $a_o = 7.85$ Å, $c_o = 6.94$ Å. The value of c_o is approximately twice that of those found for c_o in the cases of Mg_2Tl and Mg_2In, and the volume of the unit cell is approximately twice as large.

---

*The determination of the precise dimensions of the unit cell was carried out in the manner already described.

The reflections for which ℓ is odd, which necessitate the doubling of the value of c_o, are of low intensity, and the possibility that the structure was grossly the same as that found for Mg_2Tl and Mg_2In was suggested**. Reflections of the type h-k = 3n, ℓ = 4m were strong and reflections h - k $\neq$ 3n, ℓ = 4m were weak. This can be taken as confirmatory evidence that the structure of Mg_2Ga is grossly isomorphous to that of Mg_2Tl and Mg_2In. As a start, therefore, the structure previously found was assumed for Mg_2Ga and the values of x_1 and x_2 were determined in the usual way with the assumption of minimum magnesium - gallium and magnesium - magnesium distances of 2.50 Å. The best values of $\frac{x}{2}_1$ and $\frac{x}{2}_2$ seemed to be in the neighborhood of 0.182 and 0.147, respectively. The temperature factor was estimated in the usual way and the intensities of the first twenty reflections of the type hk·2m were calculated. The agreement between calculated and observed intensities was very good and confirmed the general details assumed for the structure.

In order to derive the space group of the actual structure, it was assumed that the symmetry of the space group requires a truly hexagonal lattice and that the unit cell contains six gallium atoms and twelve magnesium atoms in positions

---

**Alloys of composition Mg_5Ga_2 and MgGa were prepared and photographed in order to be sure that the reflections of type ℓ = 2n + 1 were not due to their presence in small amounts. The strongest lines of both substances were not observed in the Mg_2Ga photographs; it seems certain the doubling of the unit cell of Mg_2Ga is necessary.

which are very close to those found for the structure idealized in the manner just described. The space groups which satisfy these requirements were found to be D_{3h}^4 - C$\bar{6}$2c, D_{3h}^3 - C62m, C_{3h}^1 - C$\bar{6}$, D_3^2 - C32, C_{3v}^4 - C31c, C_{3v}^2 - C31m, and C_3^1 - C3. Of these space groups it is natural to favor the first two, D_{3h}^4 and D_{3h}^3 because of their relatively high symmetry. A systematic extinction exists for D_{3h}^4 - C$\bar{6}$2c, if $l = 2n+1$, reflections of the type hh·l are absent. No reflections of this type were observed, although in several cases it would have been possible to observe unambiguously a reflection of this type if it were of moderate intensity.

Violations of the extinction rule for D_{3h}^4 - C$\bar{6}$23 were not observed; there is no extinction rule for D_{3h}^3 - C$\bar{6}$2m. In view of the number of hh·2m + 1 absences, it was felt that the D_{3h}^3 space group D_{3h}^3 - C$\bar{6}$2m was improbable, and no systematic effort was made to find a structure based upon this space group which would be consistent with the observed intensities.

The space group D_{3h}^4 - C$\bar{6}$2c was thought to be the most probable space group because of the number of absences which could be explained by its assumption, and because of its relatively high symmetry. If the magnesium atoms are to be placed in the manner postulated, it is necessary to put six magnesium atoms in the positions

$$6\ (g)\quad x\ 0\ 0;\quad 0\ x\ 0;\quad \bar{x}\ \bar{x}\ 0$$
$$x\ 0\ \tfrac{1}{2};\quad 0\ x\ \tfrac{1}{2};\quad \bar{x}\ \bar{x}\ \tfrac{1}{2}$$

and six magnesium atoms in the positions

6 (h) u y $\frac{1}{4}$; $\bar{y}$, u-y, $\frac{1}{4}$; y-u, $\bar{u}$, $\frac{1}{4}$

y u $\frac{3}{4}$; $\bar{u}$, y-u, $\frac{3}{4}$; u-y, $\bar{y}$, $\frac{3}{4}$.

There are two possible arrangements for the gallium atoms. The first arrangement is identical to that found in Mg_2Tl, two atoms at 000; $00\frac{1}{2}$; two equivalent atoms at $\frac{1}{3}\ \frac{2}{3}\ \frac{1}{4}$; $\frac{2}{3}\ \frac{1}{3}\ \frac{3}{4}$; and two equivalent atoms at $\frac{2}{3}\ \frac{1}{3}\ \frac{1}{4}$; $\frac{1}{3}\ \frac{2}{3}\ \frac{3}{4}$. In the second arrangement two equivalent gallium atoms are in the positions $00\frac{1}{4}$; $00\frac{3}{4}$; and four equivalent atoms are in the positions

4 (f) $\frac{1}{3}\ \frac{2}{3}$ z; $\frac{2}{3}\ \frac{1}{3}\ \bar{z}$; $\frac{2}{3}, \frac{1}{3}, \frac{1}{2} + z$; $\frac{1}{3}, \frac{2}{3}, \frac{1}{2}-z$.

The first arrangement was considered to be incorrect from the following considerations. If the first arrangement were correct, the corrected intensities of reflections with the same values of h and k but different odd values of l should be the same. This is obvious because there are no general z parameters in the first possible arrangement of gallium atoms. On the other hand, if the second arrangement is correct, the intensities of hk·l and hk·l' can differ greatly. Experimentally, it was observed that the corrected intensity of the reflection $\{10\cdot3\}$ is nearly ten times that of the reflection $\{10\cdot1\}$. The second arrangement was therefore chosen for the gallium atoms; the value of z was presumed to be nearly 0.

If reflections of the type $\{h\ k\cdot 2l+1\}$ are considered, the parameter x of the magnesium positions 6 (g)

is eliminated, and it is necessary to consider only the magnesium parameters u, y and the gallium parameter z. It was assumed that the value of u 2·0.182, determined initially from the $\{hk\cdot 4n\}$, $h-k \neq 3n$ intensities was approximately correct. Intensity relationships between the observed reflections with l odd are insensitive to large variations in u from this value, and thus the explanation of the intensities of these reflections becomes essentially a two parameter problem. A consideration of the intensities of the observed reflections of type $\{hk\cdot 2m+1\}$ with the use of the preliminary value of u, led to the parameters $\bar{z} = 0.031$, $\bar{y} = 0.022$. These parameters were then used in the consideration of the $\{hk\cdot 4n\}$ intensities to correct the initial values found for u and x. It was now found from a consideration of the intensity ratios $\frac{32\cdot0}{41\cdot0}$, $\frac{40\cdot0}{32.0}$, and $\frac{21\cdot4}{30\cdot4}$ that $\frac{u}{2} = 0.192$, $\frac{\bar{x}}{2} = 0.142$. With the parameter values derived so far, the temperature factor correction was shown to be approximately

$$I_{calc} = p\,|F|^2 \exp\left\{-3.92\left(\frac{\sin^2\theta}{\lambda^2} + 1.00\,\frac{l^2}{4c_o^2}\right)\right\}$$

With the new value of $\frac{u}{2}$, 0.192, the intensities of the $\{hk\cdot 2n+1\}$ intensities were used to determine that $\bar{y} = 0.022$ and $\bar{z} = 0.034$. These values for y and z were then used in the final determination of u and x. The observed intensity ratios $\frac{32\cdot0}{41\cdot0}$, $\frac{21\cdot4}{30\cdot4}$, and $\frac{\{40\cdot2\} + \{32\cdot1\}}{\{32\cdot0\}}$ are best satisfied when u = 0.387, x = 0.284. Intensities were then calculated for all reflections observed and compared to the values

estimated visually. This comparison is given in Table 7. In general the agreement between observed and calculated intensities is rather good; there are, however, a few marked discrepancies. The agreement between calculated and observed intensities for the reflections $\{30\cdot2\} + \{22\cdot1\} + \{31\cdot0\}$, $\{22\cdot4\} + \{32\cdot3\}$, $\{33\cdot1\} + \{20\cdot5\} + \{42\cdot0\}$, and $\{31\cdot4\}$ is especially poor. Strenuous, but unsuccessful, efforts were made to explain these discrepancies in a number of ways. Errors in the indexing process were not found, and there were no gross errors in the estimation of intensities. There seemed to be no systematic effect due to preferred orientation of crystallites. Since the observed intensities in the case of marked discrepancy are always too small, the presence of impurity lines cannot be invoked to explain the difficulty. Accidental physical effects, such as the occurrence of multiple reflections[15] within each mosaic block, seem improbable for a number of reasons.

The structure found for Mg_2Ga in the present investigation is not completely acceptable in view of the inexplicable discrepancies between the calculated and observed intensities for a small number of reflections. It is quite probable that the gross structural details proposed are correct, but that the precise positions of the atoms have not been determined correctly.

A consideration of the other space groups which were proposed above would be extremely involved without additional

experimental information. In passing, it should be noted that the extinction rule for the space group C_{3v}^4 - C31c is the same as that for D_{3h}^4 - C$\bar{6}$2c. In this space group eight parameters would generally be necessary to describe a structure which is grossly the same as that of Mg_2Tl.

It is reasonable to expect that, with single-crystal data, the structure of Mg_2Ga could be completely determined. A further attack upon the structure in this direction was not possible in the present investigation.

Summary and Conclusions

An investigation of the structures of the intermetallic compounds Mg_2Tl, Mg_2In, and Mg_2Ga has been made.

The structure of Mg_2Tl was determined precisely with the use of single-crystal and powder X-ray data. The valences of the two types of thallium atoms were found to be greater than the elementary valence; it is probable that one of the three thallium atoms of each unit cell has a valence of 4.4 and the remaining thallium atoms a valence of 3.8, the magnesium valences being 2.00. No thallium-thallium valence bonds exist in the structure.

The structure of Mg_2In was found to be isomorphous to that of Mg_2Tl. It was not possible to determine the positions of the magnesium atoms with sufficient accuracy to give a discussion of valences.

The structure of Mg_2Ga is apparently similar to those of Mg_2Tl and Mg_2In in its major aspects. The positions of the atoms, however, necessitate a doubling of the length of the unit cell dimension along the c axis. It was not possible to determine the exact positions of the atoms.

Table 1

Laue photographic data for Mg_2Tl

$\underset{\sim}{\zeta}$ vertical, $\underset{\sim}{S_o} \parallel \underset{\sim}{a}$

hk·ℓ	sin θ	nλ	d(Å)*
32·4	0.302	0.479	0.792
23·3	0.245	0.474	0.967
36·2	0.300	0.474	0.790
58·0	0.384	0.471	0.613
41·5	0.344	0.469	0.682
25·2	0.242	0.461	0.951
58·1	0.380	0.460	0.605
55·4	0.380	0.458	0.603
47·2	0.339	0.456	0.672
40·5	0.339	0.456	0.673
46·3	0.338	0.452	0.668
13·2	0.170	0.451	1.32
35·3	0.292	0.450	0.770
37·1	0.290	0.445	0.766
26·1	0.237	0.442	0.933
53·5	0.370	0.435	0.588
41·5	0.329	0.433	0.658
57·3	0.368	0.430	0.584
33·4	0.284	0.425	0.754
58·2	0.366	0.425	0.581
48·1	0.327	0.424	0.648
42·5	0.322	0.411	0.638
51·6	0.356	0.402	0.564
24·3	0.225	0.401	0.893
54·5	0.355	0.400	0.564
15·0	0.158	0.397	1.25
59·1	0.353	0.395	0.560
69·2	0.384	0.393	0.511
47·3	0.314	0.390	0.621
43·5	0.310	0.381	0.615
31·5	0.267	0.375	0.702
27·0	0.215	0.370	0.860
38·1	0.264	0.367	0.695
6.10·1	0.372	0.367	0.493
15·1	0.152	0.360	1.18
10·3	0.150	0.359	1.20
49·1	0.301	0.359	0.596
52·6	0.335	0.358	0.534
31·5	0.259	0.353	0.682
14·2	0.150	0.350	1.17
27·1	0.211	0.350	0.828
11·3	0.147	0.342	1.16

Table 1
(cont.)

hk·l	sin θ	nλ	d(Å)*
25·3	0.208	0.342	0.822
5.10·1	0.328	0.342	0.521
48·3	0.293	0.339	0.578
59·3	0.325	0.334	0.514
32·5	0.251	0.333	0.663
37·3	0.250	0.329	0.658
58·4	0.322	0.327	0.509
45·5	0.286	0.323	0.564
47·4	0.285	0.323	0.566
41·6	0.285	0.322	0.564
6.11·1	0.348	0.322	0.463
4.10·1	0.280	0.318	0.552
12·3	0.139	0.307	1.10
36·4	0.241	0.305	0.632
39·1	0.240	0.305	0.634
5.11·0	0.308	0.303	0.491
49·3	0.274	0.297	0.541
26·3	0.194	0.293	0.756
39·2	0.232	0.282	0.608
28·1	0.189	0.281	0.744
13·3	0.133	0.273	1.03
16·1	0.131	0.266	1.02

*Calculated with the preliminary cell dimensions a_o = 8.04 Å, c_o = 3.64 Å.

Table 2

Laue photographic data for Mg_2Tl

$\underset{\sim}{c}$ vertical, $\angle(\underset{\sim}{s}_o, \underset{\sim}{a}) = 30°$

hk·l	sin θ	nλ	d (Å)*
10.$\bar{2}$·1	0.322	0.479	0.744
13·5	0.348	0.475	0.682
42·5	0.372	0.474	0.638
8$\bar{1}$·3	0.320	0.470	0.735
9$\bar{1}$·3	0.344	0.465	0.676
11.$\bar{2}$·1	0.340	0.458	0.674
10.$\bar{1}$·3	0.364	0.455	0.626
90·4	0.386	0.455	0.590
32·5	0.339	0.450	0.664
6$\bar{2}$·1	0.179	0.444	1.24
6$\bar{1}$·3	0.254	0.442	0.871
10·2	0.125	0.440	1.76
12.$\bar{2}$·1	0.356	0.440	0.617
11.$\bar{1}$·3	0.379	0.440	0.580
21·4	0.253	0.435	0.861
13.$\bar{2}$·0	0.372	0.427	0.574
03·5	0.305	0.425	0.696
61·5	0.350	0.421	0.601
01·3	0.175	0.420	1.20
13.$\bar{2}$·1	0.369	0.419	0.567
14·6	0.370	0.417	0.564
22·5	0.298	0.409	0.686
51·5	0.322	0.405	0.630
14.$\bar{2}$·1	0.379	0.398	0.526
7$\bar{2}$·2	0.208	0.396	0.951
5$\bar{1}$·3	0.208	0.394	0.949
13.$\bar{2}$·2	0.356	0.390	0.548
20·3	0.168	0.386	1.15
52·6	0.352	0.376	0.534
41·5	0.285	0.375	0.658
11.$\bar{1}$·4	0.350	0.375	0.536
5$\bar{2}$·0	0.115	0.368	1.60
8$\bar{1}$·4	0.284	0.368	0.648
80·5	0.327	0.366	0.559
11.$\bar{2}$·3	0.305	0.365	0.598
12·5	0.258	0.362	0.702
10.$\bar{2}$·3	0.281	0.362	0.644
12.$\bar{2}$·3	0.323	0.359	0.556
70·5	0.301	0.354	0.588
9$\bar{2}$·3	0.254	0.354	0.697

Table 2
(cont.)

hk·l	sin θ	nλ	d (Å)*
11·$\bar{4}$	0.197	0.350	0.890
11.$\bar{3}$·1	0.251	0.349	0.695
12.$\bar{3}$·1	0.275	0.348	0.634
13.$\bar{3}$·1	0.295	0.344	0.583
14.$\bar{2}$·3	0.354	0.344	0.486
31·5	0.250	0.341	0.682
10.$\bar{3}$·1	0.221	0.338	0.766
71·6	0.333	0.338	0.508
14.$\bar{3}$·1	0.311	0.336	0.540
8$\bar{2}$·3	0.220	0.332	0.756
3$\bar{1}$·2	0.110	0.330	1.50
12.$\bar{3}$·2	0.265	0.322	0.608
9$\bar{3}$·1	0.186	0.317	0.853
30·4	0.187	0.317	0.848
16.$\bar{3}$·1	0.338	0.317	0.469
15.$\bar{3}$·2	0.319	0.312	0.488
4$\bar{1}$·3	0.151	0.311	1.03
5$\bar{2}$·$\bar{1}$	0.105	0.306	1.46
13.$\bar{2}$·4	0.314	0.305	0.486
02·5	0.210	0.300	0.714
7$\bar{2}$·3	0.181	0.297	0.822
21·5	0.206	0.289	0.702
9$\bar{3}$·2	0.175	0.276	0.790
5$\bar{1}$·4	0.175	0.274	0.782
8$\bar{3}$·1	0.142	0.272	0.960

*Calculated with the preliminary cell dimensions a_o = 8.04 Å, c_o = 3.64 Å.

Table 3

Mg_2Tl Single Crystal Data

hk·0	observed intensity (corrected)	calculated intensity (scaled)
10.0	not obs.*	0.06
20.0	not obs.*	0.07
21.0	15.4	10.3
31.0	5.32	5.30
40.0	1.68	1.76
32.0	4.00	4.31
50.0	1.79	1.85
42.0	7.24	6.36
51.0	6.69	7.04
43.0	2.94	1.55
61.0	2.29	2.35
70.0	1.18	1.50
53.0	1.51	1.75
62.0	1.17	1.47
54.0	2.81	2.52
80.0	2.12	1.95
72.0	2.27	1.46
81.0	1.09	0.90

*In this region of the photograph there was a rather heavy background.

	1	2	3	4	5	6	7	8	9	10	11	12
1	$\frac{X_1}{2}$ / $\frac{X_2}{2}$	0.1885 1	0.1870 2	0.1890 2				0.1900 1			0.1850 1	
2	0.1430 2		0.1870 2									
3	0.1435 2	0.1425 2		0.1870 2	0.1865 2	0.1865 2	0.1860 2	0.1865 1		0.1870 2	0.1870 2	0.1845 2
4	0.1425 2				0.1865 1	0.1910 2	0.1850 2		0.1915 1	0.1905 1	0.1915 2	
5		0.1425 1		0.1405 1				0.1865 1		0.1850 1	0.1840 1	0.1875 1
6			0.1475 2	0.1510 1	0.1470 2				0.1885 2			
7			0.1390 1	0.1395 2				0.1855 1				0.1865 2
8	0.1425 2				0.1400 1		0.1395 2					
9						0.1490 2						
10	0.1435 1	0.1435 2	0.1435 2	0.1435 2	0.1430 2			0.1435 2				
11	0.1450 2	0.1450 2	0.1450 2	0.1455 2	0.1450 2							
12			0.1365 1		0.1385 1		0.1380 2					

Table 4

Curve No.	Intensity Ratio
1	40·0:31·0
2	32·0:40·0
3	50·0:32·0
4	42·0:50·0
5	51·0:42·0
6	70·0:61·0
7	53·0:70·0
8	62·0:53·0
9	54·0:62·0
10	80·0:54·0
11	72·0:80·0
12	81·0:72·0

Table 5

Mg_2Tl Powder Data

observed spacing Å	calculated spacing Å	hk·l	observed intensity (corrected)	calculated intensity (scaled)
	7.004	10.0	not obs.	0.00
3.992	4.043	11.0	11.7	4.09
3.628	3.672	00.1	≤0.38	0.18
	3.502	20.0	not obs.	0.00
3.225	3.252	10.1	6.10	3.50
2.696	2.718	11.1	1.46	1.28
2.618	2.647	21.0	≤0.37	0.09
2.516	2.536	20.1	5.99	4.19
2.320	2.334	30.0	7.21	5.63
2.139	2.143	21.1	7.32	6.15
2.010	2.021	22.0	3.47	2.73
1.963	1.970	30.1	0.45	0.63
	1.942	31.0	not obs.	0.05
1.830	1.836	00.2	1.09	1.12
1.763	1.776	10.2	0.53	0.73
	1.771	22.1		
	1.751	40.0	not obs.	0.01
1.711	1.715	31.1	3.93	3.40
1.663	1.672	11.2	3.46	2.92
	1.626	20.2	*	0.00
	1.606	32.0	not obs.	0.04
1.575	1.580	40.1	1.19	1.25
1.524	1.528	41.0	5.50	3.96
	1.508	21.2	not obs.	0.06
1.468	1.472	32.1	5.90	4.72
1.439	1.442	30.2	5.62	4.19
1.406	1.410	41.1	0.66	1.01
	1.401	50.0	not obs.	0.01
1.357	1.359	22.2	1.92	2.19
1.344	1.344	33.0	1.94	2.20
	1.334	31.2	not obs.	0.03
	1.823	42.0	not obs.	0.07
1.306	1.309	50.1	1.75	2.01
	1.268	40.2		
1.261	1.265	33.1	<0.43	0.41
	1.257	51.0		
1.242	1.245	42.1	1.89	2.38
	1.224	00.3	not obs.	0.02
1.202	1.209	32.2	0.49	0.57
	1.206	10.3		
1.188	1.190	51.1	2.32	2.66
1.173	1.174	41.2	3.36	3.42
	1.171	11.3		

Table 5 (cont.)

observed spacing Å	calculated spacing Å	hk·ℓ	observed intensity (corrected)	calculated intensity (scaled)
1.165	1.167	60.0	0.76	1.66
	1.155	20.3	< 0.47	0.67
	1.151	43.0		
1.120	1.121	52.0	2.08	2.22
	1.113	50.2		
1.110	1.112	60.1	0.68	1.06
	1.111	21.3		
1.097	1.098	43.1	0.91	1.25
1.085	1.087	33.2	1.80	1.99
	1.084	30.3		
	1.072	52.1		
1.058	1.071	42.2	< 0.39	0.44
	1.068	61.0		
	1.047	22.3	not obs.	0.09
1.034	1.037	51.2	0.49	0.77
	1.035	31.3		
1.024	1.025	61.1	0.73	1.23
1.010	1.011	44.0	1.18	0.90
	1.003	40.3		
1.002	1.001	53.0	< 0.35	0.29
	1.001	70.0		
0.9835	0.9850	60.2	1.09	1.32
	0.9774	32.3		
0.9727	0.9756	43.2	0.56	1.11
	0.9743	44.1		
	0.9710	62.0		
0.9641	0.9652	53.1	2.06	2.11
	0.9652	70.1		
0.9557	0.9568	52.2	2.33	2.21
	0.9552	41.3		
0.9378	0.9386	62.1	1.24	1.51
0.9265	0.9274	71.0	1.32	1.38
	0.9227	61.2		
0.9198	0.9214	50.3	< 0.25	0.48
	0.9180	00.4		
	0.9098	10.4	not obs.	0.00
	0.9060	33.3	not obs.	0.06
	0.8991	71.1		
0.8985	0.8984	42.3	0.62	1.11
	0.8964	54.0		
	0.8949	11.4		
0.8848	0.8880	20.4	0.92	0.85
	0.8855	44.2		

*The absence of this line was not certain because of the presence of the lines of either Mg_2Tl or Mg_5Tl_2.

Table 6

Mg_2In Powder Data

observed spacing Å	calculated spacing Å	hk·ℓ	observed intensity (corrected)	calculated intensity (scaled)
	7.209	10.0	not obs.	0.00
4.127	4.162	11.0	6.05	1.99
	3.605	20.0	not obs.	0.00
3.416	3.451	00.1	0.33	0.10
3.096	3.113	10.1	2.80	1.83
2.700	2.724	21.0	<0.19	0.16
2.647	2.657	11.1	1.24	1.16
2.481	2.493	20.1	3.36	2.78
2.390	2.403	30.0	5.82	4.05
2.131	2.139	21.1	4.42	3.67
2.072	2.081	22.0	1.64	1.27
	2.000	31.0	not obs.	0.08
1.963	1.972	30.1	0.44	0.34
	1.802	40.0	not obs.	0.01
1.776	1.783	22.1	0.60	0.53
1.723	1.730	31.1	2.31	2.28
	1.726	00.2		
	1.678	10.2	not obs.	0.00
1.647	1.654	32.0	<0.26	0.07
1.590	1.598	40.1	1.20	1.70
	1.594	11.2		
1.567	1.573	41.0	2.00	1.88
	1.556	20.2	not obs.	0.00
1.487	1.492	32.1	3.22	3.28
	1.457	21.2	not obs.	0.11
	1.442	50.0	not obs.	0.01
1.428	1.431	41.1	0.66	0.70
1.398	1.401	30.2	2.90	2.88
1.385	1.387	33.0	1.34	1.33
1.360	1.362	42.0	<0.29	0.13
1.326	1.330	50.1	2.49	2.30
	1.328	22.2		
1.304	1.306	31.2	<0.30	0.06
	1.295	51.0	not obs.	0.12
1.281	1.287	33.1	<0.30	0.14
1.266	1.267	42.1	0.87	1.16
	1.246	40.2	not obs.	0.01
1.210	1.212	51.1	1.23	1.54
1.200	1.201	60.0	0.78	0.85
	1.194	32.2	not obs.	0.03
	1.193	43.0		
1.162	1.162	41.2	1.29	1.60

Table 6
(cont.)

observed spacing Å	calculated spacing Å	hk·l	observed intensity (corrected)	calculated intensity (scaled)
1.153	1.154	52.0	0.94	1.08
	1.150	00.3		
	1.136	10.3		
1.134	1.134	60.1	0.29	0.41
1.120	1.120	43.1	0.38	0.61
1.107	1.109	11.3	<0.29	0.17
	1.106	50.2		
	1.100	61.0		
1.093	1.096	20.3	0.58	0.62
	1.094	52.1		
1.079	1.081	33.2	1.05	1.13
	1.069	42.2	not obs.	0.10
1.057	1.060	21.3	0.55	0.66
1.047	1.047	61.1	0.38	0.54
	1.040	44.0		
1.039	1.038	30.3	0.38	0.60
	1.035	51.2		
	1.030	53.0	not obs.	0.30
	1.030	70.0		
	1.007	22.3	not obs.	0.09
	1.000	62.0		
0.9961	0.9970	31.3	0.42	0.46
	0.9962	44.1		
	0.9868	70.1		
0.9858	0.9868	53.1	1.84	1.98
	0.9860	60.2		
	0.9769	43.2	not obs.	0.02
	0.9696	40.3	not obs.	0.09
0.9592	0.9602	62.1		
	0.9594	52.2	1.70	2.60
0.9539	0.9548	71.0		
0.9429	0.9443	32.3	0.56	0.58
	0.9286	41.3		
0.9275	0.9271	61.2	<0.19	0.16
	0.9229	54.0	not obs.	0.03
0.9194	0.9201	71.1	<0.19	0.18
0.9078	0.9080	63.0	0.60	0.55
0.8981	0.9012	80.0	0.18	0.15
	0.8992	50.3		
	0.8915	44.2		
0.8909	0.8915	54.1	0.80	0.68
	0.8856	33.3	not obs.	0.03
	0.8842	53.2		
	0.8842	70.2	not obs.	0.03

Table 6
(cont.)

observed spacing Å	calculated spacing Å	hk·l	observed intensity (corrected)	calculated intensity (scaled)
	0.8807	72.0		
0.8780	0.8789	42.3	0.30	0.35
	0.8783	63.1		
0.8718	0.8718	80.1	0.27	0.20
	0.8650	62.2	not obs.	0.02
	0.8627	00.4	not obs.	0.07
	0.8599	51.3		
0.8596	0.8567	10.4	0.30	0.33
0.8533	0.8533	72.1	0.32	0.35
	0.8448	11.4		
0.8438	0.8437	81.0	$\leq$ 0.11	0.15
	0.8390	20.4		
0.8354	0.8354	71.2	0.72	0.67
	0.8324	55.0		
0.8325	0.8310	60.3	0.13	0.24
	0.8270	64.0		
0.8252	0.8254	43.3	$<$ 0.09	0.12
	0.8225	21.4		
0.8195	0.8196	81.1	0.32	0.48

Table 7

Mg_2Ga Powder Data

observed spacing Å	calculated spacing Å	hk·l	observed intensity (corrected)	calculated intensity (scaled)
	6.900	00.1	not obs.	0.00
	6.764	10.0	not obs.	0.00
4.827	4.830	10.1	0.08	0.07
3.935	3.904	11.0	2.07	1.83
3.454	3.450	00.2	0.11	0.09
	3.398	11.1	not obs.	0.00
	3.382	20.0	not obs.	0.03
3.080	3.074	10.2	1.78	1.76
	3.037	20.1		
2.577	2.586	11.2	2.50	2.33
2.553	2.556	21.0	0.24	0.76
2.417	2.415	20.2	4.80	5.22
	2.397	21.1		
	2.300	00.3	not obs.	0.00
2.259	2.255	30.0	7.01	6.25
2.179	2.178	10.3	0.71	0.65
	2.143	30.1	not obs.	0.01
2.057	2.054	21.2	4.72	4.48
	1.982	11.3	not obs.	0.00
1.955	1.952	22.0	1.50	1.64
1.906	1.902	20.3	0.38	0.40
	1.887	30.2		
1.883	1.879	22.1	0.41	0.98
	1.875	31.0		
1.815	1.810	31.1	< 0.07	0.05
1.729	1.725	00.4	1.13	1.12
1.704	1.710	21.3	0.78	1.15
	1.699	22.2		
	1.691	40.0	not obs.	0.07
	1.671	10.4	not obs.	0.04
1.649	1.648	31.2	1.09	1.08
	1.642	40.1		
	1.610	30.3	not obs.	0.00
1.579	1.578	11.4	0.52	0.51
1.552	1.552	32.0	0.16	0.16
	1.537	20.4	not obs.	
1.516	1.518	40.2	0.35	0.37
	1.513	32.1		
	1.488	22.3	not obs.	0.00
1.477	1.476	41.0	2.41	2.42
1.454	1.454	31.3	0.75	0.73
	1.442	41.1	not obs.	0.04
1.430	1.429	21.4	0.46	0.44
1.415	1.415	32.2	4.83	4.88
	1.380	00.5	not obs.	0.00

Table 7
(cont.)

observed spacing Å	calculated spacing Å	hk·l	observed intensity (corrected)	calculated intensity (scaled)
1.372	1.370	30.4	3.14	3.17
	1.362	40.3		
	1.357	41.2		
1.356	1.352	10.5	0.69	0.82
	1.355	50.0		
	1.326	50.1	not obs.	0.03
1.302	1.301	11.5	1.32	1.29
	1.301	33.0		
1.290	1.293	22.4	0.14	0.93
	1.286	32.3		
	1.279	33.1		
1.277	1.278	20.5	0.48	0.75
	1.278	42.0		
1.269	1.270	31.4	< 0.12	0.30
1.259	1.259	50.2	1.71	2.08
	1.257	42.1		
	1.242	41.3	not obs.	0.02
	1.218	33.2		
1.215	1.214	21.5	0.98	1.17
	1.214	51.0		
	1.207	40.4	not obs.	0.11
1.199	1.198	42.2	1.09	1.08
	1.196	51.1		
	1.177	30.5	not obs.	0.00
1.166	1.166	50.3	< 0.13	0.15
1.156	1.153	32.4	< 0.13	0.16
	1.150	00.6		
1.146	1.145	51.2	1.83	1.69
	1.133	10.6	not obs.	0.05
	1.133	33.3	not obs.	0.00
1.128	1.127	22.5	0.46	0.63
	1.127	60.0		
1.121	1.121	41.4	0.76	0.99
	1.117	42.3		
	1.112	60.1		
1.113	1.111	31.5	0.23	0.47
	1.111	43.0		
1.103	1.103	11.6	0.15	0.20
	1.097	43.1	not obs.	0.04
1.090	1.092	20.6	0.20	0.30
	1.083	52.0		
1.083	1.080	51.3	0.87	1.43

Table 7
(cont.)

observed spacing Å	calculated spacing Å	hk·ℓ	observed intensity (corrected)	calculated intensity (scaled)
	1.071	60.2		
	1.070	52.1		
1.073	1.070	40.5	<0.13	0.41
	1.064	50.4		
1.058	1.058	43.2	≤0.13	0.21
1.049	1.049	21.6	0.16	0.22
1.038	1.039	33.4	0.62	0.55
	1.033	52.2		
1.031	1.031	61.0	0.30	0.38
	1.031	32.5		
	1.027	42.4		
1.027	1.024	30.6	≤0.17	0.23
	1.020	61.1	not obs.	0.01
	1.012	60.3	not obs.	0.02
	1.007	41.5	not obs.	0.01
1.001	1.001	43.3	0.24	0.29
	0.9932	51.4		
0.993_8	0.9910	22.6	0.16	0.22
	0.9882	61.2		
0.988_2	0.9857	00.7	0.37	0.39
	0.9804	31.6	not obs.	0.04
	0.9805	52.3	not obs.	0.02
	0.9758	10.7		
0.976_1	0.9760	44.0	0.54	0.56
	0.9665	44.1		
	0.9662	70.0		
0.966_2	0.9662	53.0	0.11	0.22
	0.9660	50.5		
	0.9567	70.1		
	0.9567	53.1	not obs.	0.02
	0.9560	11.7		
	0.9510	40.6	not obs.	0.00
	0.9469	33.5	not obs.	0.00
	0.9465	20.7	not obs.	0.07
	0.9435	60.4		
0.943_4	0.9407	61.3	0.25	0.42
	0.9395	44.2		
0.937_5	0.9377	42.5	0.29	0.63
	0.9375	62.0		
	0.9346	43.4		
	0.9304	53.2		
0.929_5	0.9304	70.2	0.98	0.98
	0.9297	62.1		

Table 7
(cont.)

observed spacing Å	calculated spacing Å	hk·l	observed intensity (corrected)	calculated intensity (scaled)
	0.9239	32.6		
0.923_1	0.9220	21.7	0.31	0.48
0.916_5	0.9172	52.4	0.38	0.55
0.911_0	0.9117	51.5	0.26	0.24
	0.9071	41.6	not obs.	0.02
	0.9051	62.2		
0.904_5	0.9051	30.7	1.03	0.80
	0.8986	44.3	not obs.	0.00
0.894_8	0.8958	71.0	0.65	0.62
	0.8908	53.3		
0.890_0	0.8908	70.3	0.20	0.27
	0.8887	71.1		
	0.8852	61.4	not obs.	0.04
	0.8798	22.7	not obs.	0.00

(1) L. Pauling, Proc. Roy. Soc. (London), A 196, 343 (1949).

(2) L. Pauling, J.A.C.S., 69, 542 (1947).

(3) W. Haucke, Naturwiss., 26, 577 (1938).

(4) G. Grube and J. Hill, Z. Elektrochem., 40, 101 (1934).

(5) N. A. Pushin and O. D. Micic, Z. anorg. Chem., 234, 229 (1937).

(6) K. Weckerle, Dissertation, Freiburg, 1935.

(7) E. Zintl and G. Brauer, Z. phys. Chem., B 20, 245 (1933).

(8) J. J. deLange, J. M. Robertson, and I. Woodward, Proc. Roy. Soc. (London), A 171, 398 (1939).

(9) "International Tables for the Determination of Crystal Structures, Gebruder Borntraeger, Berlin, 1935, Vol. II, pp. 583-585.

(10) J. B. Nelson and D. P. Riley, Proc. Phys. Soc. (London), 57, 160 (1945).

(11) M. Straumanis and O. Mellis, Z. Physik, 94, 185 (1935).

(12) A. Taylor and H. Sinclair, Proc. Phys. Soc. (London), 57, 126 (1945).

(13) L. Pauling, J. Chem. Soc., 1461 (1948).

(14) Handbuch Der Metallphysik, Vol II, Leipzig (1937), p. 231 ff.

(15) M. Renninger, Z. Phys., Lpz., 106, 141 (1937).

II. METALLIC VALENCE AND X-RAY EMISSION FINE STRUCTURE: A DISCUSSION

Metallic Valence and X-ray Emission Fine Structure: A Discussion

Theories of modern structural chemistry find many severe tests in the field of metals and alloys. In addition to questions concerning ordinary physical properties, ductility, malleability, mechanical strength, thermal and electrical conductivity, etc., there is the central question as to the reason for the existence of the various observed structure types which can vary in complexity from the cubic or hexagonal closest packing of identical spheres to the structure of $NaCd_2$, which is reported to be based on a unit cell containing nearly twelve hundred atoms[1]. One necessary subdivision of the existence question is concerned with valence, in other words, how many strongly bonding electrons does a given atom contribute in any particular metallic or intermetallic structure. In some cases such classical chemical quantities as oxidation numbers and stoichiometric proportions seem to provide a satisfactory answer; for example, the metallic valences which are predicted for the alkali and alkaline earth metals from these quantities, one and two respectively, seem to be correct. On the other hand, although in classical chemistry the valences of iron are given as two and three, convincing physical evidence has been found recently for the belief that the metallic valences of iron are as high as five and six[2a], [2b], [2c]. Iron is, of course, not unique

in this respect; most of the other transition group elements* apparently have greater valences in the metallic state than was heretofore imagined.

In view of the importance, the generality, and the unexpectedness of the recent discoveries concerning metallic valences it is worthwhile to search for additional experimental evidence bearing upon them. The following discussion is concerned with a promising physical method for the determination of valence, namely, the analysis of the fine structure of the X-ray emission spectra of solids. In the cases of such metals as sodium, aluminum, and magnesium, this method has given the correct answer; the extension of the method to the more interesting transition group elements is difficult and must be examined with care.

It is well known that the gross features of the X-ray emission spectrum of a given element are not affected by chemical or physical changes. Closer examination of spectral details, however, reveals the existence of small effects, especially in the highest frequency line of a given emission series**. In these instances one of the states concerned in

---

*The use of this term is that of L. Pauling (General Chemistry, Freeman and Co., San Francisco, 1947, p. 146). The elements of the first transition series, for example, are Sc to Zn.

**See, for instance, Manne Siegbahn, "Spektroskopie der Roentgenstrahlen", Second Edition, Julius Springer, (Berlin) 1931, pp. 160 ff., 278 ff.

a particular electronic transition is an outer state; one in which the electron is for the most part relatively far removed from the nucleus in question, and it is understandable that the energy of such a state should be perturbed appreciably by neighboring atoms. The perturbations arising from adjacent atoms are large in metals and the energy of a particular outer atomic state is given a nearly continuous set of values over a range which is of the order of several electron volts, such a set being called a band. A line emitted as a result of transitions from outer occupied states in a metal, therefore, is much wider than in the case of the corresponding gaseous spectral line, with a fine structure which is dependent upon the nature of the interatomic interactions.

The fine structure of a broadened solid spectral line is related explicitly to the energy distribution of outer occupied electronic states in the following manner. If the energy range of the inner state concerned is assumed to be negligibly small, at absolute zero:

(1) $I(E) \propto \nu^3 P(E) N(E), \quad E \leq E_m$

(2) $I(E) = 0, \quad E > E_m$

The number of outer electronic states in the energy range E to E + dE is given by N(E)dE; I(E) is the intensity of radiation emitted with spontaneous transitions from outer electronic states in the range E to E + dE; P(E) is the

square of the electric dipole moment integral*; and E_m is the maximum energy of the filled levels. If the form of the function P(E) were known, Equation 1 would enable N(E) to be found directly from the measurement of I(E). There is, however, a theoretical limit to the resolution of the features of the distribution function which arises from the finite width of the inner level, radiation damping, and Auger effects; features of the function which are within 1 ev of one another cannot be resolved in the X-ray region which extends from a few Angstroms upwards[3].

The function P(E) is generally difficult to determine, but a convenient reduction of the problem can be made[4], [5]. The form of P(E) is given by $\left|\int \psi_i \psi_v x \, d\tau\right|^2$** and it is reasonable to assume that ψ_i, the wave function of an inner state, is localized about each nucleus without appreciable perturbations from neighboring atoms***. In order to evaluate P(E), therefore, it is necessary to calculate the outer wave function, ψ_v, only in the immediate neighborhood of each

---

*It has been assumed by most workers that the probabilities of transitions which violate the electric dipole moment selection rules are negligible.

**If the outer electronic states are degenerate, P(E) should be represented by a weighted average of terms of this type.

***This assumption may be open to question; Parratt[6], for example, found that the half widths of the Kα lines of Mn, Fe, Cr, and Ni can be varied by as much as 23 percent by alloying.

nucleus. In the neighborhood of a nucleus ψ_v can be expanded as a series of functions ψ_s, ψ_p, ψ_d ..., the s, p, d wave functions of the free atom. Thus,

(3) $$\psi_v = A_s\psi_s + A_p\psi_p + A_d\psi_d + \ldots$$

If now ψ_i is an s function, as it is in the instances of K or L_I* spectra,

(4) $$\left|\int \psi_v \psi_s x\, d\tau\right|^2 = P_{ps}^2 A_p^2(E) = P(E).$$

For L_{II} or L_{III} spectra,

(5) $$P(E) = \left\{P_{sp} A_p^*(E) + P_{dp} A_d^*(E)\right\}^2$$

Since the functions P_{ps}, P_{sp}, etc. are to be regarded as independent of the energy of the outer wave functions, and as known for each given type of atom, the problem of the form of P(E) has been reduced to the determination of the functions $A_s(E)$, $A_p(E)$, etc.

Alkali and Alkaline Earth Metals

In the case of metals such as lithum, sodium, beryllium, magnesium, and aluminum, low energy electrons in the band formed from the outer atomic s states, the valence band, can be regarded to move in a field of nearly constant potential energy within a given specimen and in a field of very much higher or infinite potential energy outside the specimen.

---

*For an explanation of these symbols see Compton and Allison, "X-Rays in Theory and Experiment", D. Van Nostrand Co., (New York) 1935, p. 630.

The wave functions in this instance can be given the form $\exp\left\{2\pi i(\underset{\sim}{k}\cdot\underset{\sim}{r})\right\}$ (7) where the vector $\underset{\sim}{r}$ locates a particular point in the metal specimen with reference to an origin which may be arbitrarily chosen and $\underset{\sim}{k}$ is a vector having a discrete set of values which depend upon the dimensions of the metal specimen. (For metals based on a cubic lattice the specimen is usually considered to be a cube as a matter of convenience.) The distribution function N(E) has a parabolic form,

$$(6)\quad N(E) = \frac{2\pi M}{h^3 \rho N}(2m)^{3/2}(E - E_o)^{1/2}$$

where M is the atomic weight, ρ is the density, N is Avogadro's number, m is the electronic mass, and E_o is the energy of the lowest valence state.

As the kinetic energy of the valence electrons increases, however, a region is encountered in which the electrons, considered as de Broglie waves, can undergo a Bragg reflection as a result of interactions with the crystal lattice; in this region N(E) fluctuates markedly from the parabolic form of Equation (6). This situation can be treated more precisely if a <u>k space</u> is conceived in which vectors drawn from the origin to a set of points based upon an appropriate lattice are the vectors $\underset{\sim}{k}$. If the metal specimen is a cube with edge length La, such a lattice is cubic with a period $\frac{1}{La}$ along each axis, and the corresponding components of k have the form $\frac{n}{La}$, where n and L are integers. We shall

assume that the crystal lattice is cubic; the crystal lattice is aligned with the k space lattice in such a manner that the points ($\frac{n_1}{a}$, $\frac{n_2}{a}$, $\frac{n_3}{a}$) in k space form the reciprocal lattice of the crystal. An electron in the state $\exp\{2\pi i(\underset{\sim}{k}\cdot\underset{\sim}{r})\}$ can be reflected according to the Bragg condition from the crystallographic plane (l m n) if $\underset{\sim}{k}$ touches a plane which is at a distance

$$\left[\left(\frac{ls}{2a}\right)^2 + \left(\frac{ms}{2a}\right)^2 + \left(\frac{ns}{2a}\right)^2\right]^{1/2}$$

from the origin, with a unit normal vector

$$\left[\left(\frac{ls}{2a}\right)^2 + \left(\frac{ms}{2a}\right)^2 + \left(\frac{ns}{2a}\right)^2\right]^{-1/2} \cdot \left[\frac{la}{2a}\underset{\sim}{b}_1 + \frac{ma}{2a}\underset{\sim}{b}_2 + \frac{na}{2a}\underset{\sim}{b}_3\right],$$

where $\underset{\sim}{b}_1$, $\underset{\sim}{b}_2$, and $\underset{\sim}{b}_3$ are unit vectors directed along the axes of the k lattice. If the angle between the vector k and the unit normal vector is $\frac{\pi}{2} - \theta$,

$$(7)\quad |\underset{\sim}{k}| \sin\theta = \left[\left(\frac{ls}{2a}\right)^2 + \left(\frac{ms}{2a}\right)^2 + \left(\frac{ns}{2a}\right)^2\right]^{1/2}$$

The de Broglie wave length of the electron considered is $|\underset{\sim}{k}|^{-1}$ and its momentum is therefore $h|\underset{\sim}{k}|$. Thus

$$(8)\quad E - E_0 = \frac{p^2}{2m} = \frac{h^2}{2m}|\underset{\sim}{k}|^2 = \frac{h^2}{2m\sin^2\theta}\left[\left(\frac{ls}{2a}\right)^2 + \left(\frac{ms}{2a}\right)^2 + \left(\frac{ns}{2a}\right)^2\right] = \frac{h^2}{2m\lambda^2}$$

$$(9)\quad \text{Therefore, } s\lambda = \frac{2a\sin\theta}{(l^2+m^2+n^2)^{1/2}} = 2d_{lmn}\sin\theta$$

Since the crystallographic plane (l m n) is perpendicular to the vector ($\frac{ls}{2a}\underset{\sim}{b}_1 + \frac{ms}{2a}\underset{\sim}{b}_2 + \frac{ns}{2a}\underset{\sim}{b}_3$) from the properties of the reciprocal lattice, Equation (9) is the condition for Bragg reflection from (l m n).

If E($\underset{\sim}{k}$) is plotted against $|\underset{\sim}{k}|$, the k's being collinear, a parabolic curve, given by Equation (6), is obtained until $\underset{\sim}{k}$,

drawn from the origin in k space, is in the neighborhood of a plane corresponding to a crystallographic plane (l m n). In this neighborhood the curve flattens sharply and has a discontinuity when $\underset{\sim}{k}$ lies in the plane. As $\underset{\sim}{k}$ increases, the curve, still flat, quickly increases in slope until the parabolic law is again satisfied. This behavior is in general repeated for each plane as $\underset{\sim}{k}$ is further increased. Discontinuities along different lines in k space may overlap; that is, energies which are forbidden an electron traveling along a certain direction may be allowed for another direction.

Mott and Jones[8] have shown that in the case of a monatomic solid and loosely bound electrons the magnitude of each discontinuity is roughly proportional to the structure factor for Bragg reflection from the corresponding crystallographic plane. Discontinuities are non-existent when corresponding structure factors are exactly zero. In the case of a polyatomic solid this proportionality is assumed, but may be in serious error[9], [10].

The planes of energy discontinuity in k space form a series of polyhedra, concentric about the origin. For a primitive cubic lattice, the first of such polyhedra is generally a cube defined by the crystallographic planes $\{100\}$. This polyhedron is then called the first Brillouin zone and its boundaries Brillouin zone boundaries. The space

between the dodecahedron defined by the crystallographic planes {110} and the cube {100} forms the second Brillouin zone, and so on. In the primitive cubic case, with no vanishing structure factors, each zone contains 2N (twice the number of unit cells of the cubic block) electronic states, when spin degeneracy is taken into account.

When the electrons of the valence band are loosely bound, theory predicts an N(E) function of the types shown in Figure 1. At small kinetic energies the curves follow the parabolic law, Equation (6). As the kinetic energy is increased and $\underset{\sim}{k}$, drawn from the origin in k space, approaches the first zone boundary, the N(E) curve rises sharply to point P. At a point in the neighborhood of P, the total number of states with lower energies are given by the number of points of the k space lattice which lie within the inscribed sphere of the first zone polyhedron[11]. As the energy is increased the N(E) curve falls sharply to point K because of the energy discontinuity at the zone boundary. The N(E) curve rises sharply from K because of the contribution of states in the second zone.

A detailed consideration of the function P(E) indicates that points P and K of Figure 1 cannot both be found in one emission band[5], and, therefore, that the K and L_{III} emission curves of an element for which N(E) is appreciably greater than zero at point K should differ greatly in appearance. Aluminum and magnesium both have filled zones and

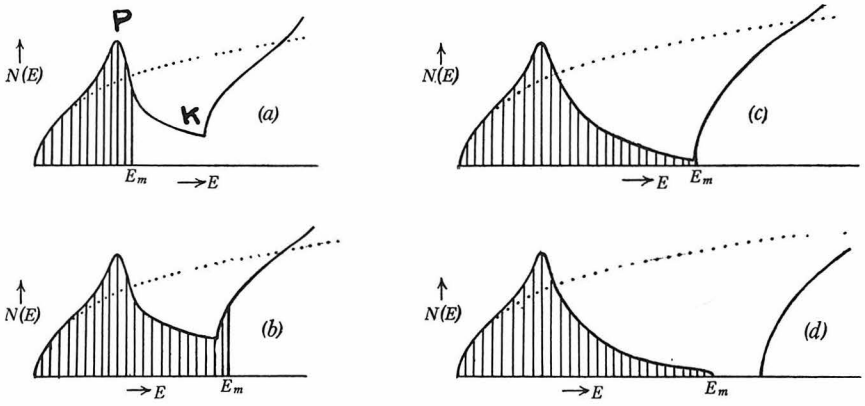

Figure 1

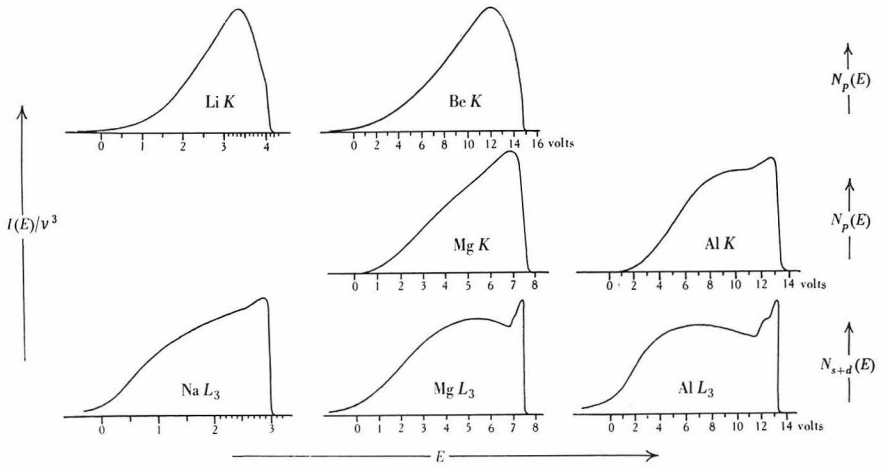

Figure 2

in each case the K and L_{III} emission bands differ in appearance, as can be seen in Figure 2. Further consideration of P(E) shows that, at low energies, I(E) should vary as $(E - E_o)^{3/2}$ and $(E - E_o)^{1/2}$ in the K and L_{III} bands, respectively[3], [5]. On the other hand, the curves of Figure 2, especially the L_{III} curves, extend toward very low frequencies with a small but finite ordinate. This behavior has been explained by advanced considerations of the radiation processes of solids which are quite beyond the scope of this discussion[5]. The high frequency edges of the bands shown in Figure 2 have nearly infinite slopes in accordance with Fermi-Dirac statistics.

The widths of the bands of Figure 2, as measured by Skinner[3], are given in Table 1 together with valences calculated from them with the use of Equation (6)*.

Table 1

Metal	Band	Measured Breadth (ev)	Calculated valence
Li	K	4.1 ± 0.3	0.77
Be	K	14.8 ± 0.5	2.02
Na	L_{III}	3.0 ± 0.2	0.88
Mg	K	7.3 ± 1	2.02
Mg	L_{III}	7.6 ± 0.3	2.14
Al	K	12.7 ± 1	3.32
Al	L_{III}	13.2 ± 0.5	3.52

---

*Skinner obtained the low frequency edges of the bands, that is, E_o by the linear extrapolation of the L_{III} tails to zero; K tails were extrapolated by the use of an E^2 form. This seems to have been done on the basis of expediency.

The agreement between observed valences and those ordinarily assigned to these elements is very good, even in the cases of beryllium, magnesium, and aluminum, where marked deviations in the form of the N(E) curve from that of Equation (6) must occur at filled zone boundaries.

The only investigation of alloys between the metals of Table 1 has been made by Farineau, who studied the alloys Mg_3Al_2 and Al_3Mg_2[12]. The L_{III} bands of the two components were found to be superposable in both cases, indicating that an electron of the valence band can approach either type of atom with nearly equal probability. The observed widths of the bands of the two alloys are identical, 11.5 ±1.5 ev, which differs somewhat from the corresponding widths for Mg_3Al_2 and Al_3Mg_2 calculated with the assumption of normal valences by application of Equation (6), 9.0 ev and 9.4 ev, respectively.

Transition Group Metals

The outer electrons of transition group metals are more tightly bound than in the case of the alkali or alkaline earth metals and it would be unsound to assume that the distribution function N(E) follows the parabolic law of Equation (5) even at low kinetic energies. Various theoretical calculations of N(E) have been made for transition metals with the use of the molecular orbital approximation, and some degree of experimental verification has been claimed.

Prominent features of N(E) calculated for copper by Rudberg and Slater[13] can be placed in correspondence with prominent features of K emission and absorption curves for copper, as has been shown by Beeman and Friedman[14]: on the other hand, the experimental verification of the Manning-Chodorow distribution function for tungsten[15] has not been carried through as successfully[16]. The theoretical N(E) curve of Rudberg and Slater shows that the energies of all the outer, that is, 3d and 4s electrons lie in a continuous band for copper, but this does not mean that all the outer electrons are necessarily valence electrons. There is good evidence, in fact, that of 5.44 of the eleven outer electrons of copper are valence electrons. This conclusion is a result of a general scheme for the distribution of the outer electrons of transition group metals which has been proposed by Pauling[2a]. In this distribution the outer electrons are considered to be divided into two overlapping bands. The first band contains electronic states which cover a large range of energy with a small density; the second band has a small energy range with a high density of states and overlaps the first band at the high energies. The electrons of the broad band are valence electrons, while those of the narrow band are tightly bound to individual atoms and do not contribute appreciable to binding. In fact, although Fermi-Dirac statistics governs the filling of the states of the valence band, the electrons of the narrow

non-bonding band tend to remain unpaired with parallel spins in accordance with Hund's rule of maximum multiplicity and are responsible for ferromagnetic properties. Now the presence of a narrow band of tightly bound electrons overlapping in energy a broad valence band might well be expected to render the experimental determination of the distribution of occupied states in the valence band difficult or impossible. In addition, the effects of gross changes in crystal structure upon the distribution of states in the valence band could be at least partially obscured by the presence of a relatively unchanging distribution of tightly bound states. Furthermore, changes in I(E) where no overlapping occurs might not be apparent because of the relatively low density of occupied states in the valence band. The nature of the emission band studied is important, to be sure. Pauling has indicated that the states of the narrow, non-bonding band are formed from atomic d states[2a]; therefore, it might be assumed that, if a K emission band were studied, the complications described above could be avoided because of the dipole selection rules. There is a certain amount of experimental evidence, however, which indicates that this method of attack is unavailing. Bearden and Friedman[17] have studied several alloys in the copper-zinc system and found only small systematic changes in K spectral detail with composition, although corresponding structural changes are gross and unsystematic. It is quite possible then,

that the quantities A_s and A_p in the expansion of Equation (3) are rather appreciable for the wave functions of the non-bonding band. A certain percentage of the observed intensity might result from electric quadropole transitions which in some cases have a probability of about one-tenth that of dipole transitions[18]; the selection rules for this type of transition of course, permit d - s transitions. Studies of transition metals and alloys between transition metals, therefore, would seem rather fruitless as sources of information concerning the distribution of occupied states in the valence band; this conclusion may be premature because of the small amount of experimental information available, but it is certain that such studies can be made fruitful only after formidable complications have been overcome.

It is possible, however, to gain information concerning the valences of transition elements from spectral studies without regard for the difficulties in the interpretation of transition element emission bands. In order to explain this statement let us consider the probable nature of the emission bands of both components in an alloy of the copper-~~nickel~~ aluminum system. The copper emission band would be expected to result from transitions involving states of both the broad valence band and the narrow non-bonding band in accordance with the previous discussion. On the other hand, it seems plausible that there should be no appreciable

contributions to the aluminum emission band from transitions of the copper non-bonding stetes. Since there are no non-bonding states centered about aluminum atoms in the energy region concerned, the aluminum emission band should be the result of transition from valence states alone. Consideration of the observed form of the aluminum emission band should thus lead to some information about the distribution of valence states in the alloy.

Farineau has investigated the fine details of the outermost emission bands of aluminum-copper and aluminum-nickel alloys[19]. His spectral curves are shown in Figure 3. The copper emission bands shown are $L\alpha$ bands, that is, the transitions involve outer occupied states and inner atomic p states. Accordingly, the masking effect of the outer narrow non-bonding band would be expected to be large; however, considerable changes in spectral detail with changes in aluminum content are to be seen. (Curves I to VII contain 0, 19, 35, 49, 60, 82, and 96 atomic percent of aluminum, respectively.) No attempt will be made to discuss the features of these curves. The nickel $L\alpha$ emission bands, in contrast to those of copper, show little detail, as would have been predicted in the present discussion.

The aluminum $K\beta_x$ emission bands of Figure 3a possess a considerable amount of structure which suggest fluctuations in corresponding N(E) functions at the surfaces of important Brillouin zone boundaries. It is of interest,

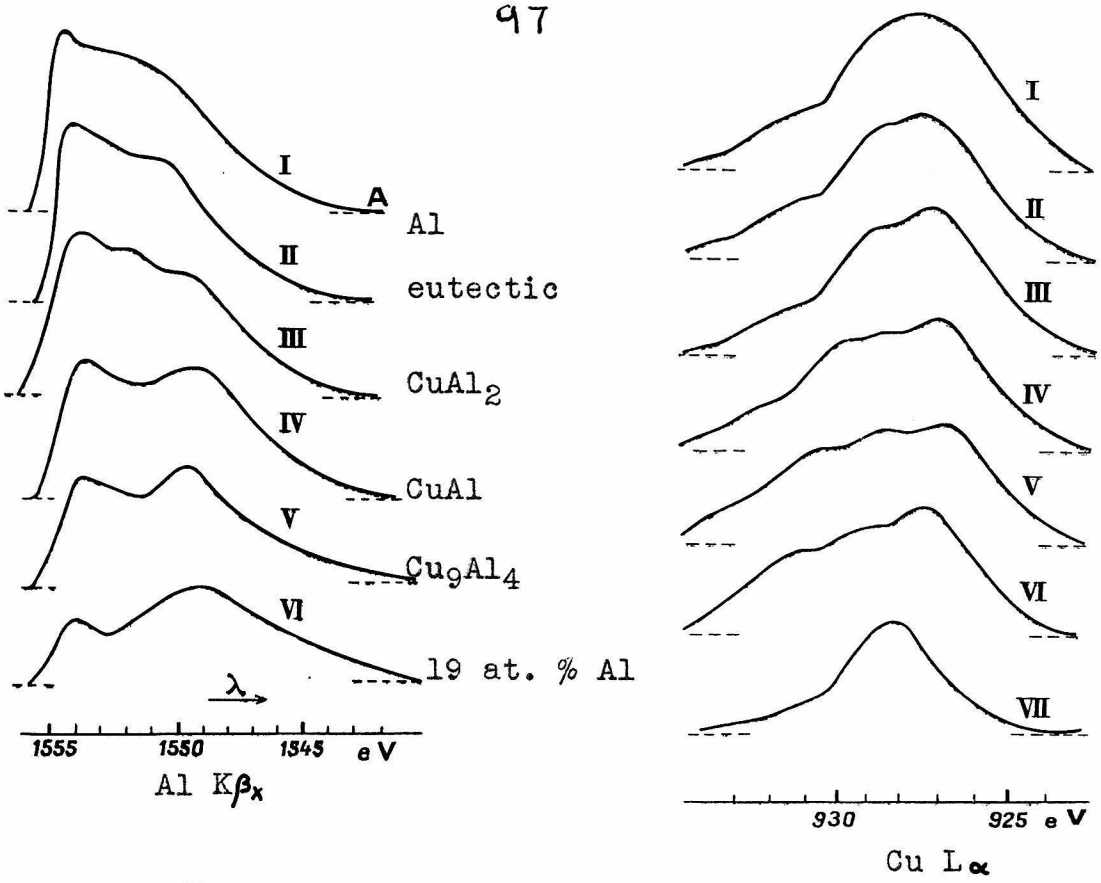

Figure 3a: Copper-Aluminum

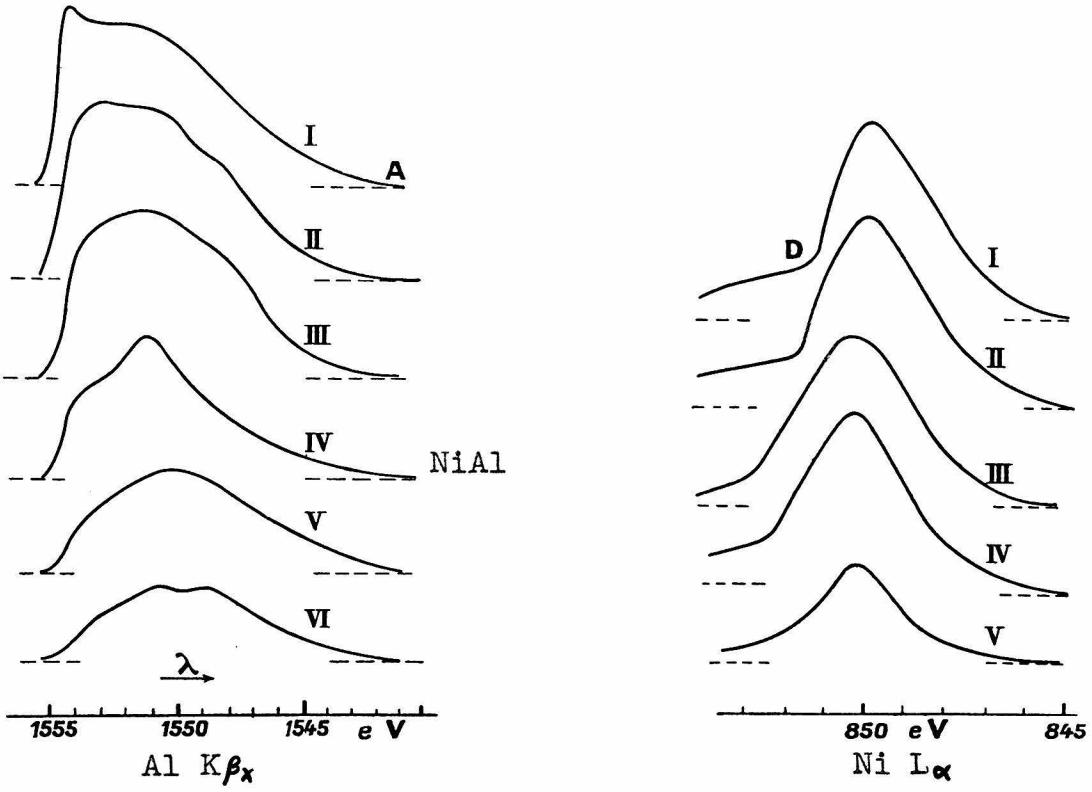

Figure 3b: Nickel-Aluminum

accordingly, to find the important zone boundaries for the valence bands of each of these alloys. This is done in the following manner. The importance of a given boundary is estimated from the magnitudes of the structure factors of the set of planes involved; this procedure has been discussed previously*. Next, the extent to which an important zone is filled by occupied states is estimated by calculating the number of states in the inscribed sphere of the zone polyhedron. If the number of valence states is greater than the number of states contained by the inscribed sphere, the zone is at least approximately filled**. At the value of the energy for which the occupied states just fill the inscribed sphere, the N(E) curve rises to a maximum, the points P of Figure 1[8]. When the next zone overlaps appreciably and the region of occupied states extends well into it, the points of discontinuity K of Figure 1 are contained in the filled portion of the N(E) curve. In general it is difficult

---

*In many cases it is either inconvenient or impossible to calculate structure factors. The alternate procedure in these cases is to use observed intensities, if possible, corrected with frequency factor, and, in any event, corrected with the appropriate Lorentz and polarization factors.

**The number of states in an inscribed sphere is calculated from the volume of the sphere and the density of states in k-space, 2V, where V is the volume of the crystal parallelepiped with the edges La, Mb, and Nc in the orthorhombic case.

to calculate the function $E(\underline{k})$. In the discussion of the features of the aluminum bands of Figure 3, the free electron approximation will be used to calculate the positions of the points P, with the recognition that this approximation may be quite crude.

In Tables 2-7 the calculations outlined in the preceding paragraph are given for the substances Al, Cu_2Al, CuAl, Cu_9Al_4, 19% Al-Cu solid solution (α phase) and NiAl. In the first column of each table the indices of the observed reflections are given; in the second, the uncorrected observed intensities; in the third, the Lorentz and polarization factors; in the fourth, the frequency factor; in the fifth, the number of states per unit cell (crystallographic unit cell) in a sphere tangent to the corresponding set of planes in the first column; in the sixth, the radius of the sphere in Å^{-1} units; and in the seventh, the value of $E(\underline{k}) - E(o)$ calculated from the radius of the inscribed sphere with the use of the free electron approximation.

The number of occupied states in the valence bands of each of the alloys is calculated in two ways. The first value is obtained with the use of 5.44 for the valence of copper and 5.76 for the valence of nickel; these are the valences proposed by Pauling[2a]. The second value is derived from the assumption of the valences 1 and 0.6 for

copper and nickel respectively, following Mott and Jones[20]*.

Inspection of Tables 2-7 shows that important Brillouin zones of the different structures are filled with either set of valences. In general, however, there is better correspondence between the features of the emission bands and the filled-zone scheme obtained with the larger valences. The form of the aluminum emission band for the intermetallic compound $CuAl_2$ suggests that at least two, and perhaps three important zones are filled. From Table 3 it is seen that the inscribed spheres of the two most important sets of planes $\{22\cdot0\}$, $\{11\cdot2\}$, and $\{31\cdot0\}$, $\{20\cdot0\}$ can be filled with either set of valences. The sphere inscribed in the polyhedron bounded by the planes $\{31\cdot0\}$, $\{20\cdot2\}$ contains 27 states per unit cell; the number of occupied states with the valences of Mott and Jones is 28, hardly more than enough to fill the inscribed sphere. It might be reasonably expected, therefore, that the emission band would exhibit two instead of the observed three maxima, if the idea of

---

*It has recently been shown by Pauling[2c], [2d] that the valences of copper and nickel can assume a variety of values, the maximum values being about 7.0 and 6.0 respectively. The use of the valence 5.44 for copper has been previously justified for the γ-brass structure, Cu_9Al_4[10], and the interatomic distances found in the structure of $CuAl_2$[21] are consistent with valence 5.44 for copper. The structure of CuAl is unknown[22] and a check of the valences from structural data is impossible. It seems likely that the valence of copper in the 19% Al α-brass structure is also 5.44.

monovalancy for copper is correct. If the valence of copper is about $5\frac{1}{2}$, however, the number of filled states greatly exceeds that contained by the second sphere, and three maxima in the emission curve would be expected, the third maximum resulting from the abrupt decrease in the number of filled levels in the region of maximum energy due to Fermi-Dirac statistics. The positions of the two maxima which are to correspond to the filling of the two inscribed spheres are calculated to be 8.6 and 10.1 ev, respectively, from the low frequency edge of the emmission band. (In calculating these positions the free electron approximation is assumed as before stated, with the additional assumption that the low frequency edge of the emission band corresponds to a transition from the lowest state of the valence band.) The respective observed maxima seem to be about 7.5 and 10.0 ev from the low frequency length edge, if we may take the edge as given by the long wave length extremity of the curve in Figure 3a*. The correspondence between calculated and

---

*This seems a reasonable choice, especially from comparison with the indicated edge for the band of 100% Al, the point A in Figure 3. Farineau does not report his low frequency edges explicitly. He does state, however, that the observed maxima in question lie between 5 and 6 ev and at 8.5 ev, respectively, from the low frequency edge. An inspection of the curve for $CuAl_2$ given in Figure 3a shows that, if the positions reported by Farineau are correct, the low frequency edge would be situated at some distance to the left of the indicated extremity. The values reported by Farineau thus seem in error; one explanation for this discrepancy might lie in Farineau's desire to ascribe the first maximum to the presence of a filled sphere inscribed to the set {20·0} , {00·2} at calculated energies 4.2 - 6.1 ev. As Table 3 shows {20·0} and {00·2} are much less prominent than either {22·0} , {11·2} , or {31·0} , {20·2} .

observed positions is as good as can be expected in view of the roughly approximate nature of the calculation. The calculated width for 45.8 occupied states per unit cell is 14.7 ev, which seems somewhat high.

It is difficult to choose important planes in the case of CuAl. For one thing, the intensities of the planes have been reported on a qualitative basis only. For another, there are a large number of closely spaced, heavily reflecting planes. An appreciable concentration of important planes seems to occur in the vicinity of the planes 200, however, and the first marked fluctuation in the N(E) curve may occur at this point, calculated to be 8.6 ev from the low frequency edge. The observed maximum is about 8.0 ev from the edge, in reasonable agreement. The inscribed sphere to the planes 200 contains 49 states, and is filled in either valence scheme. If copper is monovalent in this structure, however, it is hard to understand why there are two very pronounced maxima with one broad minimum in the observed emission curve. The free electron width for 64 occupied states per unit cell is only 10.4 ev, which is about the position of the minimum of the observed curve. The assumption of the higher valence for copper can explain the shape of the curve very well -- there is again a discrepancy, even more pronounced than in the first case, between calculated and observed widths, 17.0 ev and about 14 ev, respectively.

The Brillouin zones of the Hume-Rothery γ-phases are well known[10]. The first important zone is formed by the

planes {411} , {300} , and the second by the planes {600} , {442} . The inscribed sphere of the first zone would just be filled, with the monovalent assumption; both inscribed spheres are filled with the use of the valence 5.44. The calculated position of the maximum which corresponds to the filling of the first sphere is 8.9 ev, the valculated position of the second maximum is 17.8 ev. The observed emission curve shows two maxima, one at approximately 8.9 ev and one near the high frequency edge of the curve at about 13.5 ev. It would again be difficult to understand the presence of two maxima in the observed curve if copper were assumed to be monovalent since the first inscribed sphere contains 80 of the 84 occupied states. Again, the discrepancy between the observed width, c.a. 14.5 ev, and that calculated with the 5.44 valency, 19.2, is quite pronounced.

In order to carry out a discussion of the 19% Al-Cu solid solution, it will be necessary to assume that the method of determining the importance of a given plane, i.e. the magnitude of the energy discontinuity in the region of k-space adjoining it, is not to be altered because of the existence of a disordered arrangement of atoms in the structure. This assumption seems plausible because the relative magnitudes of the structure factors are unchanged by the existence of a solid solution.

The only planes with a finite structure factor are {111} , {200} , {220} , etc. The sphere inscribed to the {111} planes

contains 5.4 of the 5.5 occupied states calculated with the Mott and Jones valences. It would be predicted, therefore, that the observed emission curve should exhibit but one maximum, actually two are observed, at 9.0 and 14.0 ev, respectively. The appearance of the emission curve is thus more reasonably explained with the assumption of 5.44 ($5\frac{1}{2}$) valent copper. Again, the calculated position of the first maximum, 8.4 ev, agrees well with the observed position. As before, with the high valent copper, the width of the emission curve is less than the width of the filled portion of the free electron N(E) curve; the discrepancy between calculated and observed widths, 20.0 ev and c.a. 15 ev, respectively, is very large.

The general appearance of the aluminum emission curves for the copper alloys is, then, more reasonably explained if the metallic valence of copper is assumed to be much greater than the value 1, which was commonly accepted a few years ago. It is somewhat difficult to estimate the precise valences exhibited by copper in the various structures, however. With increasing copper contents the free-electron widths calculated with the assumption of 5.44 ($5\frac{1}{2}$) valent copper become progressively larger than the observed widths, which are approximately constant. This would indicate that the valence exhibited in each case is much smaller than $5\frac{1}{2}$, being close to 3. On the other hand, as is indicated in a previous footnote, there is reliable evidence that the valence of copper is approximately $5\frac{1}{2}$ in the structures of

$CuAl_2$ and Cu_4Al_9. It may be that the free electron approximation is completely invalid here; this seems improbable for the low energy region of the band at least, since the calculated position of the first maximum in the emission curve agrees well with the observed position in every case. Even if the free electron approximation is valid except in regions close to zone boundaries, the large deviations from the parabolic N(E) curve at points corresponding to the filling of important zones may cause the large discrepancies found between calculated and observed widths. If this were the case, it might reasonably be expected that the widths of the various aluminum curves would vary irregularly and markedly in view of the large structural differences exhibited in the series.

An explanation of the disagreement between calculated and observed widths which should be advanced at this point lies in the recognition that the one-electron approximation, which has been implicitly assumed throughout the discussion, may be inadequate to explain completely the features of the various emission curves. It is possible that, although in each case the width of the filled portion of the N(E) curve is reasonably that calculated for the free-electron form, exchange effects prevent electrons in one region of the band from approaching the aluminum atoms frequently enough to give rise to much radiation of frequencies corresponding to the energies of such a region. Thus, if electrons in the

high energy region of each band were prevented from approaching the aluminum atoms frequently, the observed widths of the corresponding emission curves would be smaller than if this mechanism did not obtain. In the present explanation this is the effect postulated to exist. The observed widths of the emission bands indicate that no more than about three of the $5\frac{1}{2}$ valence electrons of copper can approach the aluminum atoms frequently. The remaining $2\frac{1}{2}$ valence electrons, situated in the high energy region of each band, are forced to remain in the neighborhood of copper atoms. Such a situation seems fairly plausible although a specific theoretical justification for it is lacking.

It is reasonable to expect that a high energy emission cutoff due to exchange effect should be less abrupt than a cutoff of the type described by the elementary theory of the introductory section. Indeed, Figure 3a shows that as the copper content is increased, the slope of the cutoff generally decreases.

In the aluminum-nickel series the aluminum curves are for the most part featureless. It is likely that many of the compositions are in two-phase regions; the only known structure is that of NiAl (Curve IV). With either valence for nickel, the first important inscribed sphere, containing 2.8 occupied states per unit cell, is filled. The appearance of the emission curve indicates the filling of at least one inscribed sphere. The width of the emission band is again nearly the same as that for pure aluminum.

Conclusions

The study of the fine structure of X-ray emission bands of metals, alloys, and intermetallic compounds seems to offer a chance to gain valuable information concerning metallic valences. In many cases, however, it will be necessary to have an extremely refined theoretical description of the situation in metallic structures before the interpretation of the spectral data can be made with confidence. In other cases there is some hope that the roughly approximate picture, that developed in this discussion, will be effective in the interpretation of the data.

In any event there is a great need for more experimental information; the study of alloys and intermetallic compounds can be said to have just begun.

Table 2

Aluminum
Structure: A 1 type
Number of occupied states per unit cell: 12.0

hkl	intensity	Lorentz & polarization factor	Frequency factor	no. of states in inscribed sphere	radius of sphere ($Å^{-1}$)	$E(\underline{k})-E(0)$ (ev)
111				5.4	0.21	6.9
200				8.4	0.25	9.2
220				2.4	0.35	18.3

Table 3

$CuAl_2$

Structure[23]: D_{4h}^{18}; $a_o = 6.054$ Å; $c_o = 4.864$ Å; $Z = 4$

Number of occupied states per unit cell: 45.8 (Pauling); 28.0 (Mott and Jones)

hkl	intensity	Lorentz & polarization factor	frequency factor	no of states in inscribed sphere	radius of sphere ($Å^{-1}$)	E(k)-E(o) (ev)
11.0	440	60	4	2.4	0.12	
10·1	not obs.					
20·0	200	28	4	6.7	0.16	3.8
21·1	420	16	16	14	0.21	
22·0	660	13	4	20	0.24	8.6
11·2			8			
31·0	910	9.7	8	27	0.26	10.1
20·2			8			
30·1	not obs.					
22·2	86	6.5	8	45	0.31	
32·1	not obs.					
10·3	not obs.					
40·0	not obs.					
31·2	66	5.5	16	55	0.33	

Table 4

CuAl

Structure[22]: a = 4.08 Å, b = 12.0 Å, c = 8.63 Å; Z = 16

Number of occupied states per unit cell: 135 (Pauling), 64.0 (Mott and Jones)

hkl	intensity	Lorentz & polarization factor	frequency factor	no. of states in inscribed sphere	radius of sphere (Å^{-1})	E(k) - E(o) (ev)
020	M		unity			
021	MW	4.1	throughout			
002	MS				0.12	
110	S				0.13	
111	S				0.14	
022	S	3.2			0.15	
040	W					
003	MS				0.17	
130	S				0.17	
023	S	2.2			0.19	
132	MW					
113	MS				0.21	
043	W					
150	S				0.24	
200	VS				0.24	
024	MS	1.6		49	0.24	8.6
133	VS				0.24	
151	S				0.25	
060	S				0.25	
061	W					
220	S	1.4			0.25	
221	M					
202	S				0.27	

Table 4 (cont.)

hkℓ	intensity	Lorentz & polarization factor	frequency factor	no of states in inscribed sphere	radius of sphere ($Å^{-1}$)	$E(\underline{k}) - E(o)$ (ev)
222	S	1.3	unity throughout		0.28	
044	VW					
005	M					
134	W					
240	MW					
203	S	1.2			0.30	
063	W					
223	S			105	0.31	
154	W					
135	MW					
081	MW					
224	S				0.35	
006	S	1.0		150	0.35	

Table 5

Structure: T_d^1; Cu_9Al_4 a = 8.700 Å; Z = 4

Number of occupied states per unit cell: 244 (Pauling); 84 (Mott and Jones)

hkl	intensity	Lorentz & polarization factor	frequency factor	no. of states in inscribed sphere	radius of sphere ($Å^{-1}$)	E(k) - E(o) (ev)
210	128	53	24			
211	264	43	24			
300	258	25	6			
221			24			
222	90	19	8			
321	110	16	48			
410	43		24			
322			24			
411	2920	11	24	80	0.24	8.9
330			12			
331	26		24			
420	34		24			
421	31		48			
332	142	9.0	24			
422	183		24			
510	66		24			
431			48			
511	59		24			
333			8			
520	38		24			
432			48			
522	31		24			
441			24			
530	20		24			
433			24			
531	14		48			
600	366	5.0	6	226	0.34	17.8
442			24			

Table 5 (cont.)

hkl	intensity	Lorentz & polarization factor	frequency factor	no. of states in inscribed sphere	radius of sphere ($Å^{-1}$)	E(k) - E(o) (ev)
610	11		24			
611	62		24			
532			48			
621	16		48			
540			24			
443			24			
541	25		48			
622	10		24			
630	20		24			
542			48			
631	75		48			
444	137		8	348	0.40	

Table 6

Cu - Al (19 at. o/o Al)
Structure[23]: A 1 solid solution; a=3.65 Å; Z = 4
Number of occupied states per unit cell: 19.9 (Pauling); 5.52 (Mott and Jones)

hkℓ	intensity	Lorentz & polarization factor	frequency factor	no. of states in inscribed sphere	radius of sphere ($Å^{-1}$)	E(k) - E(o) (ev)
111				5.4	0.24	8.4
200				8.4	0.27	11.2
220				24	0.38	22.4

Table 7

NiAl
Structure[24]: L21: a = 2.88 Å
Number of occupied states per unit cell: 8.87 (Pauling); 5.52 (Mott and Jones)

100						
110				2.8	0.25	9.0
111						
200				8.4	0.35	17.2
211				(11)		

References

(1) C. B. Jordan, Unpublished Research.

(2a) L. Pauling, Phys. Rev., 54, 899 (1938).

(2b) L. Pauling, J.A.C.S., 69, 542 (1947).

(2c) L. Pauling, Proc. Roy. Soc. (London) A196, 343 (1949).

(2d) L. Pauling, Physica, XV, 23 (1949).

(3) H. W. B. Skinner, Reports on Progress in Physics, V, 257 (1938).

(4) H. Jones, N. F. Mott, and H. W. B. Skinner, Phys. Rev., 45, 379 (1934).

(5) H. W. B. Skinner, Roy. Soc. Phil. Trans., A239, 95 (1940).

(6) L. G. Parratt, Phys. Rev., 44, 328 (1933); 45, 364 (1934).

(7) F. Seitz, "The Modern Theory of Solids", McGraw Hill, (New York and London) 1940, p. 272.

(8) N. F. Mott and H. Jones, "The Theories of the Properties of Metals and Alloys", (Oxford) 1936, p. 154.

(9) F. Seitz, op. cit., p. 296.

(10) L. Pauling and F. J. Ewing, Rev. Mod. Phys., 20, 112 (1948).

(11) H. Jones, Proc. Phys. Soc. (London), 49, 243 (1937).

(12) J. Farineau, Ann. de Phys., 10, 20 (1938).

(13) E. Rudberg and J. C. Slater, Phys. Rev., 50, 150 (1936).

(14) W. W. Beeman and H. Friedman, Phys. Rev., 56, 393 (1939).

(15) M. F. Manning and M. I. Chodorow, Phys. Rev., 56, 787 (1939).

(16) J. A. Bearden and J. M. Snyder, Phys. Rev., 59, 162 (1941).

References (cont.)

(17) J. A. Bearden and H. Friedman, Phys. Rev., 58, 387 (1940).

(18) A. H. Compton and S. K. Allison, "X-Rays in Theory and Experiment", D. Van Nostrand Co., (New York) 1935, p. 632.

(19) J. Farineau, J. Phys. et Rad., 10, 327 (1939).

(20) Mott and Jones, op. cit., p. 315 ff.

(21) J. B. Friauf, J. A. C. S., 49, 3107 (1927).

(22) G. D. Preston, Phil. Mag., 12, 980 (1931).

(23) A. J. Bradley and P. Jones, J. Inst. Metals, 51, 131 (1933).

(24) A. J. Bradley and A. Taylor, Proc. Roy. Soc. (London) A159, 56 (1937).

III. CRYSTAL STRUCTURES OF CERTAIN INORGANIC COMPOUNDS

(a) Crystal Structure of Sodium Borohydride

[Reprinted from the Journal of the American Chemical Society, **69**, 987 (1947).]

CONTRIBUTION FROM THE GATES AND CRELLIN LABORATORIES OF CHEMISTRY, CALIFORNIA INSTITUTE OF TECHNOLOGY, No. 1086]

Crystal Structure of Sodium Borohydride

BY A. M. SOLDATE

The unexpected properties of sodium borohydride, such as its stability in vacuum at temperatures as high as 400°,[1] give interest to an investigation of its structure, hitherto unreported.

Experimental Methods and Results.—A sample of powdered sodium borohydride was kindly supplied by Dr. H. C. Brown of Wayne University, who reported it as being 98–99% pure. Specimens suitable for X-ray photography were obtained by sealing powdered material in thin-walled Pyrex capillaries about 0.5 mm. in diameter. To ensure adequate protection of this hygroscopic substance, the procedure was carried out over sulfuric acid in a sealed enclosure.

Powder photographs were made with copper $K\alpha$ radiation filtered through nickel in a cylindrical camera with a 5-cm. radius. The twenty reflections observed were indexed on the basis of a cubic cell with $a_0 = 6.15$ Å. More precise lattice constant measurements using sodium chloride as an internal standard gave 6.151 ± 0.009 kX for the value of a_0. No reflections with mixed indices were observed, the lattice is, therefore, face-centered.

The unit cell, being face-centered, must contain a multiple of four sodium borohydride molecules. It was assumed that the correct number of molecules in the unit cell is four. The density calculated with this assumption is 1.074 g./cc. No experimental value is known to us, but this value is a reasonable one. There are two ways in which the sodium and boron atoms can be arranged in the unit cell:

(1) Private communication from Dr. H. I. Schlesinger, The University of Chicago.

(A) 4Na at 0 0 0, 0 1/2 1/2, 1/2 0 1/2, 1/2 1/2 0
4B at 1/2 1/2 1/2, 1/2 0 0, 0 1/2 0, 0 0 1/2

(B) 4Na at 0 0 0, 0 1/2 1/2, 1/2 0 1/2, 1/2 1/2 0
4B at 1/4 1/4 1/4, 1/4 3/4 3/4, 3/4 1/4 3/4, 3/4 3/4 1/4.

By use of Pauling–Sherman f values[2] and by neglect of the scattering power of the hydrogen atoms, intensities were calculated for both arrangements of the sodium and boron atoms. Table I shows good agreement between intensities calculated on the basis of arrangement A and observed intensities. The net effect of absorption and temperature corrections, omitted here, was estimated to be small.

TABLE I

A COMPARISON OF OBSERVED INTENSITIES AND INTENSITIES CALCULATED WITH SODIUM AND BORON ATOMS IN ARRANGEMENT A

(*hkl*)	Calcd. intensity	Obs. intensity[a]
111	231	m+
200	562	vs
220	386	s
311	138	m
222	130	m−
400	72	f
331	51	f
420	145	m−
422	105	f+
333–511	31	f−
440	33	f−
531	24	vf
442–600	65	f
620	45	f−
533	7	vvf
622	38	f−
444	15	vvf+
711–551	14	vvf
640	47	f−
642	108	f

[a] s, Strong; m, medium; f, faint.

Intensities calculated for the second arrangement were in marked disagreement with those observed. For example, the calculated intensity of the line {220} is much greater than that of {200} and the calculated intensity of {331} is greater than that of {420}.

With the assumptions that each boron atom is surrounded by a tetrahedral configuration of four hydrogen atoms and that the structure consists of BH_4^- and Na^+ ions, intensities were calculated for two arrangements of BH_4^- tetrahedra: (1) a completely random distribution of tetrahedra in positive and negative configurations (mirror images) with hydrogen atoms on cube diagonals; (2) tetrahedra all positive or all negative throughout the structure with hydrogen atoms on cube diagonals. In both instances the calculated intensities of {111} and {400} were the only values which differed from corresponding values of Table I by more than 20%. Agreement between observed and calculated intensities was not improved over that shown in Table I with either arrangement of tetrahedra. It was decided that it was impossible to reach any conclusion as to the positions of the hydrogen atoms from the intensity data obtained here.

With the assumption of a covalent boron–hydrogen bond distance of 1.16 Å., a van der Waals radius of 1.00 Å. for hydrogen, and a crystal radius of 0.95 Å. for sodium, it can be seen that the boron–sodium distance of 3.07 Å. and the boron–boron distance of 4.35 Å. are large enough to cause very little steric hindrance to rotational displacements of BH_4^- tetrahedra. Thus, rotating or oscillating BH_4^- tetrahedra can be reasonably presumed to exist in the structure and statistical distributions of tetrahedra, such as the one already considered, are of relevance.

I thank Dr. Linus Pauling for the suggestion of the problem and for helpful advice during the preparation of this report.

Summary

Powder photographic X-ray data have been used to show that the structure of sodium borohydride is based on a face-centered cubic lattice. The unit cell contains four sodium and four boron atoms arranged in the following manner:

4 Na at 0 0 0, 0 1/2 1/2, 1/2 0 1/2, 1/2 1/2 0
4B 1/2 1/2 1/2, 1/2 0 0, 0 1/2 0, 0 0 1/2.

The value 6.151 ± 0.009 kX was found for a_0.

It is probable that the structure consists of tetrahedral BH_4^- ions and Na^+ ions. The dimensions of the ions would permit oscillation or rotation of the BH_4^- tetrahedra.

PASADENA, CALIFORNIA RECEIVED NOVEMBER 26, 1946

(2) L. Pauling and J. Sherman, *Z. Krist.*, **81**, 1 (1932).

III. CRYSTAL STRUCTURES OF CERTAIN INORGANIC COMPOUNDS

(b) A Redetermination of the Structural Parameters in the Cubic Modification of Arsenious Oxide

A Redetermination of the Structural Parameters in the Cubic Modification of Arsenious Oxide

Introduction

The structure of the cubic modification of arsenious oxide, which occurs naturally as the mineral arsenolite, is based upon the packing of As_4O_6 molecules in the positions of the A-4 (diamond type) arrangement[1]. Interest in the structure was stimulated by the discovery that in the molecular state the arsenic-oxygen distance, 1.80 ± 0.02Å, is somewhat shorter than the corresponding distance of 2.01 Å reported in Bozorth's original crystal structure study[2].

Because the precision of Bozorth's determination did not exclude the possibility that this difference is only apparent, another investigation of the crystal structure was undertaken, which led to a confirmation of Bozorth's result[3]. Accordingly it was concluded that the arsenic-oxygen intramolecular distance is lengthened in the formation of the molecular crystal; this lengthening was attributed to the formation of weak intermolecular oxygen-arsenic bonds[4]. The structure of cubic arsenious oxide was therefore considered to be well understood. Recently, however, another redetermination of the structural parameters of the cubic modification has been made, and it is reported that the intramolecular arsenic-oxygen distance is 1.80 + 0.05 Å[5],

the same distance found in the molecular state*. The results of the reported crystal structure determinations are discrepant, and it was considered that still another crystal structure determination was worthwhile.

Experimental Methods and Parameter Evaluations

Bozorth[1] found that the structure of the cubic modification of arsenious oxide is based upon the space group O_h^7 - Fd3m and that the length of the unit cell edge is 11.06 kX. The density of the substance indicates that there are 32 arsenic atoms and 48 oxygen atoms in the unit cell. The arsenic atoms are in the positions which may be conveniently given as

$$(\,0\;0\;0;\ \tfrac{1}{2}\;\tfrac{1}{2}\;0;\ 0\;\tfrac{1}{2}\;0;\ 0\;0\;\tfrac{1}{2}) +$$

$$(\tfrac{1}{8}\;\tfrac{\bar{1}}{8}\;\tfrac{\bar{1}}{8}) + (x\;x\;x,\ x\;\bar{x}\;\bar{x};\ \text{½}),$$

$$(\tfrac{\bar{1}}{8}\;\tfrac{1}{8}\;\tfrac{1}{8}) + (\bar{x}\;\bar{x}\;\bar{x},\ \bar{x}\;x\;x;\ \text{½}),$$

and the oxygen atoms are in the positions

$$(\,0\;0\;0;\ \tfrac{1}{2}\;\tfrac{1}{2}\;0;\ 0\;0\;\tfrac{1}{2}) +$$

$$(\tfrac{1}{8}\;\tfrac{\bar{1}}{8}\;\tfrac{\bar{1}}{8}) + (0\;0\;v;\ \text{½};\ 0\;0\;\bar{v};\ \text{½}),$$

$$(\tfrac{\bar{1}}{8}\;\tfrac{1}{8}\;\tfrac{1}{8}) + (0\;0\;v;\ \text{½};\ 0\;0\;\bar{v};\ \text{½}).$$

These conclusions were based upon Laue photographic data and the plausible assumption that all the arsenic atoms and

---

*The value for the arsenic-oxygen distance in molecular arsenious oxide was found to be 1.78 ± 0.02 Å in the electron diffraction investigation of Lu and Donohue, J.A.C.S., 66, 818 (1944).

all the oxygen atoms are crystallographically equivalent. In addition, the parameters χ and v were determined with enough precision from the Laue data to establish beyond doubt that the structure is based upon the packing of As_4O_6 molecules.

It was not deemed necessary to make a systematic check of the gross structural details given above; the good agreement between observed and calculated intensities to be reported subsequently can be considered to confirm them. The main purpose of the present investigation, therefore, was to obtain values of the parameters x and v with enough precision to decide whether or not a significant difference in the molecular dimensions is caused by crystallization.

Initially the problem of the determination of the parameters x and v was attacked with the use of powder photography. A heavy multiple-film exposure[6] was made with Cu K radiation filtered through nickel. The specimen photographed consisted of a thin Pyrex fiber which was coated with the powdered substance by means of a small amount of vaseline. Reagent grade arsenious oxide was used and the powder was prepared by sublimation. Absorption errors were considered to be negligible.

A preliminary determination of the value of the arsenic parameter x was made by a consideration of the intensities of reflections of the type $h + k + \ell = 4n + 2$, which are independent of the positions of the oxygen atoms. Structure

factors were calculated for these reflections in the region $0.100 \leq x \leq 0.110$ with the use of Pauling-Sherman atomic scattering factors[7]. The permissible range for x was found to be $0.102 \leq x \leq 0.105$ by the observations that $F^2_{662} < 2\ F^2_{842}$ and $F^2_{662} > 2\ F^2_{842}$, the intensity ratio for the latter inequality being large enough to insure that it is not reversed when corrections for Lorentz, polarization, or reasonable isotropic temperature factors are made. Structure factors were then calculated in the region $0.102 \leq x \leq 0.105$, $0.160 \leq v \leq 0.230$. It was found that v must be less than 0.185 because of the observation that $F^2_{620} > F^2_{533}$. On the other hand, if $v = 0.160$ the general agreement between calculated and observed intensities becomes appreciably less satisfactory. A further limitation of the permissible values of x and v was found to be impossible with the powder photographic data. It became necessary, therefore, to secure single-crystal data.

Single crystals were prepared by the slow cooling of a hydrochloric acid solution of the substance. The crystals were octahedral in habit and, at first, it did not seem advisable to grind them to cylinders even though the linear absorption coefficient for Cu Kα radiation is rather high, 236 cm^{-1}. Oscillation and rotation photographs were taken with crystals of small dimensions, 0.1 mm to 0.3 mm on an edge. Selected intensity ratios were corrected for

the effect of Lorentz and polarization factors, and the magnitudes of absorption errors were estimated by the use of the graphical method first suggested by Albrecht[8]. The permissible range for x was then more precisely defined as $0.102 \leq x \leq 0.104$ by the observation that $F^2_{12.0.0} \leq 3F^2_{880}$, and the permissible range of v as $0.165 \leq v \leq 0.178$ by the observation that $F^2_{220} \approx F^2_{600}$.

A precise measurement of the positions of the large angle powder reflections, which were clearly resolved into the $K\alpha_1$ and $K\alpha_2$ components, led to the value of 11.04 ± 0.01 kX for a_o, the unit cell edge*. The values of the structural parameters and the length of the unit cell edge reported above fix the intramolecular arsenic-oxygen distance as 1.78 ± 0.04 Å, a value which is in essential agreement with that of Almin and Westgren 1.80 ± 0.05 Å.

As a final step in the investigation, the intensities of the powder reflections were estimated visually, the best value for the isotropic temperature factor estimated by graphical means, and a list of calculated and observed intensities prepared.

During a verbal report of the investigation made in a seminar on structural chemistry at the California Institute

---

*The value of a_o was found to be 11.0457 ± 0.0002 kX by F.Lihl, Z. Kryst., 81, 142 (1931) and 11.05208 ± 0.00010 kX by M. Straumanis et al, Z. Phys. Chem., B 42, 143 (1937).

of Technology, it was pointed out that the agreement between the calculated and observed intensities of the powder reflections was not wholly satisfactory, and it was suggested that the existence of an anisotropic temperature effect of the type found for crystalline hexamethylenetetramine[9] might explain the discrepancies*. Since such a correction is not a smooth function of the angle of reflection, the parameter determination reported above conceivably could be incorrect. Accordingly it became necessary to estimate the magnitude of the anisotropic temperature effect.

A consideration of the data led to the conclusion that the anisotropic temperature effect was not large; however, the method used in the determination of the parameters is in principle extremely sensitive to even small effects of this type. Furthermore, it seemed that the intensities of the powder reflections could not be estimated with enough precision to decide whether or not the effect really exists.

---

* I am indebted to Professor V. F. H. Schomaker for this suggestion. It is made plausible by the fact that the crystal structure of hexamethylenetetramine is based upon the packing of $(CH_2)_6 N_4$ molecules, the configuration of the carbon and nitrogen atoms of each molecule being identical to that of the arsenic and oxygen atoms of the As_4O_6 molecule.

Before the single-crystal data at hand could be used it was necessary to apply the absorption correction calculated for an octahedral shape. Since the calculation of these corrections, even by graphical means was found to be laborious, it was decided to obtain single-crystal data with the use of a cylindrically shaped specimen.

A rather large octahedron was ground to a cylinder 0.5 mm. in length and 0.2 mm. in diameter. The axis of the cylinder was parallel to one of the four-fold axes. A heavily exposed multiple-film rotation photograph was prepared with the use of copper K radiation filtered through nickel. The cylinder axis was aligned with the axis of rotation.

The intensities of the observed reflections were estimated visually with the use of the film factor 3.7, which is appropriate for normal incidence upon Eastman No-Screen X-ray film[10]*. The intensities were corrected for the effect of Lorentz, polarization, frequency, and absorption factors. Absorption corrections were obtained in the following manner. The corrections of Claassen[11] ($\mu r = 2.4$) were used for the equatorial reflections. The correction curves for the second and fourth layer lines

---

*Because of an oblique angle of incidence, the film factor for each layer line above the equator is somewhat greater than 3.7. The film factors used for the first, second, third, and fourth layer lines were 3.7, 3.9, 4.2, and 4.9 respectively.

were estimated from a comparison of the intensities of a given reflection which appeared on the equatorial layer line and one or the other of the higher layer lines. The curves for the first and third layer lines were estimated by interpolation and a similar intercomparison of intensities. The visually estimated intensities corrected in the manner outlined above are listed in Table 1.

The magnitude of the anisotropic temperature effect was estimated from a consideration of the intensities of type $h+k+\ell = 4n+2$. First, the value of the arsenic parameter x was estimated from the observed structure factor ratios of reflections which occurred on the same layer line and which were close to one another. In this way, an isotropic temperature correction effect could be omitted in the first approximation and possible errors in absorption corrections ignored. Calculated curves of four intensity ratios were found to have large slopes in the range $0.095 \leq x \leq 0.115$. The values of x derived from the observed ratios $\frac{442}{622}$, $\frac{842}{662}$, $\frac{10.2.2}{842}$, and $\frac{10.2.2}{882}$ are 0.1025, 0.1026, 0.1029, and 0.1035, respectively. These values are, of course, derived with the neglect of an anisotropic temperature factor as well as an isotropic temperature factor. Since the variations in the observed structure factor ratios due to an anisotropic temperature effect would be expected to be more or less random,

the average value of x should not be greatly in error. Structure factors were then calculated for all observed reflections of the type $h+k+\ell = 4n+2$ for $x = 0.103$ and the function $\ln\left\{\frac{|F|_{calc.}}{|F|_{obs.}}\right\}$ plotted against $\frac{\sin^2\theta}{\lambda^2}$ This plot is shown in Figure 1. With the exception of the point for 222, the points lie very close to a straight line of slope 2.2 Å^2. Thus, a reasonable value of the isotropic temperature factor is obtained and the magnitude of the anisotropic temperature effect is indicated to be small. With the use of the isotropic temperature coefficient 2.2, the values of x and v were found from a comparison of observed and calculated structure factor ratios. In Figure 2 curves are given which represent the loci of points for which calculated structure factor ratios are equal to observed structure factor ratios. The various points of intersection are centered about the point $x = 0.1029$, $v = 0.1749$ with an average deviation of 0.0003 and 0.0030 respectively. The parameter values derived here are in essential agreement with those derived previously and with those found by Almin and Westgren[5] $x = 0.103 \pm 0.001$, $y = 0.175 \pm 0.010$. Table 1 shows good general agreement between corrected observed intensities and intensities calculated with the structural and isotropic temperature parameters given above.

The value of the parameter x seems particularly well fixed and can be used to gain a quantitative estimate of the

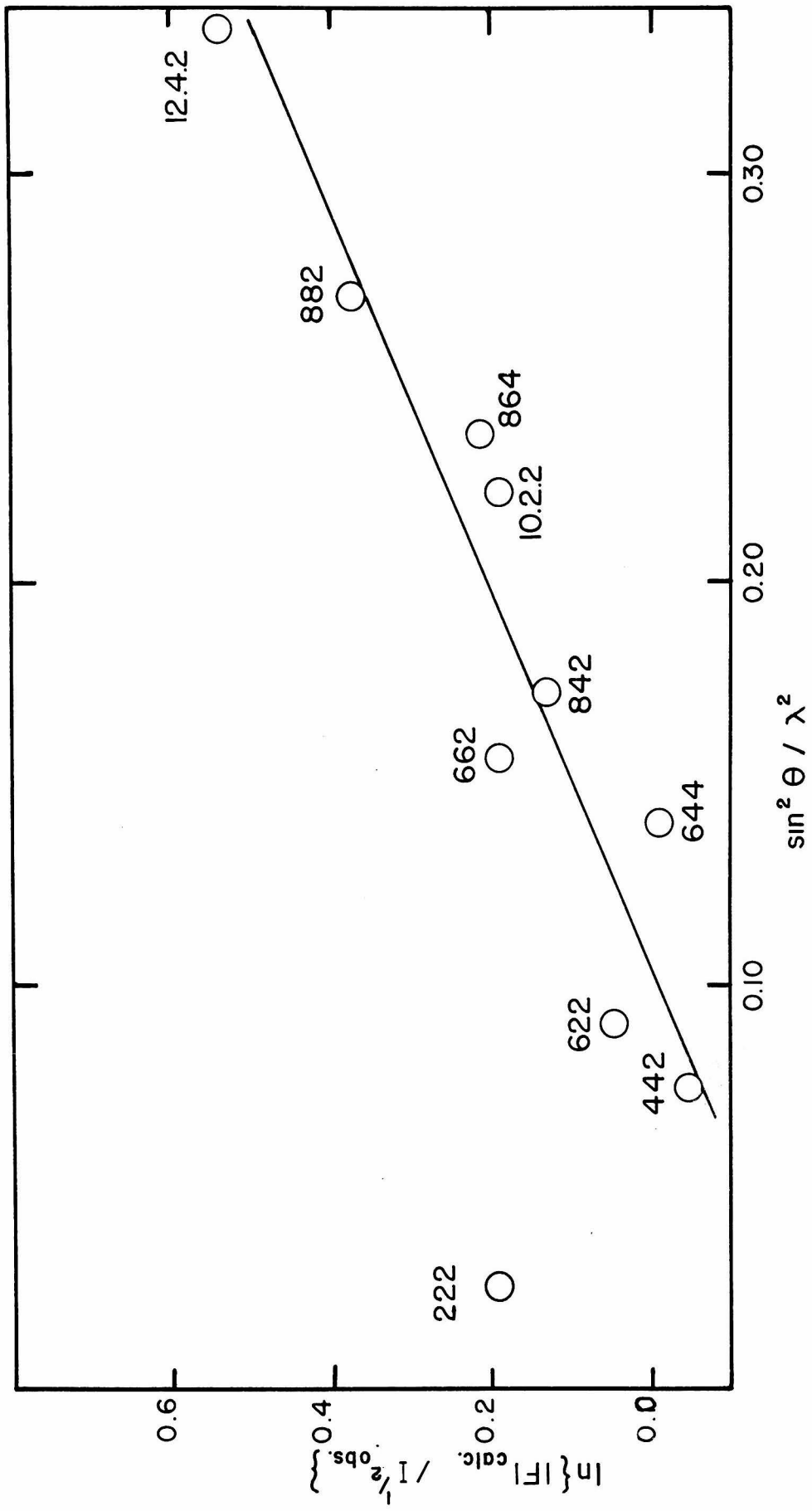
12.4.2
882
864
10.2.2
842
662
644
622
442
222
0.0
0.2
0.4
0.6
0.10
0.20
0.30
$\sin^2\theta / \lambda^2$
$\ln\{|F|_{calc.} / I^{1/2}_{obs.}\}$

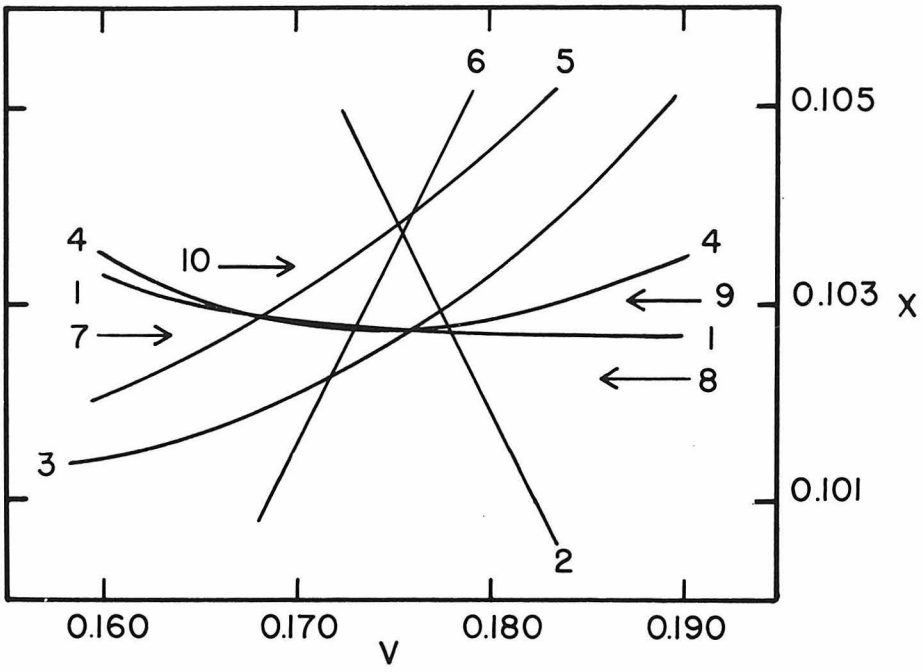

curve no.	ratio
1	933:953
2	513:533
3	620:800
4	884:10.6.4
5	11.5.3:993
6	822:662
7	442:622
8	662:842
9	842:10.2.2
10	10.2.2:882

magnitude of the anisotropic temperature factor. The anisotropic temperature factor to be considered here arises from the possibility that the As_4O_6 molecules can under go small torsional vibrations about the various molecular centers of gravity. These small vibrations should be very nearly symmetric with respect to direction and would cause a smearing of the charge distribution of each atom in a plane normal to a line drawn through the atom and the molecular center of gravity. The calculation of the effective atomic scattering factor for a smearing of this type has been discussed previously[9] and no report will be made here concerning its details. The specific form of the correction used here will be given for convenience in the subsequent discussion. If following Shaffer, F_As and F_0 are defined by the expression

$$F = \exp\left\{-B\frac{\sin^2\theta}{\lambda^2}\right\}\left[F_0 + F_{As}\right],$$

we find that

$$F_0 = 16 f_o \cos\frac{2\pi}{8}(h+k+l)\left[\cos 2\pi l v \exp\left\{\frac{-b}{4a_0^2}(h^2+k^2)\right\} + \cos 2\pi k v \exp\left\{\frac{-b}{4a_0^2}(h^2+l^2)\right\} + \cos 2\pi h v \exp\left\{\frac{-b}{4a_0^2}(k^2+l^2)\right\}\right],$$

$$F_{As} = 8 f_{As} \exp\left\{\frac{-b}{6a_0^2}(h^2+k^2+l^2)\right\}\left[\cos 2\pi\left\{\frac{h+k+l}{8} + (h+k+l)x\right\}\exp\left\{\frac{-b}{6a_0^2}(-hk-hl-kl)\right\} + \cos 2\pi\left\{\frac{h+k+l}{8} + (h+\bar{k}+\bar{l})x\right\}\exp\left\{\frac{-b}{6a_0^2}(hk+hl-kl)\right\} + \cos 2\pi\left\{\frac{h+k+l}{8} + (\bar{h}+\bar{k}+l)x\right\}\exp\left\{\frac{-b}{6a_0^2}(-hk+hl+kl)\right\} + \cos 2\pi\left\{\frac{h+k+l}{8} + (\bar{h}+k+\bar{l})x\right\}\exp\left\{\frac{-b}{6a_0^2}(hk-hl+kl)\right\}\right].$$

The value of the parameter b determines the magnitude of the anisotropic temperature effect. It is quite plausible that in most cases the changes in the terms of each expression due to the exponential factors tend to cancel when the value of b is small. In a few instances, however, the various changes might reinforce each other. Even so, the effect of an anisotropic temperature factor for small values of b would be slight unless the various terms of each expression, especially that for F_{As} tend to cancel when no exponential factors are applied. The agreement between calculated and observed structure factors is quite appreciably improved in the case of the weak reflections 10.6.2, and 10.4.4 when b is 0.5 and B is 1.9. The positions of the curves of Figure 2 are not appreciably shifted by an anisotropic temperature factor of 0.5, however. It is clear that, although the final agreement between calculated and observed structure factors may be somewhat improved by the anisotropic temperature factor, the structural parameters will be left essentially unchanged.

Discussion of Structure

The parameters $x = 0.1029 \pm 0.0003$ and $v = 0.1749 \pm 0.0030$ determine the intramolecular arsenic-oxygen distance as 1.80 ± 0.02 Å. The intramolecular arsenic-arsenic distance is 3.22 Å. The most probable O - As - O angle is 99°12'; the

most probable As - O - As angle is 127°24'. The dimensions of the As_4O_6 molecule in the cubic modification of arsenious oxide are thus nearly identical to those found for the free As_4O_6 molecule, As - O = 1.78 ± 0.02 Å, As - As = 3.20 ± 0.02 Å ∠ O - As - O = 99°, ∠ As - O - As = 128° (12).

The arsenic-oxygen distance of 1.80 Å is appreciably smaller than the sum of the single bond radii, 0.66 Å + 1.21 Å = 1.87 Å(13). If the equation relating distance to bond order

$$R(1) - R(n) = 0.300 \log n \quad (13)$$

is used, it is found that the bond order, n, for the arsenic-oxygen distance of 1.80 Å is 1.31. The increase in bond number over the value 1.00 is presumably due to the use of the unshared electron pairs of the oxygen atoms(4). It is of interest to calculate the bond number for the smallest intermolecular arsenic-oxygen distance. This distance is 3.03 Å and the corresponding bond number is 0.012 which is so small as to have no significance(13).

The structure of the cubic modification of arsenious oxide, therefore, can be described in terms of the packing of undistorted As_4O_6 molecules which are attracted to one another by secondary valence or Van der Waals forces.

Summary

The structural parameters of the cubic modification of arsenious oxide have been redetermined by means of X-ray powder and single-crystal photography and found to agree

closely with those reported by Almin and Westgren[5].

The structure is based upon the packing of As_4O_6 molecules which have the same dimensions as those found for the molecules of the gas[2],[12].

Table 1

hkl	$\|F\|_{obs.}$	$\|F\|_{calc.}$
111		11.5
220	2.00	1.69
311	2.06	2.13
222	18.7	26.4
400	15.0	18.7
331	9.47	11.2
422	5.62	5.71
511	6.55	7.22
333	6.64	7.32
440	15.0	17.0
531	3.81	3.88
442	5.69	5.66
620	1.30	1.20
533	2.37	2.49
622	11.4	12.1
444	13.5	13.0
711 551	13.0	14.7
642	3.27	3.03
731	7.06	7.06
553	5.29*	3.65
800	8.85	8.94
733	11.0	11.5
644	3.16	2.84
822	2.02	2.25
660	10.9	11.9
751	3.49	3.25
662	5.86	6.24
840	5.70	5.40
911	7.41	6.98
753	1.94	1.54
842	6.22	6.00
664	4.69	4.16
931	5.81	5.70
844	2.58	2.44
933	2.43	2.17
771	4.61	4.15
10.2.0	3.63	3.44
862	1.30*	1.45
951	6.16	5.69
773	6.45	6.61
10.2.2	2.07	1.90
953	2.22	1.97
864	3.60	3.30

Table 1 (cont.)

hkl	$\|F\|_{obs.}$	$\|F\|_{calc.}$
10.4.2	3.24	3.02
11.1.1	6.29	5.86
880	>1.10; <1.52	1.45
11.3.1	3.86	3.84
971	0.55*	0.73
10.4.4	>0.84; <1.00	0.44
882	7.19	7.10
10.6.0	6.07	5.23
11.3.3 973	6.75	7.11
10.6.2	>0.74; <0.87	1.06
12.0.0	2.75	2.56
884	2.37	2.68
11.5.1	2.64	2.42
12.2.2	<0.67	0.17
10.6.4	5.02	5.39
11.5.3	1.94	1.97
12.4.0	<0.59	0.30
991	2.66	2.25
12.4.2	3.71	3.72
10.8.2	<0.60	0.09
13.1.1 11.7.1	6.20	5.26
993	1.73	1.56
12.4.4	<0.47	0.53
13.3.1	2.84	2.74
11.7.3	2.78*	3.00

*These intensities determined by difference, that is, when crystal in reflecting position, another reflection also possible.

References

(1) R. M. Bozorth, J. A. C. S., 45, 1621 (1923).

(2) G. C. Hampson and A. J. Stosick, J. A. C. S. 60, 1814 (1938).

(3) D. Harker and J. Eskijian, Unpublished Research.

(4) L. Pauling, "The Nature of the Chemical Bond", Second Edition, Cornell University Press, Ithaca, N.Y., (1942), p. 248.

(5) K. E. Almin and A. Westgren, ArkIV KEMI, MinerolGeol, 15 B, No. 22, (1942).

(6) J. de Lange, J. M. Robertson, and I. Woodward, Proc. Roy. Soc. (London), A 171, 398 (1939).

(7) L. Pauling and J. Sherman, Z. Krist., 81, 1 (1932).

(8) G. Albrecht, Rev. Sci. Instruments, 10, 221 (1939).

(9) P. A. Shaffer, Jr., J. A. C. S., 69, 1557 (1947).

(10) D. P. Shoemaker, Thesis, Calif. Inst. of Tech., (1947).

(11) "International Tables for the Determination of Crystal Structures", Gebrueder Borntraeger, Berlin, 1935, Vol. 2, pp. 583-585.

(12) Chia-Si Lu and Jerry Donohue, J. A. C. S.,66, 818 (1944).

(13) L. Pauling, J. A. C. S., 69, 542 (1947).

IV. PROPOSITIONS

IV. Propositions

1. A relationship between the band structure of nearly free electrons and diffraction patterns of liquids exists which is closely analogous to that between the band structure of nearly free electrons and crystalline diffraction patterns. The demonstration of this relationship can be easily generalized to include the case of disorder in crystalline solids. Some systems in which the proposed relationship might fruitfully be applied are the alkali metal-ammonia systems, metallic liquid systems, and metal-molten salt systems[1].

2. Mott and Jones[2] have given a discussion of the Brillouin zones of graphite and find that the valence electrons just fill the zone bounded by the planes $\{11\cdot0\}$ and $\{00\cdot2\}$. This zone has the form of a flattened hexagonal prism with the ratio of the perpendicular distance of the $\{00\cdot2\}$ planes to that of the $\{11\cdot0\}$ planes equal to 0.362. Because of the marked flattening it might be expected that the $\{00\cdot2\}$ zone boundaries are overlapped by the Fermi-surface, with resultant vacancies at the zone vertices. This expectation is supported by the abnormally low value

of the specific resistivity, $2 \cdot 10^{-5}$ ohm cm. at 0° C, and the high diamagnetic susceptibility, $-3.5 \cdot 10^{6}$ emu[3].

3. A. F. Wells[4] has stated that there are no hydrogen bonds in the diaspore structure, and that one-half of the oxygen atoms exist as hydroxyl groups and the other half as oxygen atoms; accordingly, the most representative chemical formula for diaspore would be AlO(OH). As evidence for this conclusion Wells cites the existence of an absorption band at 3 μ. Cl. Duval and J. Lecomte[5], ~~however~~ indeed, find an OH absorption band at 1521 cm^{-1} ~~(1.5 μ)~~. The result of Duval and Lecomte, however, is in accordance with the conclusion reached by Pauling[6] that there are no hydroxyl groups in the structure and that all hydrogen bonds exist in such a way as to give the structure a residual entropy of R log 2.

It is probable that Wells' conclusion is incorrect.

4. Phase transformations which are extremely sluggish at low temperatures might be carried out by the presence of suitably unstable isotopes which by their disintegration would furnish the required energy of activation.

5. In section 3 of this thesis, it was found that

the interatomic distances in the structure of sodium borohydride permit the existence of freely rotating or oscillating BH_4^- tetrahedrons. It would be of interest to carry out a determination of the C_p and C_v curves from about 50° K to room temperature in order to investigate this possibility further.

6. The famous relationship of Gibbs

$$-\Gamma = \frac{1}{RT}\frac{d\sigma}{d\ln a} \quad (7)$$

has general validity for planar surfaces of two component systems, in the absence of external fields. A previous suggestion that it be modified in view of properties peculiar to one or both of the components, such as a tendency for long chain hydrophobic molecules to orient themselves at the surface [8] is unwarranted.

7. Slow exchange reactions might be studied in an electrical migration apparatus with a scanning counting device. In such a manner, complications introduced by precipitation separations could be avoided as could the necessity for the separation of enriched solutions [9].

8. Zachariasen [10] has developed a general theory for the calculation of structure factors of disordered structures. The initial model for his calculations

is an assemblage of crystallites of uniform dimensions. This model seems reasonable; it is, however, immediately modified to consist of but one average crystallite. Although such a modification seems plausible and does enable the development of a rather elegant treatment, it might be thought to lead to some degree of error, possibly of serious proportions. In order to check the validity of Zachariasen's treatment several of his examples were recalculated by a more direct, less elegant procedure in which the averaging process was carried out directly over the crystallites of the assemblage; this procedure led to identical results in every instance and lends confirmation to Zachariasen's treatment.

9. The presence of a protein has been noted to markedly affect the reduction of such substances as organic dyes at the dropping mercury electrode[11]. With reference to this phenomenon the following calculation may be of interest. The flux-time relationship is calculated for the linear flow of a solute at initial concentration c_o to a moving, initially clean, plain surface upon which the solute is adsorbed instantaneously according to a linear isotherm, $x = Kc$ (limiting form of Langmuir isotherm at low concentrations). If the flux, taken in the

direction toward the surface is ϕ , t the time, c_o the initial concentration, and k the diffusion constant,

$$\phi = c_o k K e^{\frac{kt}{K^2}} \left[1 - \mathrm{erf}\left(\frac{1}{K}\sqrt{kt}\right)\right]$$

10. It would be of great assistance and convenience to have a continuing index of all propositions submitted by candidates for the degree of Doctor of Philosophy in Chemistry at the California Institute of Technology. In this manner unintentional duplications of propositions and the embarrassment of an innocent plagiarism could be avoided.

References

1. D. D. Cubicciotti and C. D. Thurmond, J. A. C. S., 71, 2149 (1949)
2. N. F. Mott and H. Jones, "The Theory of the Properties of Metals and Alloys", (Oxford) 1936, p. 163
3. F. Seitz, "The Modern Theory of Solids", McGraw Hill (New York) 1940, p 61
4. A. F. Wells, "Structural Inorganic Chemistry", (Oxford) 1945, p. 356.
5. Cl. Duval and J. Lecomte, Bull. Soc. franc. mineral., 66, 284 (1943)
6. L. Pauling, J. A. C; S., 57, 2680 (1935)
7. "The Collected Works of J. Willard Gibbs", Longmans, Green and Co, (New York) 1928, Vol. I, p. 229 ff.
8. J. W. McBain and G. F. Mills, Reports on Progress in Physics, V, 30 (1938)
9. V. J. Linnenbom and A. C. Wahl, J. A. C. S., 71, 2589 (1949)

10. W. H. Zachariasen, "Theory of X-ray Diffraction in Crystals", John Wiley & Sons, Inc., (New York) 1945, p. 213 ff.

11. B. Keilin, J. A. C. S., 70, 1984 (1948)